Strength, Transport Efficiency and Selectivity of Novel Extractants for the Recovery of Base Metals

Tai Lin

Doctor of Philosophy

University of Edinburgh

2009

Preface and Declaration

The author graduated from Peking University, China in 2003 with a Bachelor of Science degree in chemistry, and has been engaged in a programme of full time research under the supervision of Professor Peter A. Tasker at the University of Edinburgh since 2005.

The work presented in this document is the original work of the author, except where references are made to other sources. It has been composed by the author and has not been submitted previously in whole or in part for another degree or qualification from this or any other university or institute of learning. In accordance with the regulation, this thesis does not exceed 70,000 words in length.

Tai Lin

September 2009

Abstract

This thesis concerns the development of new types of solvent extractants for use in the hydrometallurgical recovery of base metals, and addresses the ligand design features which are needed to control the strength, transport efficiency and selectivity of these extractants.

Chapter 1 provides background on the development of extractive metallurgy, e.g. pyrometallurgy and hydrometallurgy, and introduces the history, basic terminology and various processes and reagents involved. Solvent extraction as a hydrometallurgical technique to achieve the recovery of base metals is discussed in most detail. The design criteria of extractants are highlighted as the focus of the whole thesis.

Chapter 2 investigates the potential of salicylaldehyde hydrazones as cation exchange extractants for hydrometallurgical recovery of copper, and studies substituent effects, e.g. electronic, steric and particularly "buttressing" of ligand-ligand hydrogen bonding, on the strength and efficacy of the extractants. A series of 3-substituted (X) and N-substituted salicylaldehyde hydrazones has been developed. Solvent extraction experiments show that the 3-substitution can increase the distribution coefficient of the methylhydrazone for copper extraction by more than three orders of magnitudes along the series (X) Me < OMe ≤ H < Br < NO_2. Both the phenol acidity and intermolecular hydrogen bonding are significantly influenced by the 3-substituent as judged by a systematic NMR study on the solution speciation of the free ligands. Electron-withdrawing groups which also act as hydrogen bond acceptors (X = NO_2 or Br) are particularly effective in enhancing the strength of the methylhydrazones. Compared to the commercially applied salicylaldoximes, the hydrazones are weaker extractants, and the strength varies in

the order: oximes > methylhydrazones > phenylhydrazones. This order probably arises from a combination of variations in the phenol acidities and the strength of the hydrogen bonding motifs, which are also probed in the free ligands using NMR techniques.

Chapter 3 considers reagents capable of extracting metal salts and deals with the development of polytopic salicylaldimine ligands bearing pendant tertiary amine groups for the hydrometallurgical recovery of zinc chloride. These extractants show extremely high transport efficiency of metal salts with more than two moles of $ZnCl_2$ loaded per mole of ligand, and high chloride over sulfate selectivity in solvent extraction experiments. The unusual multiple loading suggests the extraction of chlorozincate as anion species, which is supported by the elemental analysis and ESI MS spectra of the formed complexes. The zinc chloride dependent extraction and stripping experiments further indicate that the extraction process is controlled by the Cl^- activities in the aqueous solutions. ^1H NMR studies show that two different complexes are successively formed in solution as the ligand to zinc stoichiometry is increased to 1L : 2$ZnCl_2$, with the first formed by extracting the zinc cation at low $ZnCl_2$ concentrations and the second likely resulting from the further extraction of chlorozincate at high $ZnCl_2$ concentrations. An extraction mechanism is proposed in which a tritopic assembly [Zn**L**Cl_2] forms by binding the Zn^{2+} cation with the $N_2O_2^{2-}$ site of the "salen" type ligands and two Cl^- anions with the protonated pendant amine groups and then a ditopic assembly [Zn**L**($ZnCl_4$)] forms by extracting the $[ZnCl_4]^{2-}$ anion when the reagent is contacted with high tenor $ZnCl_2$ feed. The possible formation of tritopic assemblies [Zn**L**$(ZnCl_3)_2$] accounts for Zn-loadings higher than 200%. The ligand design features such as the benefits of combining cation and anion binding sites in the same molecule are indicated by comparing the polytopic ligands with a series of dual host pairs of the salen ligand and hydrophobic amines. The polytopic ligands show potential for industrial application as $ZnCl_2$ extractants.

Finally chapter 4 focuses on the anion binding and selectivity involving simple anions and chlorometallates in solvent extraction by the polytopic ligands discussed in chapter 3 and their metal complexes. A novel and reliable method for chloride analysis in the presence of complexing metal cations has been developed using excess silver(I) to precipitate chloride and then analyze the silver content by ICP-OES technique. Multiple loadings of chloride are achieved by the polytopic ligands, which confirms the uptake of metal salt as $ZnCl_2$, and is desirable for excellent material balances in hydrometallurgical processes. The anion binding of the copper-only complex [Cu(**L**-2H)] supports the proposed extraction mechanism by indicating that one mole of zinc is extracted in the likely form of chlorozincate anions when the cation binding site is occupied by Cu^{2+}. The polytopic ligands and their copper-only complexes [Cu(**L**-2H)] show the same anion selectivity following the order $[ZnCl_4]^{2-} > Cl^- > SO_4^{2-}$, which can be explained by the hydration energies of these anions. Extractions from $ZnCl_2$, $ZnSO_4$, $Zn(NO_3)_2$ or mixed feed solutions indicate that the zinc transport efficiency is also dependent on the nature of counter anions.

Acknowledgements

I would like to thank a lot of people who have made my life much easier and happier throughout the last four years at Edinburgh. Firstly my supervisor Professor Peter Tasker, it is a real privilege to know you and work with you. All your time, patience, advice, support and encouragement are truly appreciated. You are an inspiration for my life and my career. Also Siggi and the rest of the Taskers, I am touched that your home is always opened to me, even at Christmas! Your kindness and friendship will be cherished.

I am also grateful for all the help from past and present members of the Tasker group. Your guys kept me in the right track along this adventure, and made the lab a fun and friendly place to work at. Thanks in particular to Dr Vesna Gasperov who helped me start my first project and to Heiko Bauer who contributed to part of the synthesis in the other project.

I would also like to thank the School of Chemistry and EaStCHEM for the funding of my studentship and for the excellent facilities here. I extend my gratitude to Dr Juraj Bella for helping me obtain a number of NMR spectra, Professor Simon Parsons and Dr Fraser White for solving my crystal structures, and Dr Lorna Eades for her advice on ICP-OES problems.

So many thanks are due to all the friends I made in Edinburgh, who carried me over the highs and lows. A special thank you to Yi Wang, Michael Pounds, Iain Robertson, Dr Christine Tong and Dr Arjan Westra for all the laughs, dinners and movies shared with me.

And Xuan Ye, thanks for visiting me from time to time. Our trips in Europe were

always full of fun and surprises. I am sure there will be more for us in the future.

Last but definitely not least, my greatest thanks to my parents, my sister and all my family. You are the reason to get me this far. Thank you so much for loving me, supporting me and putting up with my moaning and sometimes juvenility. I could not have done it without your guys!

Content

Ligands

Structure	Ligand	R	X
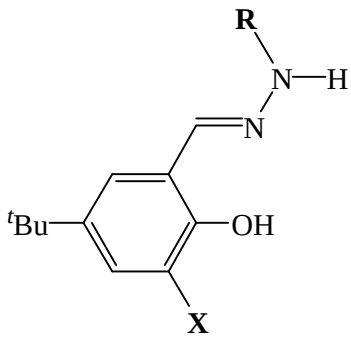	**L1**	Methyl	H
	L2	Methyl	Me
	L3	Methyl	NO_2
	L4	Methyl	Br
	L5	Methyl	OMe
	L6	Phenyl	H
	L7	Phenyl	Me
	L8	Phenyl	NO_2
	L9	Phenyl	Br
	L10	Phenyl	OMe

Structure	Ligand	R
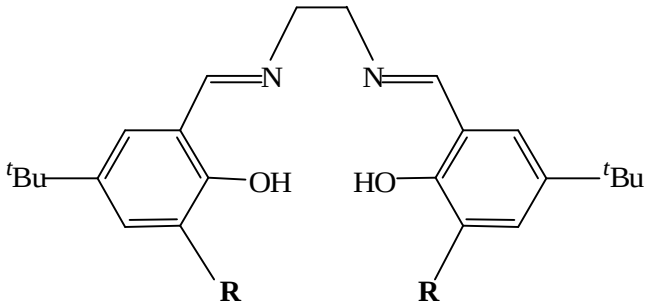	**L11**	H
	L12	$CH_2N(n\text{-}C_6H_{13})_2$
	L13	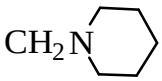
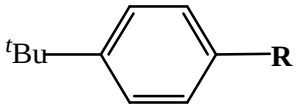	**L14**	$CH_2N(n\text{-}C_6H_{13})_2$

Abbreviations

Δ	change in
δ	chemical shift
°	degrees
°C	degree centigrade
$	dollars
=	equal to
<	less than
≤	less than or equal to
>	greater than
≥	greater than or equal to
%	percent
±	plus or minus
1D	one-dimensional
2D	two-dimensional
Å	Angstrom
AcOH	acetate acid
AD	*Anno Domini*
aq	aqueous phase
anal.	analysis
Ar	aromatic; aryl
BC	Before Christ
b.p.	boiling point
Bu	butyl
ca.	*circa* (around)
calc.	calculated
CHN	carbon, hydrogen and nitrogen

CLP	Chlorine Leach Process
CLX50	Pyridine-3, 5-dicarboxylic acid diisodecyl ester
COSY	Correlated Spectroscopy
d	doublet (NMR)
D2EHPA	di(2-ethyl hexyl)phosphoric acid
DBBP	dibutyl butyl phosphonate
DCM	dichloromethane
DFT	Density Functional Theory
DMSO	dimethylsulfoxide
EDTA	ethylenediaminetetraacetic acid
e.g.	for example
EPR	Electron Paramagnetic Resonance
ESI	electrospray (MS)
et al	*et alii* (and others)
etc	*et cetera* (and so on)
EtO	ethoxy
EtOH	ethanol
g	gram; gaseous
H	enthalpy
HF	Hartree-Fock
HMBC	Heteronuclear Multiple Bond Connectivity
HMTA	hexamethylenetetramine
hr	hour
I	nuclear spin quantum number
i	isomer
ICP-OES	inductively coupled plasma optical emission spectroscopy
i.e.	that is
in *vacuo*	under vacuum

IR	infrared
K	degree Kelvin
K_a	association constant
l	liquid
m	multiplet (NMR), metre
m	*meta*
M	molar
Me	methyl
MeO	methoxy
MeOH	methanol
MH^+	positively charged parent molecular ion (MS)
MHz	frequency (NMR)
mg	milligram
ml	millilitre
mm Hg	pressure
mmol	millimole
mol	mole
MS	mass spectrometry
m/z	mass to charge ratio
n	normal
NaOAc	sodium acetate
nm	nanometres
NMR	nuclear magnetic resonance
NOE	nuclear Overhauser effect
NOESY	Nuclear Overhauser Effect Spectroscopy
o	*ortho*
org	organic phase
p	*para*

P50	5-nonyl-2-hydroxybenzaldehyde oxime
PGM	platinum group metal
pH	$-\log_{10}[H^+]$
$pH_{0.5}$	pH when D = 0
pK_a	$-\log_{10}K_a$
ppm	parts per million
q	quartet (NMR)
s	singlet (NMR); solid
salen	*N,N'*-ethylenebis(salicylideneaminato)
SHG	special high grade
SX	solvent extraction
t	triplet (NMR)
t	tertiary
T	temperature
TBP	tri-*n*-butylphosphate
tert	tertiary
TMS	Tetramethylsilane
TOA	tri-n-octylamine hydrochloride
UV-Vis	ultraviolet-visible
via	by way of
vs.	versus
XRD	X-Ray Diffraction

CHAPTER 1

INTRODUCTION

Content

This thesis involves the development of new types of reagents for use in the hydrometallurgical recovery of base metals, and addresses the ligand design features which are needed to control the strength, transport efficiency and selectivity of new solvent extractants. Particular attention is paid to tuning the strength of salicylaldehyde hydrazones as potential copper extractants, investigating the mechanism of multiple zinc chloride loadings by polytopic salicylaldimine ligands and determining the anion binding and selectivity of these polytopic ligands for zinc salts. These topics are described successively in the following chapters.

This chapter provides a background on the chemistry of extractive metallurgy, particularly hydrometallurgical processes, and introduces the history, basic terminology and various reagents involved. More specific information relevant to an individual project is provided in the introduction of each of the respective chapters.

1.1 Extractive Metallurgy

Extractive metallurgy is the technology used to recover metals from primary sources (metal ores) and secondary sources, generally by the unit operations of concentration, separation, reduction and refinement.[1] These unit operations arise from the nature and composition of metal ores. Metals are usually found in low concentration, mixed ores, which require "concentration and separation". As a consequence of the changes to the composition of the Earth's atmosphere, a metal deposit typically consists of a lower sulfide layer, a middle mixed sulfide/oxide layer and a top metal oxide layer,[2] all of which require "reduction" to obtain the metal values. When a high-purity product is required, "refinement" is additionally needed. Extractive metallurgy dates back to 4000 BC or earlier[2] when copper smelting was discovered. Pyrometallurgy, hydrometallurgy and other methods are currently used to process metal ores.

1.2 Pyrometallurgy

Pyrometallurgy produces metals or intermediate products directly from the ore by use of high-temperature oxidative or reductive processes.[3, 4] Carbon is commonly used as a reductant for extraction from a metal oxide such as Fe_2O_3 and carbon monoxide or dioxide is formed.[5] The thermodynamically stable oxides of carbon favour the production of the metal. In the case of metal sulfides, carbon is unsuitable for the reduction because the analogues, carbon sulfide and carbon disulfide, have only small free energies of formation.[5] Consequently the sulfidic ores are often roasted in air to convert them to metal oxides prior to the reduction step,[5] e.g.

$$ZnS + {}^3/_2O_2 \rightarrow ZnO + SO_2 \qquad \textbf{Equation 1.1}$$

$$ZnO + 2C \rightarrow Zn + 2CO \qquad \textbf{Equation 1.2}$$

Reducing agents are not always required. When copper sulfide is heated to a temperature of approximately 1300 °C, copper can be recovered by a two-stage process in air.[4]

$$2CuS + O_2 \rightarrow Cu_2S + SO_2 \qquad \textbf{Equation 1.3}$$

$$Cu_2S + O_2 \rightarrow 2Cu + SO_2 \qquad \textbf{Equation 1.4}$$

The driving force is therefore the thermodynamically favoured formation of sulfur dioxide.

The process based on Equation 1.3 and 1.4 was first used in copper smelting 6000 years ago.[2] Pyrometallurgy consequently came into being and has been the dominant branch of extractive metallurgy. It has been widely applied for the recovery of copper, iron, zinc, nickel and many other metals.[5] During the last century pyrometallurgy

underwent some significant development with the advance of science and engineering.[3] This was spurred by not only the increasing demands for the commonly used metals mentioned above, but also the exotic metals such as titanium, uranium, zirconium and niobium which were required for the nuclear and space applications.[3]

Pyrometallurgy, as a mature technology, is most economically successful when used for high-grade ores on extremely large scales.[6] However, it has some unavoidable disadvantages.[6] Large amounts of fossil fuels are required for the high energy consumption due to the high temperature involved.[6] Toxic gases such as SO_2 and greenhouse gases such as CO_2 are emitted, carrying fine dust.[6, 7] As a result pryrometallurgy has become undesirable with the wakening awareness of the environmental and global-warming effects and the tightening regulations.[6, 7] Also the technique cannot efficiently process complex or low-grade ores which are of increasing importance to extend the lifetimes of reserves.[6] Consequently other techniques such as hydrometallurgy have been developed and gained more attention in recent years.

1.3 Hydrometallurgy

Hydrometallurgy involves the processing of an ore or a secondary source of metal by the dissolution, concentration, separation, purification, reduction and precipitation of the dissolved metal using aqueous solutions.[1, 4, 6] As the following sections will show, hydrometallurgy can overcome many of the environmental and technical problems associated with pyrometallurgy.[6] The much lower temperatures involved in solution processing significantly decrease energy consumption and costs.[1, 6] Sulfidic ores can be treated without the release of SO_2 and fewer fuels are utilized to avoid generating greenhouse gases.[1, 6] Low-grade ores, transition ores, mixed metal ores and waste streams have the potential to be extracted by hydrometallurgical methods.[1, 6]

The beginning of hydrometallurgy may be marked by the discovery of aqua regia in the 8th century[6] which is a mixture of HCl and HNO_3 to dissolve gold. In the 16th century heap leaching of copper was practised in Rio Tinto, Spain and Harz mountain area, Germany.[6] Pyrite containing copper sulfide was exposed to rain and air for months to allow oxidation and dissolution of copper, and the resulting solution was used to precipitate metallic copper by scrap iron.[6] The birth of modern hydrometallurgy dates back to 1887 when two important processes were invented, the cyanidation process for gold and silver recovery and the Bayer process for the production of aluminium.[6] The cyanidation process was based on the leaching of gold by an alkaline cyanide solution and the precipitation by zinc dust.[6, 8]

$$4Au + 8CN^- + 2H_2O + O_2 \rightarrow 4[Au(CN)_2]^- + 4OH^- \quad \textbf{Equation 1.5}$$

$$2[Au(CN)_2]^- + Zn \rightarrow [Zn(CN)_4]^{2-} + 2Au \quad \textbf{Equation 1.6}$$

The reactions in Equation 1.4 and 1.5 are complicated processes and the chemistry involved is still under investigation.[1, 6] Despite the toxicity of cyanide solutions, the cyanide leaching remains the most widely used technique for both Au and Ag recovery at present.[1] The Bayer process leaches the ore bauxite (AlO(OH)) with sodium hydroxide solution above its boiling point in a pressure reactor.[5, 6] After separating insoluble materials, the solution is then seeded to precipitate pure crystalline aluminum hydroxide which was calcined (1250 °C) to generate pure Al_2O_3 suitable for electrolytic reduction cell.[5, 6]

$$AlO(OH) + OH^- + H_2O \rightarrow Al(OH)_4^- \quad \textbf{Equation 1.7}$$

$$2Al(OH)_3 \rightarrow Al_2O_3 + 3H_2O \quad \textbf{Equation 1.8}$$

The Bayer process based on Equation 1.7 and 1.8 is still used in its original form.[6] During the last century, the development of hydrometallurgy has made significant

progress.[6, 9] One of the milestones is the first application of liquid-liquid solvent extraction for the recovery of uranium in the 1940s.[6] The technique was introduced in connection with the Manhattan Project aiming to produce an atomic bomb.[10] Since then solvent extraction has proved to be a robust and flexible technique for metal recovery from aqueous solutions, and widely applied for uranium,[11] plutonium,[11] thorium,[11] gold,[12] platinum group metals,[13] copper,[9] zinc,[14] nickel,[15] cobalt,[15] *etc.*

A hydrometallurgical process typically consists of unit operations of leaching, separation, concentration and reduction as shown in Figure 1.1, which are further discussed.

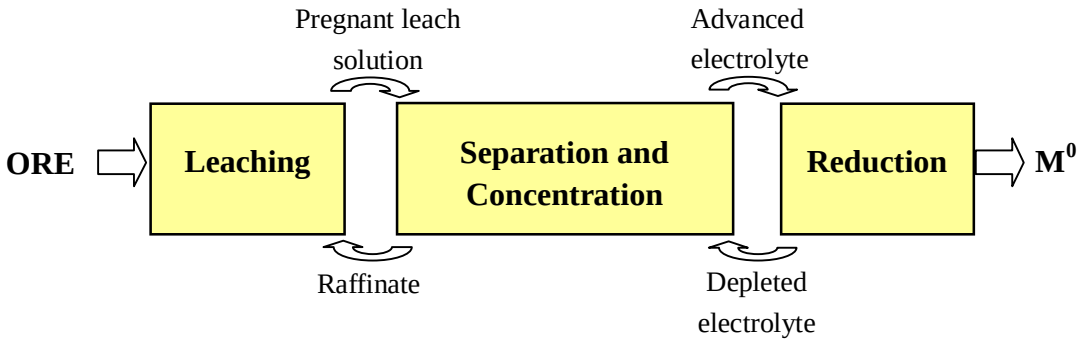

Figure 1.1 A simplified flowsheet for a hydrometallurgy process

1.3.1 Leaching

Leaching is the primary process in hydrometallurgy which transfers the metal values from a solid material into an aqueous solution by the action of a lixiviant.[1] Leaching can be applied to ores, metal scraps, spent catalysts, pyrometallurgically derived intermediates, by-products from metal refining and so on.[1] There are many physical, chemical and biochemical techniques and engineering involved, and the leaching agents can be water, acids such as H_2SO_4, HCl, HNO_3 and aqua regia, bases such as NaOH and NH_3, aqueous salt solutions of $FeCl_3$, Na_2CO_3, NH_4Cl and so on.[6] From

the point of view of chemistry, leaching processes can be divided into two categories, those in which the metals remain the formal oxidation states and those where dissolution is accompanied by a redox reaction.[1] The most relevant and commonly used processes will be discussed.

1.3.1.1 Leaching into Sulfate Media

As mentioned above, the heap leaching of copper ores is a process established 500 years ago to generate the feed solution in sulfate media for the metal recovery.[6] In the 1950s, the Moa Bay plant first commercially applied acid pressure leaching of limonitic nickel ores.[1, 6] Since then sulfuric acid leaching under atmosphere or high pressure has been utilized for the recovery of copper,[16-18] zinc,[14] nickel[19, 20] and cobalt.[19, 20] The non-oxidative leaching can be used for oxidic ores as shown in Equation 1.9.

$$MO + H_2SO_4 \rightarrow MSO_4 + H_2O \qquad \textbf{Equation 1.9}$$

One of the applications is the leaching of the lateritic ores which represent *ca.* 70% of the world's nickel reserves and are also major resources for cobalt.[20] These oxidic ores are located close to the surface and can be mined at a significantly lower cost than sulfidic ores from which the majority of nickel is extracted.[1] The limonitic laterites are rich in iron contents, and sulfuric acid leaching can efficiently reduce the iron to nickel ratio by precipitating iron as hematite and regenerate the consumed acid in Equation 1.10 and 1.11.[19, 20]

$$FeOOH + 3H^+ \rightarrow Fe^{3+} + 2H_2O \qquad \textbf{Equation 1.10}$$

$$2Fe^{3+} + 3H_2O \rightarrow Fe_2O_3 + 6H^+ \qquad \textbf{Equation 1.11}$$

Oxidative pressure acid leaching is often applied to sulfidic ores, e.g. chalcopyrite ($CuFeS_2$) as shown in Equation 1.12 and 1.13.[16-18] The products depend on the reaction conditions such as the pressure and temperature.[17, 18] Copper is leached as a sulfate salt and iron is precipitated as hematite. In the partial oxidation at lower temperature, elemental sulfur is formed in Equation 1.12, and the total oxidation at higher temperature converts sulfur to sulfate in Equation 1.13.[17] In both cases the emission of H_2S or SO_2 is avoided.

$$2CuFeS_2 + 2.5O_2 + 2H_2SO_4 \rightarrow 2CuSO_4 + Fe_2O_3 + 4S + 2H_2O \quad \textbf{Equation 1.12}$$

$$2CuFeS_2 + 8.5O_2 + 2H_2SO_4 \rightarrow 2CuSO_4 + Fe_2O_3 + 2H_2SO_4 \quad \textbf{Equation 1.13}$$

1.3.1.2 Leaching into Chloride Media

Chloride leaching was first applied in the production of platinum group metals (PGM) when a process was established in 1810 to dissolve raw materials containing platinum values in aqua regia.[21] The resulting hexachloroplatinate was then precipitated by ammonium chloride and further purified.[21] This breakthrough laid the foundation of modern PGM production and chloride hydrometallurgy.[21] The aqua regia leaching is still used at present, along with other chloride leaching techniques for the recovery of PGM.[22, 23]

Chloride leaching has been gradually applied to base metal recovery in recent years due to its efficiency.[14, 24-26] The metal values can be transferred into aqueous chloride media by either an oxidative or non-oxidative lixiviant. The latter usually consists of a high strength brine containing HCl which dissolves the metal ore as shown in Equation 1.14.[27]

$$MO + 2HCl \rightarrow MCl_2 + H_2O \quad \textbf{Equation 1.14}$$

The mechanism has been suggested to involve the adsorption of HCl onto the surface of the ore,[28-30] which is demonstrated by the leaching of copper oxide in Equation 1.15 and 1.16.[27]

$$CuO + HCl \rightarrow Cu(OH)Cl \qquad \textbf{Equation 1.15}$$

$$Cu(OH)Cl + HCl \rightarrow CuCl_2 + H_2O \qquad \textbf{Equation 1.16}$$

Consequently the non-oxidative chloride leaching is very effective in high strength brines because the adsorption of HCl is highly efficient due to the elevated proton activity.[31] The presence of metal salts significantly reduces the water activity and therefore increases the proton activity,[32] which makes the leaching remarkably effective.

The oxidative chloride leaching has recently drawn more interest as it can be the ideal technique for sulfidic ores.[1] The oxidative lixiviant, e.g. $FeCl_3$, efficiently transfers the metal value into chloride media and generates elemental sulfur as a by-product in Equation 1.17.

$$MS + 2FeCl_3 \rightarrow MCl_2 + 2FeCl_2 + S \qquad \textbf{Equation 1.17}$$

Common oxidants also include Cl_2 and $CuCl_2$. The latter is particularly effective because Cu(I) forms stable chloride complexes which drive the reaction to the reduction of Cu(II).[31] Ferric and cupric oxidants are more efficient in chloride media than sulfate media due to more favourable redox couples.[31]

These oxidative leaching processes are proposed to be acid catalyzed, involving the initial dissolution of sulfur as H_2S and the following oxidation to elemental sulfur as shown in Equation 1.18 and 1.19.[33] This mechanism is supported by investigations

on the morphology of the deposited sulfur and the dependence of leaching rate on the proton activity.[33]

$$MS + 2HCl \rightarrow MCl_2 + H_2S \qquad \textbf{Equation 1.18}$$

$$H_2S + 2FeCl_3 \rightarrow 2FeCl_2 + 2HCl + S \qquad \textbf{Equation 1.19}$$

1.3.1.3 Bioleaching

The use of bioleaching is considered to go back thousands of years in China, Spain, Sweden, Germany and so on.[34, 35] However, it was not recognized until the 1950s that microorganisms were involved in bioleaching.[34] Since the early 1980s, bioleaching of sulfidic ores has particularly received much attention.[1, 35, 36] In the last decade, it has become an established technique for the recovery of metals such as copper, cobalt, nickel, zinc and uranium.[17, 25, 35, 36] The major application of bioleaching today is the recovery of copper from low grade ore.[34] The process pulverizes and piles the ore into heaps sprinkled with sulfuric acid, which promotes the activity of endogenous acidophilic microorganisms that oxidize ferrous iron and sulfur present in the ores using the energy gained for growth.[34] The ferric iron produced in these reactions then oxidizes Cu(I) in the ore to the more soluble Cu(II) form which enters the sulfuric acid solution.[34] Two different reaction mechanisms control the dissolution of metal sulfides: the thiosulfate and the polysulfide pathways.[35] At present about 10-15% of the world's copper production is recovered by this technique.[34] It is reasonable to believe that a wider range of applications will be realized with better understanding of the involved reactions and the advance of biological techniques.

1.3.2 Separation and Concentration

A variety of techniques can be applied to separate and concentrate target metals from other materials in aqueous solutions for hydrometallurgical recovery of metal values.[1]

Selective crystallization is used to produce pure aluminum hydroxide from the pregnant leach solution in the Bayer process as mentioned above.[5, 6] Lead can be separated from other base metals by controlling the temperature and chloride activity to crystallize $PbCl_2$ out of the aqueous solution.[32, 33]

Selective precipitation is often employed to remove iron(III) by adjusting the pH in the recovery processes of metals such as zinc,[14] nickel,[37, 38] cobalt[37, 38] and so on. Precipitation also plays a key role in the purification of platinum group metals.[21]

Selective reduction is another technique which has been widely applied in extractive metallurgy for a long time, e.g. the cementation of copper by addition of scrap iron to aqueous solutions of copper(II) salts,[1, 6] or the use of zinc dust to reduce gold and silver[6, 8] as mentioned above.

Selective adsorption of ions or complexes onto solid materials can also achieve the separation and concentration of desired metal values. Activated carbon is used for the adsorption of cyanogold(I) complexes.[6] Ion exchange resins have been studied for the hydrometallurgical applications in recovering metals such as gold,[39] uranium,[40] zinc,[40] nickel,[41] cobalt,[41] *etc.*

Selective solvent extraction of metal values into water-immiscible phases is preferred for treating moderately concentrated feeds due to its transport efficiency and

capacity.[1] The application of this technique has been rapidly expanding in recent years,[11-15] and will be further discussed in section 1.4.

1.3.3 Reduction

The ability to reduce metal values using relatively clean methods which do not require large amounts of heat and carbon is one of the most desirable features of hydrometallurgy. The process can be achieved by chemical reduction, e.g. the use of hydrogen in the production of base metals,[42, 43] or more often electrolytic reduction known as electrowinning which has been applied for the recovery of various metals such as copper, zinc, cadmium, manganese, chromium, nickel, cobalt, antimony, gold, silver, tellurium, *etc*.[6, 44-48]

In electrowinning processes, inert electrodes are immersed in the aqueous solution and a direct current is passed.[6] The metal cation is usually reduced and deposited on the cathode as shown in Equation 1.20. The anodic reaction depends on the electrolytes in the solution. In sulfate media, the electrolysis of water in Equation 1.21 occurs and generates oxygen, while chlorine gas is produced from chloride media as shown in Equation 1.22.

$$M^{n+} + ne^- \rightarrow M \qquad \textbf{Equation 1.20}$$

$$H_2O \rightarrow 0.5O_2 + 2H^+ + 2e^- \qquad \textbf{Equation 1.21}$$

$$2Cl^- \rightarrow Cl_2 + 2e^- \qquad \textbf{Equation 1.22}$$

Electrowinning from sulfate media is a well-established technique conventionally used in the hydrometallurgical industry.[44-48] In theory, metals must have reduction potentials more positive than that of proton to be preferentially discharged on the cathode.[6] However, due to the phenomenon of overpotential, metals such as zinc

with reduction potentials slightly lower than that of proton can still be deposited.[6] Another factor to determine whether a metal can be deposited from aqueous solution is the hydration of the metal cation.[6] Some metals, particularly beryllium and aluminum, are strongly hydrated due to the small sizes and large positive charges of the ions. Consequently the reduction potential of the metal is much less positive than that of proton and electrolysis of water occurs instead at the cathode.[6] Eletrowinning from sulfate media generally produce metal deposits in desirable uniform sheets.[44-48] The morphology can be affected by the conditions such as impurities, current density, the concentrations of electrolytes and so on.[47-49]

Electrowinning from chloride media has not been commercially applied, mainly due to the difficulty of handling chlorine gas and the undesirable structure of the deposited metal. Electrolytic reduction of zinc in chloride media was reported to give a sponge-like product.[50] However, this technique has many potential advantages. The cathode reactions are usually more reversible in chloride than in sulfate solutions due to the possible mechanism via an adsorbed chloride species.[51] Electrical conductivity is high, resulting in low energy consumption for electrolysis.[51] Cobalt can give a better metallic product in chloride media than the nodular deposit from sulfate solution.[51] In the case of zinc, the electrolytic cell developed in the Zinclor process is proven to produce smooth zinc plates with a careful selection of operating conditions.[52, 53]

1.4 Solvent Extraction

Many processes and reagents have been developed on a large scale using liquid-liquid solvent extraction techniques to achieve hydrometallurgical recovery of metal values. Based on the target species, solvent extraction processes can be classified into three categories: cation, anion, or metal salt transport, which will be

discussed in detail. The extractants involved in the following sections are listed in Table 1.1.

Category	Reagent	Structure
Cation transport	P50	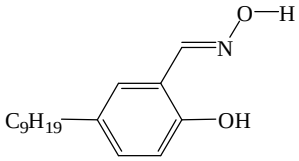
	D2EHPA	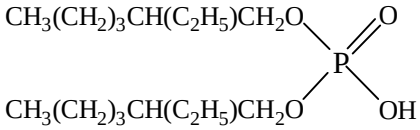
Metal salt transport	CLX50	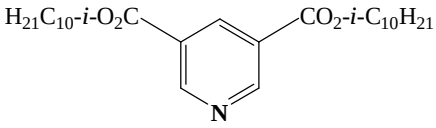
	DBBP	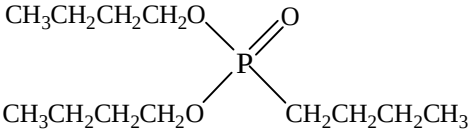
Anion transport	TOA	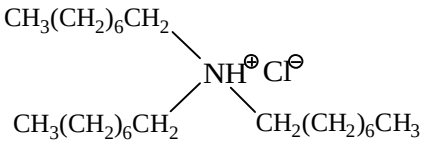

Table 1.1 Examples of cation, anion or metal salt extractants

1.4.1 Cation Transport

Metal cation can be extracted from an aqueous solution into an organic phase by displacing another cation (usually a proton) from the extractant to form an electrically neutral complex, e.g. the extraction of base metal cations by weak organic acids in Equation 1.23.

$$2LH_{(org)} + M^{2+} \rightarrow L_2M_{(org)} + 2H^{+} \qquad \textbf{Equation 1.23}$$

Phenolic oximes such as 5-nonylsalicylaldoxime (P50) in Table 1.1 are commercially successful cation extractants which account for 20-30% of the world's copper production.[54, 55] In non-polar organic solvents hydroxyoxime molecules display the association through intermolecular hydrogen bonds between the oximic hydrogen and phenolic oxygen atoms,[56-59] which provide the ideal pre-organised geometry for complexation of a square planar Cu(II) ion as shown in Figure 1.2.

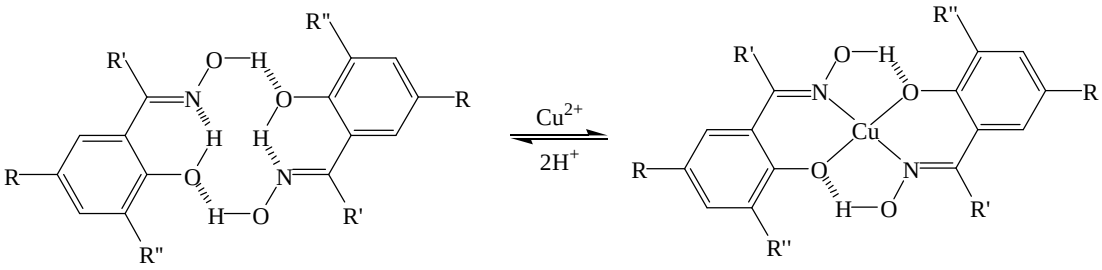

Figure 1.2 Extraction of Cu(II) cation by phenolic oxime *pseudo*-macrocycle

A simplified flowsheet for the hydrometallurgical production of copper from oxidic ores by phenolic oximes is shown in Figure 1.3.[1] The non-oxidative sulfate leaching is utilized to transfer copper(II) into the aqueous solution. The extraction and stripping equilibrium is pH-dependent, which is termed a "pH-swing" process.[1] The metal value is extracted into the organic solvent, usually kerosene,[6] at higher pH. By contacting the loaded organic phase with an aqueous sulfate solution of lower pH, the Cu^{2+} ions are stripped into the aqueous phase as a pure $CuSO_4$ electrolyte, and the extractant is regenerated in the organic phase for continuous extraction and stripping cycles.[9] Subsequent electrowinning generates conductivity grade copper and sulfuric acid to be reused in the stripping stage.[9] The overall equation in Figure 1.3 indicates the excellent material balance of the process, which ensures both its commercial and environmental success as a method for recovering copper.[55]

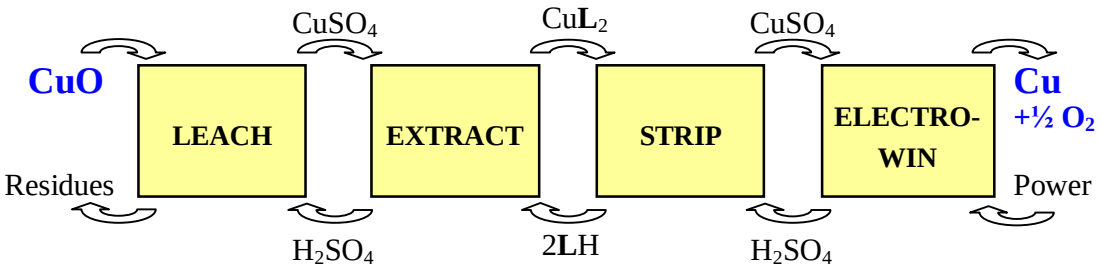

- Leach: $CuO_{(s)} + H_2SO_4 \rightarrow CuSO_4 + H_2O$
- Extract: $CuSO_4 + 2\mathbf{L}H_{(org)} \rightarrow Cu\mathbf{L}_{2(org)} + H_2SO_4$
- Strip: $Cu\mathbf{L}_{2(org)} + H_2SO_4 \rightarrow CuSO_4 + 2\mathbf{L}H_{(org)}$
- Electrowin: $CuSO_4 + H_2O \rightarrow Cu_{(s)} + ½O_{2(g)} + H_2SO_4$

- Overall: $\mathbf{CuO_{(s)} \rightarrow Cu_{(s)} + ½O_{2(g)}}$

Figure 1.3 Hydrometallurgical recovery of copper from oxidic ores by phenolic oximes

Another successful application of cation transport involves the use of the organophosphorus acids such as di-(2-ethylhexyl)phosphoric acid (D2EHPA) in Table 1.1 for the hydrometallurgical recovery of zinc. The strong interligand hydrogen bonds result in the formation of 8-membered rings in Figure 1.4, which are preserved when metal complexes are formed.[60]

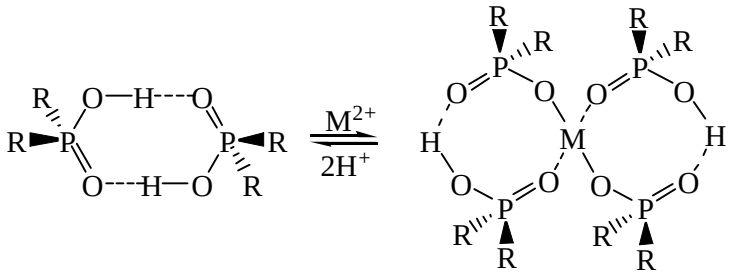

Figure 1.4 Extraction of M^{2+} cation by an organophosphorus acid to form chelated complexes

The bite angle in the 8-membered *pseudo*-macrocycle favours metal cations with tetrahedral coordination geometries such as Zn^{2+}.[60] The Skorpion project in Namibia uses D2EHPA as the extractant to recover zinc from silicate ores in a flowsheet similar to that in Figure 1.3, and produces *ca.* 150,000 metric tons special high grade zinc per annum.[14]

The process in Figure 1.3 achieves remarkable material balance for the copper recovery from oxidic ores. However, this is not the case when recovering copper from sulfidic ores as shown in Figure 1.5.

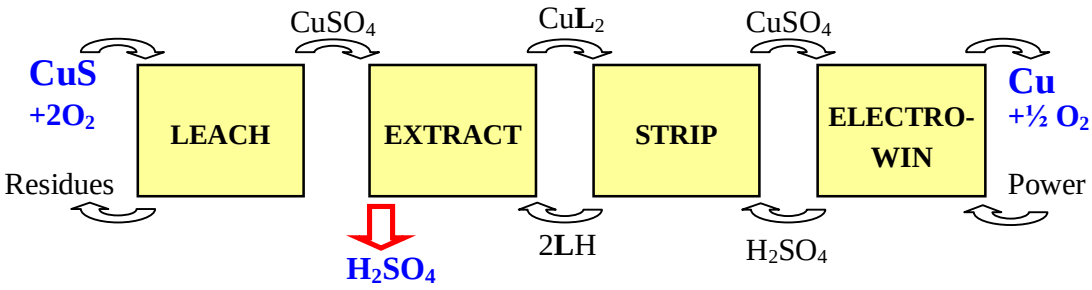

- Leach: $CuS_{(s)} + 2O_{2(g)} \rightarrow CuSO_4$
- Extract: $CuSO_4 + 2\mathbf{L}H_{(org)} \rightarrow Cu\mathbf{L}_{2(org)} + \mathbf{H_2SO_4}$
- Strip: $Cu\mathbf{L}_{2(org)} + H_2SO_4 \rightarrow CuSO_4 + 2\mathbf{L}H_{(org)}$
- Electrowin: $CuSO_4 + H_2O \rightarrow Cu_{(s)} + ½O_{2(g)} + H_2SO_4$

- **Overall:** $\mathbf{CuS_{(s)} + 3/2O_{2(g)} + H_2O \rightarrow Cu_{(s)} + H_2SO_4}$

Figure 1.5 Hydrometallurgical recovery of copper from sulfidic ores by phenolic oximes.

The oxidative sulfate leaching is used as discussed in section 1.3.1.1. Consequently one mole of sulfuric acid is generated per mole of copper extracted and is not consumed in the leaching stage. The acid built up in the front end of the circuit must

be recovered by a costly process or neutralised with base, generating a waste salt which again must be removed. To overcome this problem, a metal salt extractant could be used instead to transport the sulfuric acid in the form of sulfate. Chloride leaching followed by processing in chloride media is another option, which will be discussed in the following section.

1.4.2 Metal Salt Transport

Metal salt extractants are neutral species which impart stability and organic phase solubility to metal salts by the displacement of water molecules in the coordination sphere and hence transfer the target species into the organic solution.[1] Base metal chlorides can be extracted by weak bases with soft organic donors as shown in Equation 1.24.

$$MCl_2 + 2L_{(org)} \rightarrow L_2MCl_{2(org)} \qquad \textbf{Equation 1.24}$$

Metal salt transport of copper in chloride media has been developed in the CUPREX process to overcome the problems associated with sulfidic ores mentioned above.[1] The ester-substituted pyridine ligand CLX50 (see Table 1.1) is applied to recover $CuCl_2$ as shown in Figure 1.6.[1] The oxidative ferric chloride leaching is employed to transfer the metal value into chloride solution and generate sulfur as a by-product, which avoids the emission of SO_2 and the building up of sulfuric acid. The control of extraction and stripping involves a "chloride swing" process based on the activity of Cl^- in the aqueous solution. The $CuCl_2$ salt is loaded by the extractant at high Cl^- activity, and stripped into an aqueous solution of low Cl^- activity to generate a pure $CuCl_2$ electrolyte with the extractant regenerated in the organic phase for continuous extraction and stripping cycles. Electrowinning subsequently produce metallic copper and chlorine gas which is used to regenerate ferric chloride for the leaching

stage. Compared to sulfate-based processes, the CUPREX process fulfils current requirement for clean technology without disposal of waste.[1]

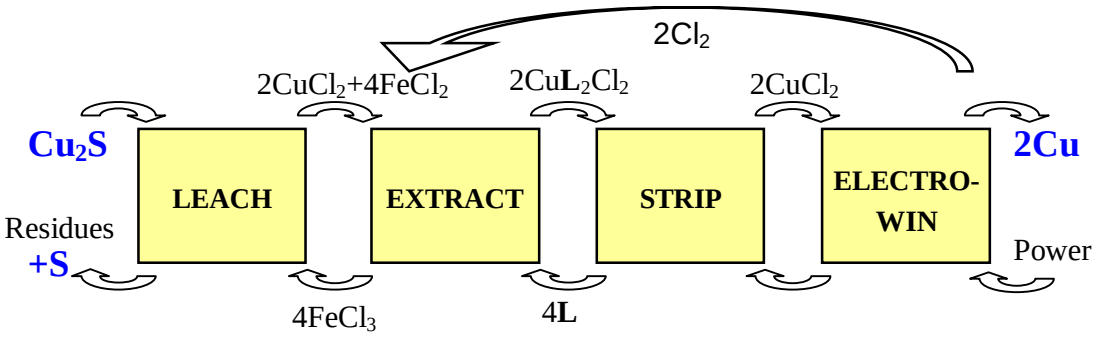

- Leach: $Cu_2S_{(s)} + 4FeCl_3 \rightarrow 2CuCl_2 + 4FeCl_2 + S_{(s)}$
- Extract: $2CuCl_2 + 4\mathbf{L}_{(org)} \rightarrow 2Cu\mathbf{L}_2Cl_{2(org)}$
- Strip: $2Cu\mathbf{L}_2Cl_{2(org)} \rightarrow 2CuCl_2 + 4\mathbf{L}_{(org)}$
- Electrowin: $2CuCl_2 \rightarrow 2Cu_{(s)} + 2Cl_{2(g)}$
- Regeneration: $4FeCl_2 + 2Cl_{2(g)} \rightarrow 4FeCl_3$

- Overall: $\mathbf{Cu_2S_{(s)} \rightarrow 2Cu_{(s)} + S_{(s)}}$

Figure 1.6 Hydrometallurgical recovery of copper from sulfidic ores by CLX50 in the CUPREX process

Extractants with P=O donors such as dibutyl butyl phosphonate (DBBP) in Table 1.1 have been investigated for the zinc recovery from sulfidic ores in the ZINCLOR process.[14] DBBP extracts zinc chloride species in a similar flowsheet to that in Figure 1.6.[14] Zn(II) can be separated from Fe(II) with a separation factor of more than 10^3.[14] The electrowinning process is reported to consume low energy due to high current efficiency and low cell voltage.[14]

1.4.3 Anion Transport

An anionic metal complex, usually chlorometallate, can be transferred from an aqueous solution by the displacement of another anion in the organic phase, e.g. the extraction of chlorometallates by alkyl ammonium chloride salts in Equation 1.25.[1] The electrostatic and hydrogen bonding interactions between the ligand and the chlorometallate complex are of great importance in anion transport.[1]

$$[MCl_4]^{2-} + 2[R_4N]Cl_{(org)} \rightarrow [R_4N]_2[MCl_4]_{(org)} + 2Cl^- \qquad \textbf{Equation 1.24}$$

One of the most successful applications involving anion transport is the Falconbridge Nikkelverk refinery in Norway which employs the Chlorine Leach Process (CLP) using tri-n-octylamine hydrochloride (TOA) in Table 1.1 to separate cobalt from nickel in chloride media as shown in Figure 1.7.[61-63] This process applies a copper-catalysed oxidative chloride leaching in which Cl_2 is consumed as the oxidant to transfer the nickel and cobalt values into aqueous solution and generate elemental sulfur.[61-63] The pregnant leach solution is contacted with excess "matte" (nickel and cobalt sulfides) to remove copper and platinum group metals by the precipitation of sulfides which are later recovered by hydrometallurgical processes.[61-63] Iron is removed by the addition of nickel carbonate to raise the pH and precipitate iron(III) hydroxides.[61-63] Cobalt is then extracted as the tetrachlorocobaltate complex $[CoCl_4]^{2-}$ by TOA and stripped into an aqueous solution to generate a $CoCl_2$ electrolyte.[61-63] After the removal of all the above impurities, the nickel chloride solution is used for electrowinning to produce metallic nickel.[61-63] The CLP has expanded the Nikkelverk plant into one of the world's largest cobalt-nickel refineries.[64]

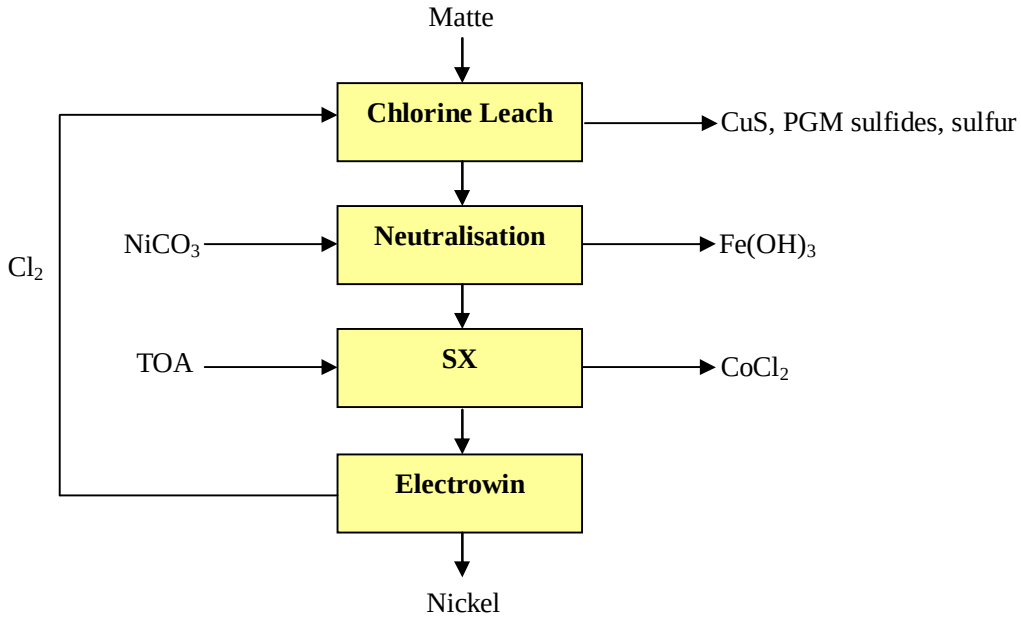

- Leach: $2Cu^{+} + Cl_{2(g)} \rightarrow 2Cu^{2+} + 2Cl^{-}$

  $Ni_3S_{2(s)} + 2Cu^{2+} \rightarrow 2NiS_{(s)} + Ni^{2+} + 2Cu^{+}$

  $NiS_{(s)} + 2Cu^{2+} \rightarrow Ni^{2+} + 2Cu^{+} + S_{(s)}$

  $Cu_2S_{(s)} + S_{(s)} \rightarrow 2CuS_{(s)}$
- Extract: $[CoCl_4]^{2-} + 2[R_4N]Cl_{(org)} \rightarrow [R_4N]_2[CoCl_4]_{(org)} + 2Cl^{-}$
- Strip: $[R_4N]_2[CoCl_4]_{(org)} \rightarrow CoCl_2 + 2[R_4N]Cl_{(org)}$
- Electrowin: $CoCl_2 \rightarrow Co_{(s)} + Cl_{2(g)}$

  $NiCl_2 \rightarrow Ni_{(s)} + Cl_{2(g)}$

Figure 1.7 A simplified flowsheet of the Chlorine Leach Process used in the Falconbridge refinery[61-63]

1.5 Reagent Design Criteria

The focus of this thesis is to develop novel extractants for the hydrometallurgical recovery of base metals. A viable extractant must be designed to meet various requirements such as synthesis, stability, solubility, strength, efficiency, selectivity,

etc, and references to these criteria will be made in the following chapters.

In chapter 2, the potential of salicylaldehyde hydrazones as cation extractants for copper recovery is investigated. Substituent effects, e.g. electronic, steric and particularly "buttressing" of ligand-ligand hydrogen bonding, are utilised to tune the strength and efficacy of the extractants.

Chapter 3 considers metal salt extractants and deals with the development of polytopic salicylaldimine ligands bearing pendant tertiary amine groups for the hydrometallurgical recovery of zinc chloride. The polytopic ligands achieve remarkably high transport efficiency of zinc chloride, which is investigated and explained by a proposed mechanism involving the extraction of both zinc cation and chlorozincate anion species.

Chapter 4 focuses on the anion binding and selectivity in solvent extraction involving simple anions and chlorometallates by the polytopic ligands discussed in chapter 3 and their metal complexes.

In summary, new solvent extractants are developed in this thesis for potential industrial application, and ligand design features are addressed to control the strength, transport efficiency and selectivity of the extractants.

1.6 References

1. P. A. Tasker, P. G. Plieger and L. C. West, "Comprehensive Coordination Chemistry II", Elsevier Ltd, Oxford, 2004.
2. D. F. Shriver and P. W. Atkins, "Inorganic Chemistry", Oxford University Press, Oxford, 2006.
3. H. H. Kellogg, Y. K. Rao and S. W. Marcuson, *Annual Review of Physical Chemistry*, 1976, **27**, 387-406.
4. M. J. Nicol, C. A. Fleming and J. S. Preston, *Comprehensive Coordination Chemistry*, 1987,

6, 779-942.

5. T. W. Swaddle and Editor, "Inorganic Chemistry: An Industrial and Environmental Perspective", Academic Press, London, 1996.
6. F. Habashi, "A Textbook of Hydrometallurgy", Quebec, 1994.
7. M. Dimitrijevic, A. Kostov, V. Tasic and N. Milosevic, *Journal of Hazardous Materials*, 2009, **164**, 892-99.
8. A. Cottrell, "An Introduction to Metallurgy", Edward Arnold Ltd, London, 1975.
9. J. Szymanowski, "Hydroxyoximes and Copper Hydrometallurgy", CRC Press, London 1993.
10. F. Habashi, *Hydrometallurgy*, 2005, **79**, 15-22.
11. C. K. Gupta and T. K. Mukherjee, "Hydrometallurgy in extraction processes", CRC Press, Boca Raton, US, 1990.
12. G. A. Kordosky, J. M. Sierakoski, M. J. Virnig and P. L. Mattison, *Hydrometallurgy*, 1992, **30**, 291-305.
13. F. L. Bernardis, R. A. Grant and D. C. Sherrington, *Reactive & Functional Polymers*, 2005, **65**, 205-17.
14. A. Deep and J. M. R. de Carvalho, *Solvent Extraction and Ion Exchange*, 2008, **26**, 375-404.
15. T. Zhu, *Mineral Processing and Extractive Metallurgy Review*, 2000, **21**, 1-24.
16. F. Habashi, *Journal of Mining and Metallurgy, Section B: Metallurgy*, 2007, **43**, 1-19.
17. S. Wang, *JOM*, 2005, **57**, 48-51.
18. D. Dreisinger, *Hydrometallurgy*, 2006, **83**, 10-20.
19. D. H. Rubisov, J. M. Krowinkel and V. G. Papangelakis, *Hydrometallurgy*, 2000, **58**, 1-11.
20. G. K. Das, S. Acharya, S. Anand and R. P. Das, *Hydrometallurgy*, 1995, **39**, 117-28.
21. H. Renner, "Platinum Group Metals and Compounds", Wiley-VCH, New York, 2005.
22. M. H. H. Mahmoud, *JOM*, 2003, **55**, 37-40.
23. F. K. Letowski and R. E. G. Robinson, "Acidic chloride leaching for recovery of precious metals from ore concentrates", 1993.
24. J.-M. Lalancette, "Recovery of nonferrous and precious metals from ores and wastes by chlorination leaching", 2002.
25. R. G. McDonald and B. I. Whittington, *Hydrometallurgy*, 2008, **91**, 56-69.
26. R. R. Moskalyk and A. M. Alfantazi, *Minerals Engineering*, 2002, **15**, 593-605.
27. G. Senanayake, *Minerals Engineering*, 2007, **20**, 634-45.
28. H. Majima, Y. Awakura and N. Misaki, *Metallurgical Transactions B: Process Metallurgy*, 1981, **12B**, 645-9.
29. Y. Awakura, S. Kamei and H. Majima, *Metallurgical Transactions B: Process Metallurgy*, 1980, **11B**, 377-81.
30. L. G. Sillen and E. A. Martell, "Stability Constants of Metal-Ion Complexes. " Chemical Society, London, 1964.
31. D. M. Muir, Chloride Metallurgy 2002, Montreal, Canada, 2002, 759-91.
32. G. Senanayake and D. M. Muir, Hydrometallurgy 2003, Vancouver, Canada, 2003, 517-31.
33. J. E. Dutrizac, *Hydrometallurgy*, 1992, **29**, 1-45.
34. D. S. Holmes, *Hydrometallurgy*, 2008, **92**, 69-72.
35. T. Rohwerder, T. Gehrke, K. Kinzler and W. Sand, *Applied Microbiology and Biotechnology*, 2003, **63**, 239-48.

36. G. J. Olson, J. A. Brierley and C. L. Brierley, *Applied Microbiology and Biotechnology*, 2003, **63**, 249-57.
37. T. Inami, K. Toyabe and T. Kanai, *Metallurgical Review of MMIJ*, 1984, **1**, 125-37.
38. S. Makino, M. Sugimoto, F. Yano and N. Matsumoto, EPD Congress 1996, Anaheim, US, 1996, 299-311.
39. V. S. T. Ciminelli, *JOM*, 2002, **54**, 35-36.
40. H.-J. Bart, *Hydrometallurgy*, 2005, **78**, 21-29.
41. F. D. Mendes and T. V. Berni, "Hydrometallurgical process for recovery of nickel and cobalt using ion exchange resins and pyrohydrolysis", 2009.
42. A. Agrawal, D. Bagchi, S. Kumari, V. Kumar and B. D. Pandey, *Materials Letters*, 2008, **62**, 2880-82.
43. M. Haemaelaeinen and O. Hyvaerinen, "Production of copper by the hydrometallurgical reduction of copper(I) oxide", 2005.
44. I. G. Sharma, P. Alex, A. C. Bidaye and A. K. Suri, *Hydrometallurgy*, 2005, **80**, 132-38.
45. E. Mostad, S. Rolseth and J. Thonstad, *Hydrometallurgy*, 2008, **90**, 213-20.
46. K. L. Hardee, L. M. Ernes and C. W. Brown, Jr., "Copper electrowinning", 2002.
47. L. Muresan, G. Maurin, L. Oniciu and D. Gaga, *Hydrometallurgy*, 1996, **43**, 345-54.
48. A. M. Alfantazi and A. Shakshouki, *Journal of the Electrochemical Society*, 2002, **149**, C506-C10.
49. D. J. MacKinnon, J. M. Brannen and P. L. Fenn, *Journal of Applied Electrochemistry*, 1987, **17**, 1129-43.
50. D. J. Mackinnon, J. M. Brannen and V. I. Lakshmanan, *Journal of Applied Electrochemistry*, 1979, **9**, 603-13.
51. R. Winand, *Hydrometallurgy*, 1991, **27**, 285-316.
52. E. D. Nogueira, L. A. Suarez-Infazon and P. Cosmen, Zinc 83, 13th Annual CanadaHydrometallurgical Meeting, Canada, 1983.
53. G. Diaz, J. M. Regife, C. Frias and F. Parrilla, *Publications of the Australasian Institute of Mining and Metallurgy*, 1993, **7/93**, 341-6.
54. P. J. Mackey, *CIM Magazine*, 2007, **2**, 35-42.
55. G. A. Kordosky, International Solvent Extraction Conference, Cape Town, South Africa, 2002, 853-62.
56. A. G. Smith, P. A. Tasker and D. J. White, *Coordination Chemistry Reviews*, 2003, **241**, 61-85.
57. P. O'Brien and J. R. Thornback, *Hydrometallurgy*, 1982, **8**, 331-9.
58. P. O'Brien, J. R. Thornback and J. Szymanowski, *Journal of Coordination Chemistry*, 1983, **13**, 11-15.
59. B. McCudden, P. Obrien and J. R. Thornback, *Journal of the Chemical Society-Dalton Transactions*, 1983, 2043-46.
60. M. J. Nicol, C. A. Fleming and J. S. Preston, *Comprehensive Coordination Chemistry II*, 1987, **6**, 779-842.
61. E. O. Stensholt, H. Zachariasen and J. H. Lund, *Transactions of the Institution of Mining and Metallurgy, Section C: Mineral Processing and Extractive Metallurgy*, 1986, **95**, C10-C16.
62. E. O. Stensholt, O. M. Dotterud, E. E. Henriksen, P. O. Ramsdal, F. Stalesen and E. Thune,

CIM Bulletin, 2001, **94**, 101-04.

63. E. O. Stensholt, H. Zachariasen, J. H. Lund and P. G. Thornhill, Extr. Metall. Nickel Cobalt, Proc. Symp. 117th TMS Annu. Meet., 1988, 403-12.

64. G. Van Weert, Chloride Metallurgy 2002, Montreal, Canada, 2002, 277-98.

CHAPTER 2

SALICYLALDEHYDE HYDRAZONES AS COPPER EXTRACTANTS

Content

2.1 Introduction

This chapter focuses on the hydrometallurgy of copper, and looks into the potential of salicylaldehyde hydrazones as copper extractants. A series of 3-substituted and N-substituted salicylaldehyde hydrazones in Figure 2.1 has been synthesized and studied. Electronic, steric and particularly hydrogen bonding effects of the substituents on the extractive properties of the ligands are reported. A comparison with salicylaldoxime reagents widely used by the mining industry is also provided.

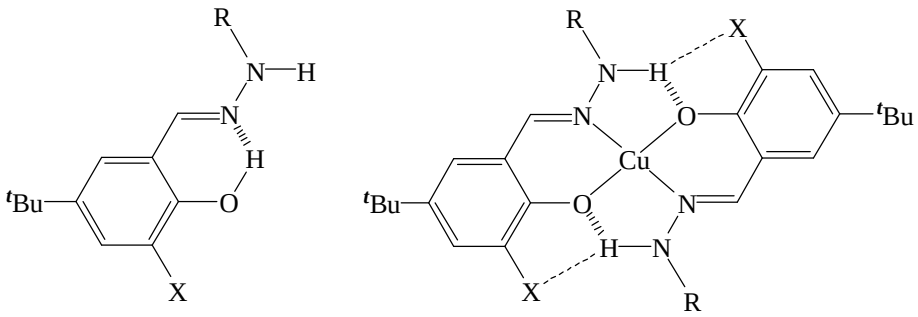

	L1	L2	L3	L4	L5	L6	L7	L8	L9	L10
X	H	Me	NO_2	Br	OMe	H	Me	NO_2	Br	OMe
R	Me	Me	Me	Me	Me	Ph	Ph	Ph	Ph	Ph

Figure 2.1 3-Substituted and N-substituted salicylaldehyde hydrazones studied as copper extractants in this chapter.

2.1.1 Copper

The use of copper by man has been significant over a long period of history,[1] and the current demand continues to increase.[2] These are due to the unique and valuable properties of copper and its alloys.

Copper is a red lustrous metal which is believed to be the 22nd most abundant element[3] and present at 68 ppm[4] in the Earth's crust. It can be found in an extremely

pure native form for example in northern Michigan[1], but most commonly exists as chalcopyrite $CuFeS_2$ which accounts for about 50% of all copper deposits.[4] Copper is the 29th element in the periodic table and a paramagnetic transition metal with electronic configuration $3d^{10}4s^1$ and spin of s = ½. It has two stable isotopes ^{63}Cu and ^{65}Cu, and can be found in oxidation states of I to IV. It exhibits excellent conducting properties of both electricity and heat, second only to silver.[1] In high purity grade (>99.95%), it is soft, ductile and malleable. It has good corrosion resistance owing to the turquoise insoluble layer of hydroxycarbonate ($Cu(OH)_2.CuCO_3$) formed by oxidative weathering to retard further corrosion.[1, 3, 5] Copper can be alloyed to give stronger materials which are similarly lustrous and malleable, yet more resistant to corrosion than the native metals.[1, 3, 6] Brass is a coloured alloy with zinc, tuned from red to yellow by respectively the amount of zinc present (5-45%).[1] Bronze is formed by alloying copper and tin (<10%) and is even stronger and more corrosion resistant than brass.[1]

Consequently, copper was the first metal used extensively by the human race,[1] and hence the metallurgy of copper came into being and continued to develop. Artefacts dating back 10,000 years have been found in Iraq.[6] Pyrometallurgical processes were established as long as 6,000 years ago, as mentioned in chapter 1,[5] and bronze was used to make not only implements for hunting and fishing but also decorative items such as keepsakes and jewellery.[1] During 3,000 to 500 BC, the use of bronze achieved such importance that it gave the name "bronze age" to the era.[1] Subsequently the production of copper peaked during the Roman Empire (250-350 AD) and the Sung Dynasty of China (960-1127 AD),[7] and then massively increased with the advent of the industrial revolution until the present day.[7] In the modern age, copper and its alloys have established widespread applications which include building and construction, industrial and domestic electrical equipment, power generation and distribution, telecommunication, transportation and coinage.[8]

Compounds of copper are also used scientifically as catalysts and fungicides.[8, 9]

As a result of these extensive applications, the demand for copper has experienced an extraordinary increase in recent years. This increase in demand and market price has been fuelled particularly by the development of Asia-Pacific countries such as China and India.[10, 11] In 2006 the production of 15 million tonnes fell short of the global consumption of 17 million tonnes,[10] and market prices reached an all time high of $8,820 per metric tonne on the 6th of March 2008.[12] Such demand has led to the commencement of many new projects around the world to increase the global supply, and thus the price is expected to be stabilised within the decade.[10]

If the consumption continues to increase at current rates, commercially important global reserves could be exhausted within 30 to 60 years.[2, 11] A few options are available to address this problem. Recycling must be increased. Currently only *ca.* 53% of discarded copper is reused[2] and *ca.* 26% will never be recovered.[8] Recovery from secondary sources can be effectively achieved by hydrometallurgical processes.[13] Also, as mentioned in chapter 1, low grade ores should be exploited to extend the lifetimes of the reserves, which could be done by the development of new technologies, particularly hydrometallurgy.

In summary, as copper is of great importance to the sustainable development of the human race, the hydrometallurgical extraction and recycling of copper has recently received much attention because of its advantages over conventional pyrometallurgical processes.

2.1.2 Phenolic Oximes as Copper Extractants

Currently between 20-30% of the world's copper is produced by hydrometallurgical

methods using phenolic oxime extractants.[10, 14] The most common commercial variants of these ligands[13, 15] are shown in Table 2.1.

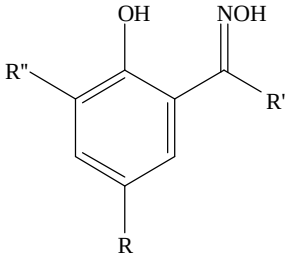

R	R'	R''	Commercial Name
C_9H_{19}	H	H	P50
C_9H_{19}	$C_6H_5CH_2$	H	P17
C_9H_{19}	CH_3	H	LIX84
$C_{12}H_{25}$	C_6H_5	H	LIX64
C_9H_{19}	C_6H_5	H	HS-LIX 65N
C_9H_{19}	C_6H_5	Cl	LIX70
$C_{12}H_{25}$	H	H	LIX860

Table 2.1 Structures of some phenolic oximes used in industry.[13, 15]

These extractants are cation exchange reagents as mentioned in chapter 1.

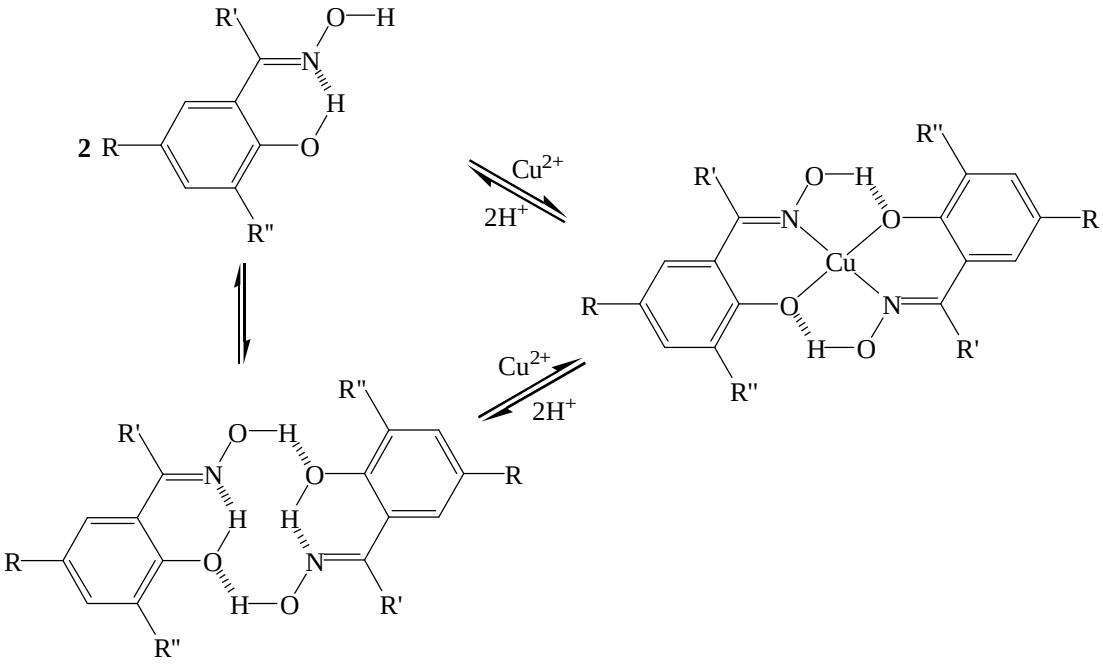

Figure 2.2 The pH-dependent complexation of copper(II) by phenolic oxime extractants

Deprotonation of the phenolic group allows metal complexation *via* the "pH swing" controlled equilibria in Figure 2.2.

Phenolic oximes have proved to be very commercially successful owing to the strength and selectivity in the recovery of copper(II), which can be assessed by determination of the metal loading as a function of pH.[15] A characteristic curve, known as an S-curve, is obtained by plotting the metal content in the organic phase as a percentage of the theoretical maximum based on the concentration of the extractant against the pH of the aqueous phase after equilibration. Extractant strength is defined by the $pH_{0.5}$ value[15] measured in the S-curve, the pH at which half of the ligand is loaded. A lower $pH_{0.5}$ corresponds to a stronger pH-swing extractant for a particular metal. The relative affinity of an extractant for different metal cations can be inferred from their $pH_{0.5}$ values. The strength and selectivity of 5-nonylsalicylaldoxime (P50 in Table 2.1) for the first transition series metals is illustrated in Figure 2.3.[15]

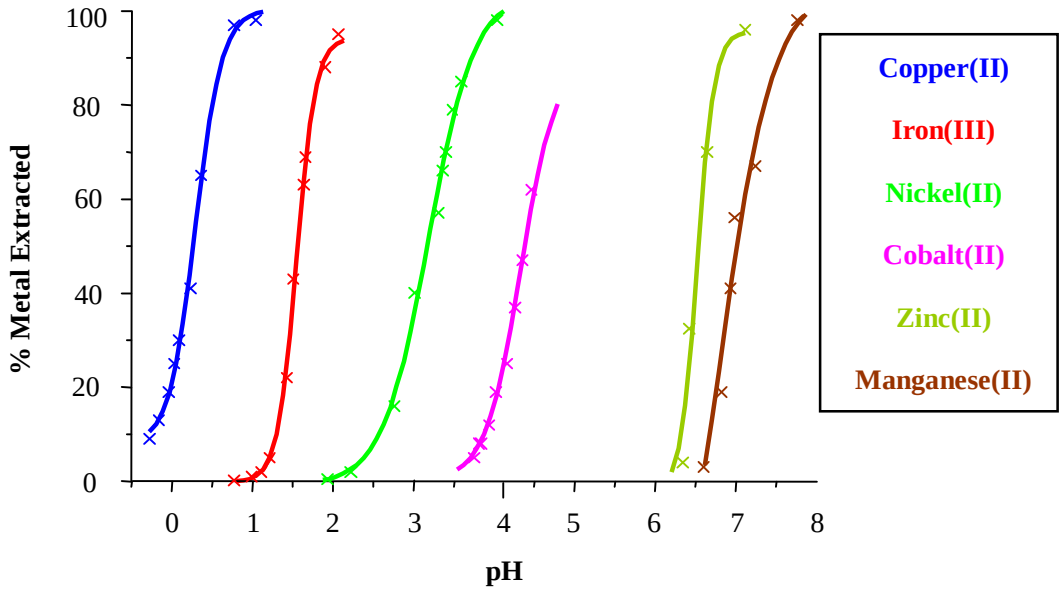

Figure 2.3 Loading S-curves for the first row transition metals by P50 (see Table 2.1) in kerosene.[15]

Clearly P50 is a strong extractant for Cu(II) and achieves excellent selectivity for copper over other first row transition metals. This is believed to arise from features of the structures shown in Figure 2.2. In non-polar organic solvents hydroxyoxime molecules display the association through intermolecular hydrogen bonds between the oximic hydrogen and phenolic oxygen atoms,[16-19] which provide the ideal pre-organised geometry for complexation of a square planar Cu(II) ion. In the neutral 2:1 complex formed, the 14-membered *pseudo*macrocyclic hydrogen bonded array imparts additional stability. The selectivity shown in Figure 2.3 is basically in accordance with the Irving-Williams series:[5, 20]

$$Ba^{2+} < Sr^{2+} < Ca^{2+} < Mg^{2+} < Mn^{2+} < Fe^{2+} < Co^{2+} < Ni^{2+} < Cu^{2+} > Zn^{2+}$$

Preference for copper(II) is supposedly due to the cavity size[15] (the mean distance of the donor atoms to the metal centre) which is close to an ideal radius for the Cu(II) ion.

In practice neat P50 proved to be slightly too strong for the copper to be released in the stripping process without use of strong acid which prompts hydrolysis of the ligand. Thus it is usually used as in blends with weaker phenolic oximes or with the addition of equilibrium modifiers. Much research has been done in industry and academia, including the Tasker group,[21] to investigate and tune the strength of the extractants shown in Table 2.1.

In principle variation of R, R' or R'' groups in the structure in Table 2.1 can be used to tune the strength. Alkyl groups as R groups do not change $pH_{0.5}$ values greatly,[15, 22] but highly branched alkyl groups impart higher solubility in the hydrocarbon diluents for industrial application. In general salicylaldoximes with R' = H are stronger extractants than ketoximes or benzophenone oximes where R' groups are alkyl or

aromatic groups.[15] The R" group has a unique and significant effect on extraction strength due to the *ortho*-position to the phenolic group, and a discussion in the case of salicylaldoximes follows.

2.1.3 Buttressing Effects in Salicylaldoxime Extractants

Generally, substituent effects on salicylaldoxime extractive efficacy arise from their electronic properties.[15, 23] Electron-withdrawing substituents such as halide and nitro groups make the ligands more acidic, and hence stronger as extractants; while electron-donating substituents such as alkyl and methoxy groups have the opposite effects.[22] The following equation was proposed[22] to account for this in a single phase,

$$K_e = \beta_2 K_a^2 \qquad \textbf{Equation 2.1}$$

where K_e is the equilibrium constant for the formation of the neutral complex in a single phase,

$$Cu^{2+} + 2LH \rightleftharpoons [CuL_2] + 2H^+ \qquad \textbf{Equation 2.2}$$

β_2 represents the overall formation constant for the 2:1 (ligand : Cu^{II}) complex,

$$Cu^{2+} + 2L^- \rightleftharpoons [CuL_2] \qquad \textbf{Equation 2.3}$$

and K_a represents the acid dissociation constant of the ligand LH.

$$LH \rightleftharpoons L^- + H^+ \qquad \textbf{Equation 2.4}$$

Ligands with higher phenol acidity (larger K_a) form conjugate phenolate ions with lower basicity, which are poorer σ-donors[24] (smaller β_2). The square dependence of K_e on K_a (Equation 2.1) suggests that the phenol acidity has a greater effect on K_e than the phenolate basicity in a single phase. This arises because *two* phenolates must coordinate to form the *neutral* complex. For a two-phase solvent extraction, the above discussion may be an oversimplification in that the distribution coefficients of the ligand and the complex should be considered. Given that the free ligands and their complexes studied in this chapter are all water-immiscible, it is difficult to determine these distribution coefficients and to study their influence on the extractant strength.

When substituents are introduced in the 3-position of salicylaldoximes, additional effects result from their influences on the intracomplex hydrogen bonding shown in Figure 2.2. Large and bulky groups may disrupt the stabilising hydrogen bonding motif. More importantly, if the 3-substituent is a hydrogen bond acceptor as the case with halide, nitro and methoxy groups, it can form an additional bifurcated hydrogen bond with the oximic proton,[25] "***buttressing***" the stabilising motif,[22] and thus increases the extractant strength.

A series of salicylaloxime ligands was developed and studied by the Tasker group[22] as shown in Table 2.2. The $pH_{0.5}$ values of the ligands in 0.01 M chloroform solutions were measured to define extractant efficiencies with different 3-substituents. Clearly 3-substitution has a major influence on extractant strength, changing the distribution coefficients for copper by two orders of magnitude in the series: Br > NO_2 > Cl > OMe > Me ≥ H > ^{t}Bu.

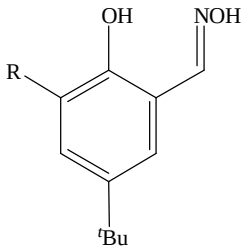

Ligand	R	$pH_{0.5}$	Calculated pK_a
O1	H	1.68	9.32 ± 0.48
O2	Me	1.67	9.66 ± 0.50
O3	NO_2	n/a[a]	6.58 ± 0.40
O4	Br	0.42	7.77 ± 0.50
O5	OMe	1.09	9.31 ± 0.50
O6	^{t}Bu	2.64	10.68 ± 0.50
O7	Cl	0.91	7.84 ± 0.50
O8	H[b]	1.73	9.33 ± 0.50
O9	NO_2[b]	0.70	6.60 ± 0.40

Table 2.2 Salicylaldoximes with different 3-substituents used as 0.01 M $CHCl_3$ solutions in Cu-extraction experiments.[22] [a]Cannot be measured due to poor solubility of the Cu^{II} complex in chloroform. [b]These ligands have *t*-octyl groups in the 5-position, instead of the *t*-butyl groups of **O1** and **O3**.

The pK_a values cannot be measured by pH titration since the ligands tend to hydrolyze in low pH solutions.[26] Instead values were calculated[22] by Daniel Tackley at Intertek ASG using ACD/Labs pK_a predictor v10.01. They vary in a generally similar fashion to the $pH_{0.5}$ values, suggesting that the electronic effects of the substituents which vary the pK_a values are important.

A combination of electronic and steric effect appears to operate in the case of **O6** (*t*-butyl) which is the weakest extractant. Buttressing could contribute to the strength of **O3** (NO_2), **O4** (Br) and **O7** (Cl), and particularly makes **O5** (OMe) much stronger than the benchmark **O1** (H) despite the electron-donating effect of the methoxy group.

A systematic study of the hydrogen bonding in the ligands and their copper(II) complexes was undertaken[22] to improve the understanding of the substituent influences, especially the buttressing effect. The most definitive results came from the solid state structure determinations and computational studies of dimerization enthalpies in the gas phase. Salicylaldoximes **O10**-**O15** (Table 2.3) were synthesized and crystallized.[22, 27]

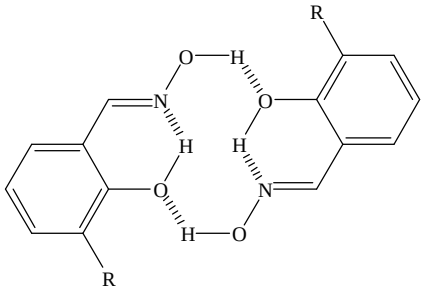

Ligand	R	Hole Size / Å
O10	H	2.0048(15)
O11	Me	2.0237(18)
O12	Br	1.9726 (53)
O13	OMe	1.9492(19)
O14	^{t}Bu	2.0367(19)
O15	Cl	1.9837(12)

Table 2.3 Salicylaldoximes studied for H-bonding in the ligands[22, 27]

All the crystal structures show the expected 14-membered *pseudo*macrocyclic dimeric arrangement.[22, 27] Cavity sizes (the mean distance of the donor N and O atoms from the centroid) were measured for the dimers, following the order **O13** (OMe) < **O12** (Br) < **O15** (Cl) < **O10** (H) < **O11** (Me) < **O14** (^{t}Bu).[22, 27] The radii of the cavities are significantly smaller in the dimers of **O12**, **O13** and **O15** with hydrogen bond accepting 3-substituents and larger in **O14** with a bulky 3-substituent, suggesting that buttressing of the hydrogen bonding by the 3-substituent is a dominant factor in stabilising the assembly. This was also confirmed by the gas phase calculations[22, 27] using the 6-31G basis set and various methods, including Hartree-Fock (HF), second order truncated Moller Plesset (MP2) and the DFT exchange function of Tao, Perdew, Staroverov and Scuseria (TPSSTPSS).

2.1.4 Salicylaldehyde Hydrazones as Potential Copper Extractants

Since the ability of 3-substituents to tune the strength of salicylaldoximes as copper extractants has been established,[22, 27] it was logical to investigate similar effects with alternative ligands. The most obvious choice was salicylaldehyde hydrazones in which the hydroxyl groups of oximes are replaced by secondary amino groups. It was hoped that these salicylaldehyde hydrazones would form copper(II) complexes with a similar *pseudo*macrocyclic H-bonding arrangement (Figure 2.4), and that the substituents could be used to tune their strength appropriate for potential commercial application, particularly by using the buttressing effect.

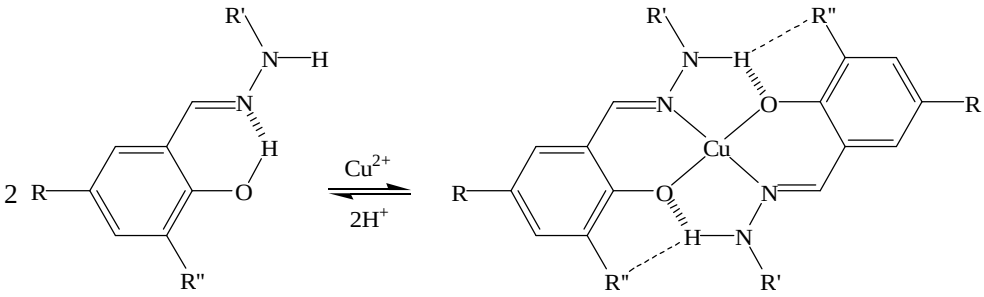

Figure 2.4 Potential buttressing of H-bonds in copper(II) complexes of salicylaldehyde hydrazones.

Hydrazones have been intensively investigated due to their facile syntheses, tuneable steric, electronic, magnetic and optical properties, excellent chelating capability, and hence widespread applications in organic, analytical, biological and industrial chemistry.[28] They function as intermediates to synthesize many heteocycles such as indoles,[29] indazole, pyrazoles,[30, 31] pyrazolidines,[32] triazoles[33] and benzofurans.[34] Certain hydrazones can be used as spectrophotometric and gravimetric reagents for the detection and determination of transition metals, including copper, nickel, iron *etc*.[35-37] Hydrazones or their complexes are magnetic,[38, 39] electronic,[40] nonlinear optically active[41-43] and fluorescent materials.[44, 45] They can also be made into optical

chemosensors for analytical purposes.[46, 47] As physiological active compounds, hydrazones are widely exploited in pharmaceutics. Phenolic hydrazones are potent inhibitors of macrophage migration inhibitory factor[48] which is critically involved in the pathogenesis of sepsis and other inflammatory disorders. Salicylaldehyde benzoylhydrazone and analogous aroyl hydrazones have been studied as chelating agents for mobilizing iron during the therapy of iron overload,[49, 50] and their transition metal complexes possess antitumour properties.[51, 52] Certain hydrazones have shown inhibition of HIV integrase for the treatment of AIDS.[53] Polyaryl mononitro/dinitrophenylhydrazones are applied to treat cancerous or precancerous cutaneous lesions.[54] Also many hydrazones and their transition metal complexes are used as antibacterial, antiviral and antifungal agents,[55, 56] and in industry they are employed as plasticizers[57] and catalysts.[58-60]

The copper coordination chemistry of hydrazones is of particular interest in this chapter. For the structure shown in Figure 2.4, the R' group could be H, alkyl, aryl or aroyl. Aroyl hydrazones[61-65] usually form 1:1 copper(II) complexes as tridentate ligands with the phenolate oxygen, azomethine nitrogen and enolimide oxygen atoms defining the binding site. An example is given in Figure 2.5 with A being water or solvent molecule.[61-65] Salicylidenehydrazones (R' = H) have been reported to form 1:2 copper(II) to ligand complexes.[35, 36] Copper complexes of salicylaldehyde alkyl/arylhydrazones, however, have been little investigated. A search in the literature indicates that salicylaldehyde phenylhydrazone forms a 1:2 copper(II) to ligand complex,[66-68] but no work has been reported on the use of salicylaldehyde hydrazones as copper extractants.

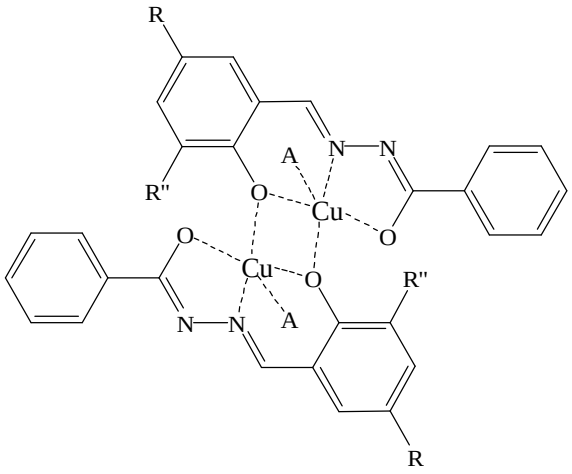

Figure 2.5 One of the copper(II) complexes of aroyl hydrazones

The aim of the research presented in this chapter is to consider salicylaldehyde hydrazones as potential copper(II) extractants for the hydrometallurgical recovery and study the substituent effects, particularly the buttressing effect, on the efficacy and strength of the ligands. The following sections cover the syntheses and characterizations of the novel ligands and their copper(II) complexes, solvent extraction results, discussions of substituent effect, a comparison with salicylaldoximes and a systematic NMR solution study.

2.2 Ligand Syntheses

2.2.1 Ligand Design

A series of salicylaldehyde hydrazones has been developed with 3-substituents and N-substituents which will affect the electronic, steric and hydrogen bonding properties of the extractants (see Figure 2.6). In theory 3-substituents with electron-drawing effect (NO_2, Br) and electron-donating effect (Me, OMe) have significant influence on the pK_a values for the phenolic proton, and hence change the

strength of the extractants. These substituents also have the potential to form attractive bifurcated hydrogen bonds (NO_2, Br, OMe) or repulsive interactions (Me) with the H-bond donating group on the adjacent ligand, which is described as "Buttressing effect" in section 2.1.3. N-substituent such as phenyl group was investigated for the steric and conjugating effect on the extractants. Each ligand includes a 5-*tert*-butyl group to increase the solubility in non-polar solvents.

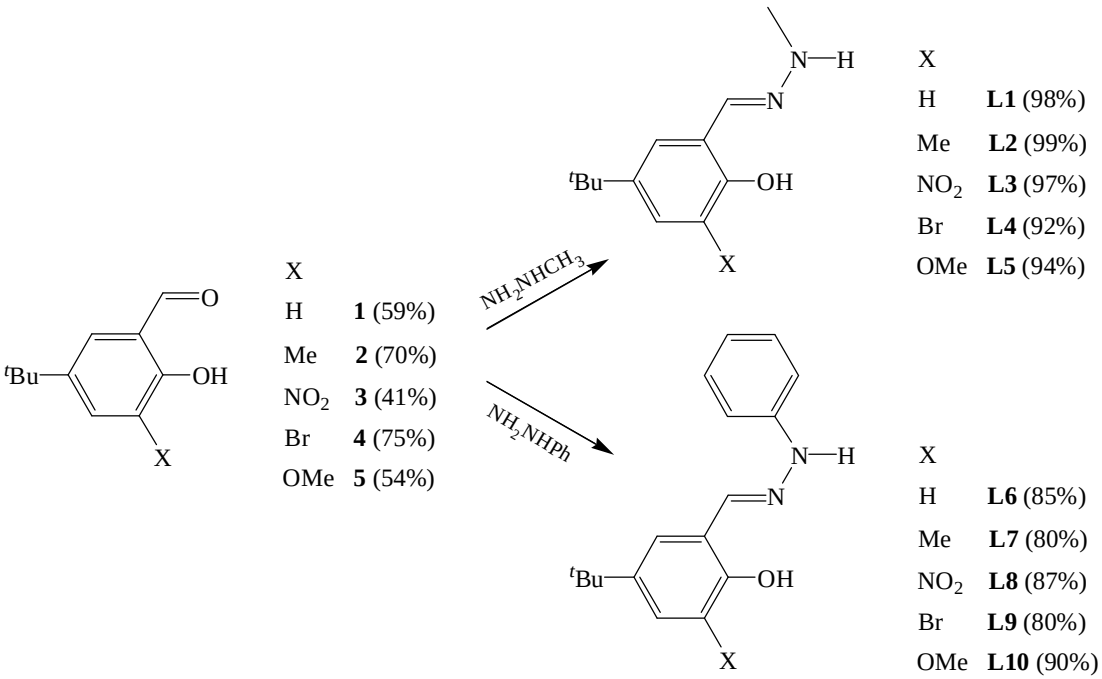

Figure 2.6 Synthesized precursors **1**-**5** and salicylaldehyde hydrazones **L1**-**L10** with yields indicated. The yields of **L1**-**L10** are only for the hydrazone formation step.

None of the hydrazones except **L6**[69, 70] has been reported in the literature. However, their salicylaldehyde precursors can be readily prepared following related literature and the methods reported below have been based on optimizing these procedures. The hydrazone formation from appropriate precursors and hydrazines was high-yielding as shown in Figure 2.6.

The synthesis of the substituted salicylaldehydes **1**-**5** generally involved two steps, formylation and inclusion of the 3-substitution of 4-*tert*-butylphenol. "Formylation first" or "substitution first" is the main issue in defining the best synthetic route. After extensive reviewing literature of methods, some of the routes used in the group were abandoned and new synthetic strategies were employed as in Scheme 2.1.

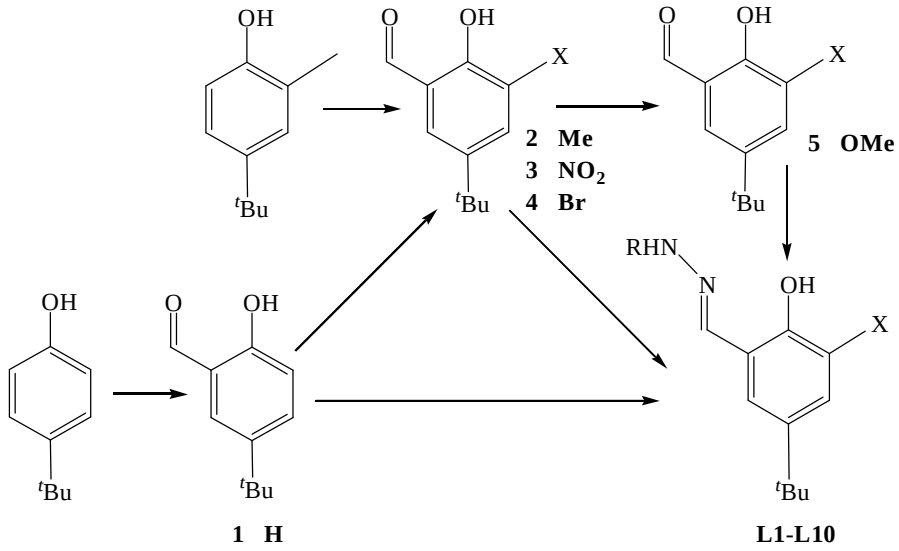

Scheme 2.1 Synthetic routes to salicylaldehyde hydrazones **L1**-**L10**.

The formylation was done before the substitution to block one *ortho* site of the phenol group, and the numbers of starting materials and steps have been significantly reduced. A stock pile of 5-*tert*-butyl-2-hydroxybenzaldehyde (**1**) was synthesized by the Levin method.[71] The nitro-substituted (**3**) and bromo-substituted (**4**) salicylaldehydes were produced from **1** under optimized conditions in literature.[72] The methoxy-substituted precursor (**5**) was prepared from **4** by a modification of the literature method.[73] Only in case of the methyl-substituted salicylaldehyde (**2**), the synthesis exploited the modified Duff reaction[74] starting with 4-*tert*-butyl-2-methylphenol, since it was commercially available and it would be difficult to methylate **1** by Friedel-Crafts reaction.

2.2.2 Formylation

2.2.2.1 The Levin Method

As the main starting material and the precursor of **L1**, **1** was prepared according to the method introduced by Levin *et al*[71] which effectively and selectively monoformylates the appropriate phenol. The reaction supposedly involves magnesium mediated *ortho*-formylation.

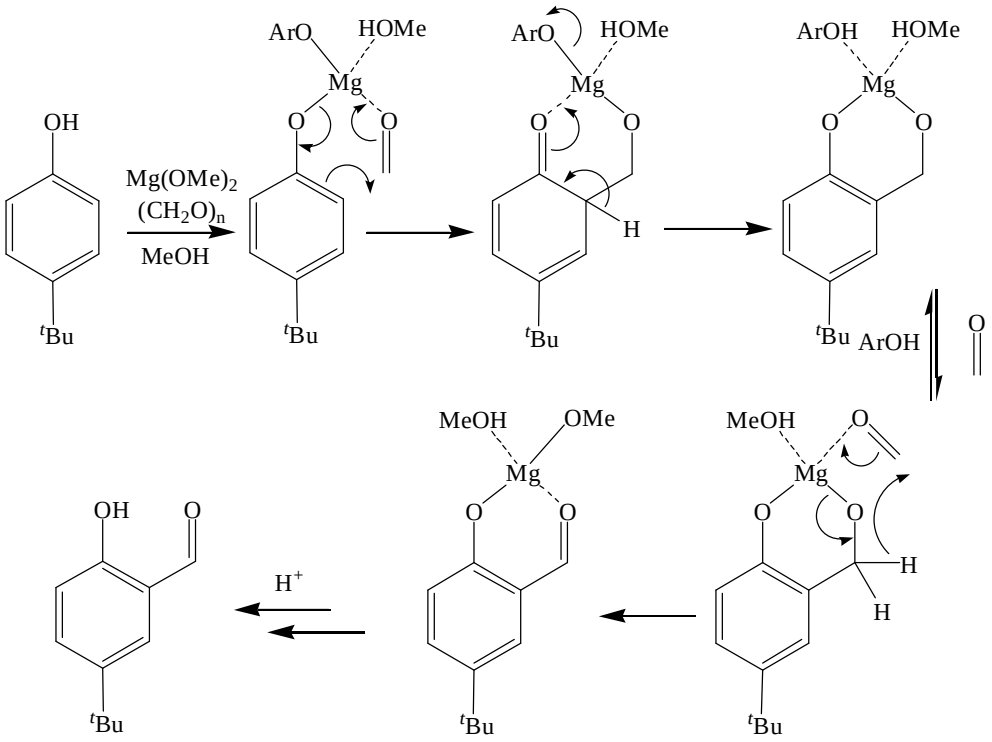

Figure 2.7 Proposed mechanism for the synthesis of **1** using the Levin method.[71]

Magnesium bis-phenoxides are formed on addition of magnesium methoxide to alkyl phenol in methanol, and react with paraformaldehyde in toluene by the mechanism proposed in Figure 2.7 to yield the product after an acidic work-up. Control of methanol level is required as high concentration can result in competition with the

phenoxides for magnesium coordination and hence it acts as an inhibitor. The reaction succeeded in producing large quantities of **1** in *ca.* 59% yield.

2.2.2.2 The Modified Duff Reaction

The Duff reaction has been modified to produce salicylaldehydes in good yields using hexamethylenetetramine (HMTA) and appropriate phenols in trifluoroacetic acid as a solvent.[74]

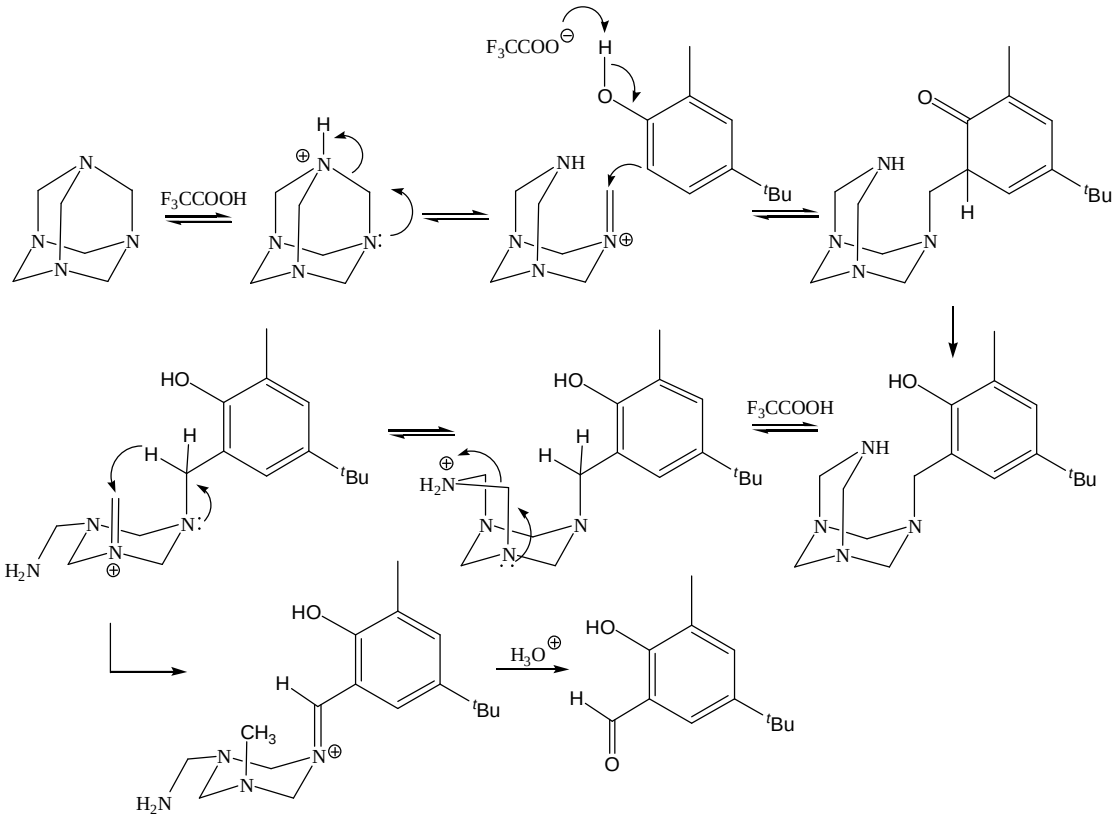

Figure 2.8 Proposed mechanism of the modified Duff reaction of **2**.[74]

The main disadvantage is the lack of selectivity. *Ortho*-, *para*- or diformylated phenols all are possible products. However, in case of 4-*tert*-butyl-2-methylphenol there is only one accessible site for formylation to give the desired compound **2** as in

Figure 2.8. The reaction was carried out in a large excess of HMTA to ensure the completion. After heating overnight the reaction mixture was poured into 2 M HCl and stirred for 6 h. The product was extracted into DCM and purified via column chromatography.

2.2.3 Introduction of 3-Substituents

2.2.3.1 Nitration

The introduction of a nitro group was achieved by electrophilic substitution using nitric acid and glacial acetic acid as described in Figure 2.9. As expected, the nitro group went in *ortho* to the phenol group and *meta* to the CHO group to give **3**. The reaction solution was heated at 55 °C for 20 h and extracted by DCM. Column chromatography gives the pure product in 41% yield.

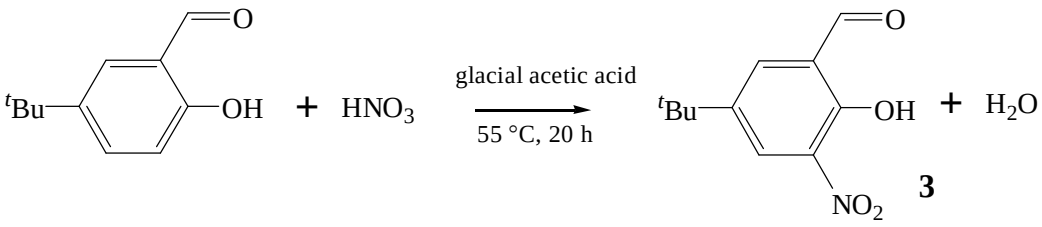

Figure 2.9 Synthesis of salicylaldehyde precursor **3**.

2.2.3.2 Bromination

A variety of methods are known for brominating salicylaldehydes,[72, 75] and the one chosen here has optimized the reaction conditions and work-up in Figure 2.10. Bromine in glacial acetic acid was added to a solution of **1** and sodium acetate in glacial acetic acid via a dropping funnel over 50 min. The reaction media, AcOH in

presence of NaOAc, removed the free hydrobromic acid as quickly as produced to eliminate its influence on the reaction.[76] As part of the work-up, the crude product in DCM was washed with $Na_2S_2O_5$ solution and saturated $NaHCO_3$ solution to remove leftover Br_2, AcOH and HBr produced by the reaction. Recrystallization in light petroleum spirits gave the pure product as pale yellow crystals.

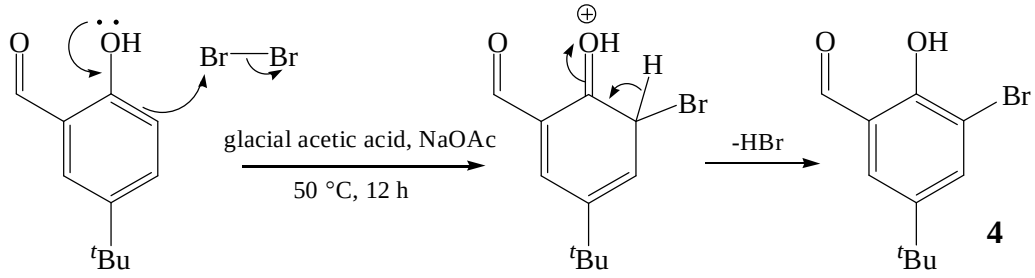

Figure 2.10 Proposed mechanism of the synthesis of **4**.

2.2.3.3 Methoxylation

Nucleophilic substitution of **4** by the methoxy group gave the desired product **5** as described in Figure 2.11.

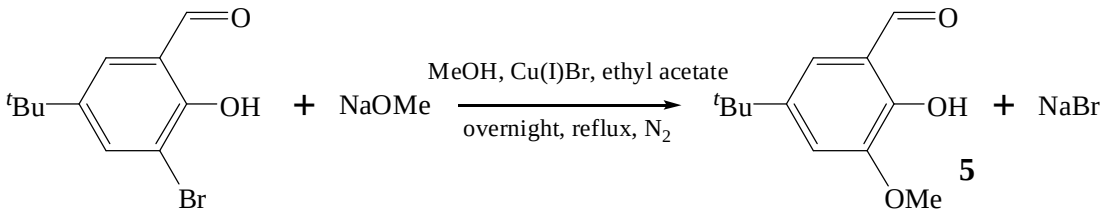

Figure 2.11 Synthesis of salicylaldehyde precursor **5**.

Different catalysts and reaction conditions have been reported in the literature.[73, 77] The reaction in this work was carried out by adding **4** in methanol into a refluxing mixture of a fresh 4 M NaOMe/MeOH solution, CuBr and small amount of ethyl

acetate under nitrogen. This system was chosen because the Cu(I) catalyst could achieve increased solubility and stabilization in the presence of ethyl acetate due to formation of an adduct with concentrated methoxide ion.[78] As a result, the substitution proceeded with great efficiency. After refluxing the reaction mixture overnight, the solvent was removed. The solid was dissolved in 3 M HCl and extracted with ethyl acetate. The product was purified by column chromatography.

2.2.4 Hydrazone Formation

All the hydrazones **L1-L10** were synthesized by slowly adding the appropriate salicylaldehyde precursors to hydrazines. The proposed mechanism is shown in Figure 2.12. The reactions in ethanol went rapidly to completion, and the pure products separated as solids.

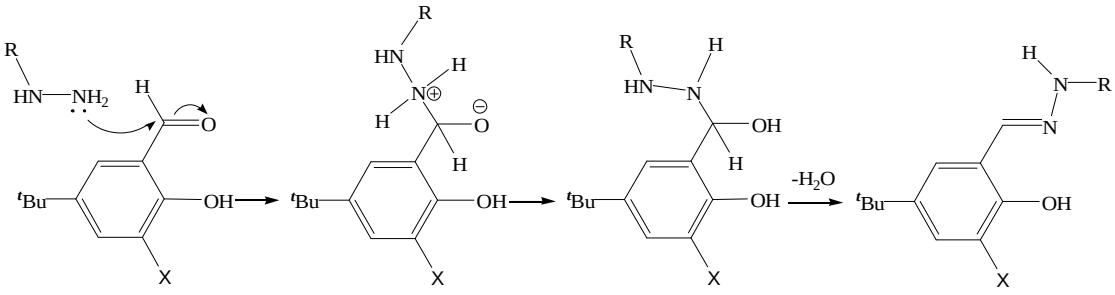

Figure 2.12 Mechanism of hydrazone formation by reaction with hydrazine.

2.3 Ligand Characterization

2.3.1 NMR Spectroscopy

The precursors **1**-**5** and ligands **L1**-**L10** were fully characterized by ^{1}H and ^{13}C NMR spectroscopy.

^{1}H NMR	**1**	**2**	**3**	**4**	**5**
C(C*H*$_3$)$_3$	1.33	1.33	1.36	1.33	1.34
Ar-*H* (4-position)	7.58	7.45	8.34	7.82	7.18
Ar-*H* (6-position)	7.52	7.36	8.15	7.52	7.15
C*H*O	9.88	9.88	10.43	9.86	9.92
3-Substituent	6.92 (Ar-*H*)	2.28 (C*H*$_3$)	/	/	3.94 (OC*H*$_3$)
^{1}H NMR	**L1**	**L2**	**L3**	**L4**	**L5**
C(C*H*$_3$)$_3$	1.34	1.30	1.33	1.29	1.31
NHC*H*$_3$	2.97	2.98	3.03	2.98	2.97
Ar-*H* (4-position)	7.23	7.10	7.90	7.43	6.88
Ar-*H* (6-position)	7.13	6.98	7.64	7.07	6.76
C*H*N	7.69	7.70	7.72	7.60	7.67
3-Substituent	6.89 (Ar-*H*)	2.28 (C*H*$_3$)	/	/	3.92 (OC*H*$_3$)
^{1}H NMR	**L6**	**L7**	**L8**	**L9**	**L10**
C(C*H*$_3$)$_3$	1.30	1.32	1.37	1.31	1.33
Ar-*H*	6.93-7.28	6.96-7.44	6.94-8.05	6.95-7.51	6.79-7.29
C*H*N	7.84	7.88	8.05	7.84	7.88
3-Substituent	6.93 (Ar-*H*)	2.34 (C*H*$_3$)	/	/	3.96 (OC*H*$_3$)

Table 2.4 Chemical shifts (δ/ppm) of aldehyde precursors **1**-**5** and ligands **L1**-**L10** in ^{1}H NMR spectra in $CDCl_3$

^{1}H NMR spectra showed that the conversion of aldehyde to hydrazone was complete as the azomethine signal appeared with the absence of the carbonyl signal. Chemical shifts in ^{1}H NMR spectra, particularly of aromatic protons, varied due to the nature of the 3-substituent as shown in Table 2.4. The peaks of **2**/**L2**/**L7** and **5**/**L5**/**L10** were generally shifted to higher field compared to those of **1**/**L1**/**L6** as a result of the electron-donating property of methyl and methoxy group, while those of **3**/**L3**/**L8** and **4**/**L4**/**L9** were shifted to lower field due to the electron-drawing nature of nitro and bromo group. This indicates the initial success of the ligand design in this chapter.

2.3.2 Mass Spectrometry

ESI MS was used to characterise all the precursors and ligands. Appropriate peaks were seen for each molecular ion (MH^+), indicating the success of the syntheses. No strong peaks were shown for the dimers of the ligands, which could be due to methanol used as the solvent.

2.3.3 X-ray Crystallography

L6 and **L10** were successfully characterised by X-ray crystallography. For **L6**, the phenolic group acts as a hydrogen bond donor to form an intramolecular bond O-H···N to the imine nitrogen atom. It also acts as a hydrogen bond acceptor to form an intermolecular hydrogen bond N-H···O with the hydrazone NH group. These hydrogen bonds interconnect the **L6** molecules into chains which are interconnected by π-π interaction to form the crystal packing as shown in Figure 2.13. The dihedral angle between the benzene rings is 40.07°. The N-N bond length, 1.3637(16) Å, is significantly shorter than that of hydrazine in the literature, 1.46 Å,[79, 80] which indicates the partial double bond property of the N-N bond due to the conjugation

effect.

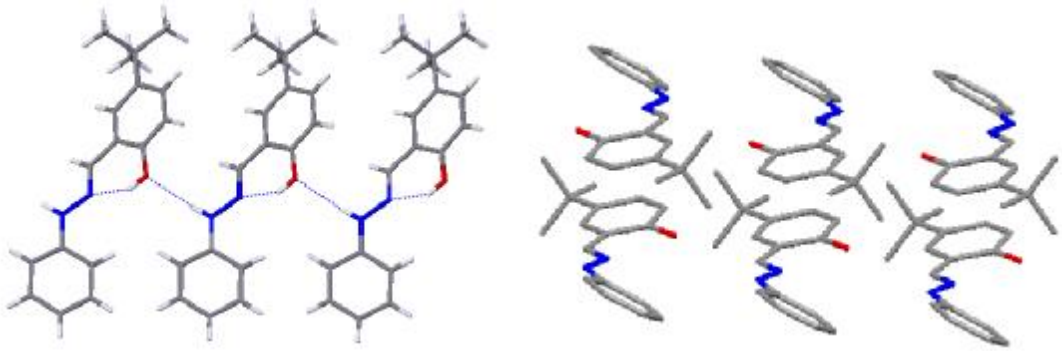

Figure 2.13 Crystal structure of **L6** showing the H-bond array (left) and the crystal packing (right)

The crystal structure of **L10** shown in Figure 2.14 consists of an ordered molecule with the dihedral angle of 6.60˚ and a disordered molecule in which the dihedral angle is 30.51˚. The N-N bond lengths are respectively 1.354(3) Å and 1.358(3) Å. The methoxy group provides an additional H-bond acceptor adjacent to phenol oxygen, prompting the formation of bifurcated hydrogen bonds. These hydrogen bonds interconnect the molecules into a three-dimensional network.

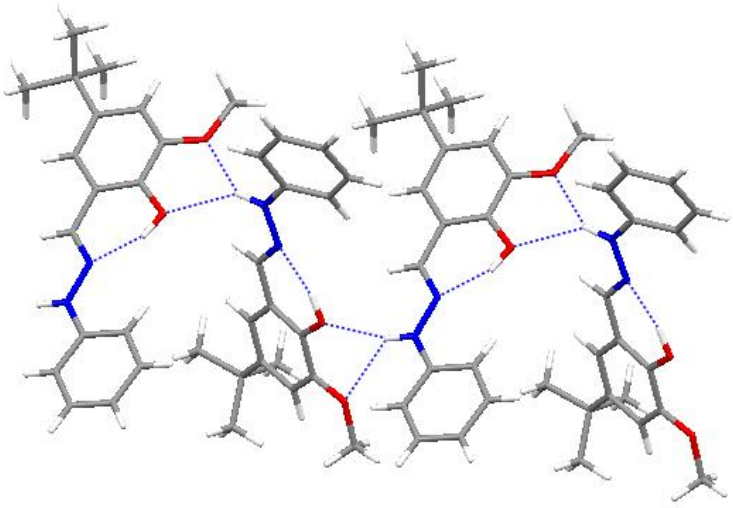

Figure 2.14 Crystal structure of **L10**

Initially it was hoped that salicylaldehyde hydrazones would dimerize to form 14-membered *pseudo*macrocyclic hydrogen bonded structures in the solid state analogous to those formed by salicylaldoximes shown in Table 2.3. However, it was not the case for salicylaldehyde phenylhydrazones. In order to discuss the structures conveniently, the conformation of the hydrazone group need to be defined. Since the N-N bond has partial double bond property, it is reasonable to adopt the concept of Z/E configuration in this case. The Z conformation refers to the structure where two higher priority groups are closest through the N-N bond, while the E conformation refers to the structure where two higher priority groups are furthest apart through the N-N bond. The steric effect of the N-phenyl group favours the E conformation of the free ligand in order to minimize the repulsion from the azomethine proton as shown in Figure 2.15, and thus it is less likely to form a dimer which adopts the Z conformation.

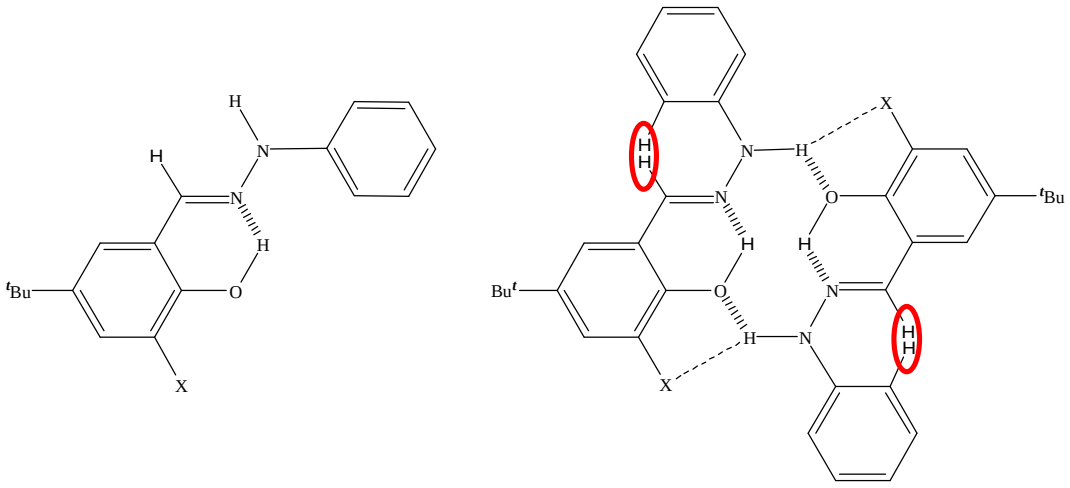

E conformation **Z** conformation in a dimer

Figure 2.15 E and Z conformation of salicylaldehyde phenylhydrazones

2.3.4 Melting Point

Melting points of **1**-**5** and **L1**-**L10** were measured in Table 2.5, which indicate the

purity of the products. The values increase in the order aldehydes < methylhydrazones < phenylhydrazones with the increase of the molecular weights. Methyl substituted ligands have much lower melting points, possibly due to smaller molecular weights and the lack of intermolecular hydrogen bonds compared to other ligands. **L6** has a markedly higher melting point, which could result from the significant π-π interaction in the crystal packing.

Substituent	**Precursor**	**M. P.**/°C	**Ligand**	**M. P.**/°C	**Ligand**	**M. P.**/°C
H	**1**	oil	**L1**	43-44	**L6**	173-174
Me	**2**	38-39	**L2**	96-97	**L7**	105-106
NO_2	**3**	87-88	**L3**	117-118	**L8**	125-126
Br	**4**	83-84	**L4**	105-106	**L9**	145-146
OMe	**5**	57-58	**L5**	80-81	**L10**	133-134

Table 2.5 Melting points of **1**-**5** and **L1**-**L10**

2.4 Syntheses and Characterization of Cu(II) Complexes

The copper(II) complexes of **L1**-**L10** were successfully synthesised by mixing stoichiometric amounts of the ligand and copper(II) acetate in ethanol. Precipitation occurred immediately, and the pure products were collected by filtration. All complexes were isolated as brownish solids.

The copper(II) complexes were characterised by CHN analysis and ESI Mass Spectrometry. Molecular ion peaks were all observed, confirming the successful syntheses.

2.5 Solvent Extraction by the Methylhydrazones

The strength of salicylaldehyde hydrazone as a potential copper extractant was assessed by solvent extraction. In the laboratory, extraction data can be obtained by conducting either loading or stripping experiment. A loading experiment uses a solution of the free ligand in a hydrocarbon solvent to contact with aqueous feeding solution of the target metal; while in a stripping experiment a solution of the metal complex in a hydrocarbon solvent is contacted with a blank aqueous solution. For a pH dependent extraction, the $pH_{0.5}$ value can be measured by varying the pH of the aqueous solution in both methods. In theory, loading and stripping experiment under identical conditions should give the same $pH_{0.5}$ value.

2.5.1 Loading Experiment

The loading experiment for **L1**-**L5** was carried out in chloroform using an aqueous solution of $CuSO_4$. The pH of the aqueous solution was adjusted by adding H_2SO_4 or NaOH. After extraction the Cu content of the organic phase was measured by taking an aliquot to evaporate to dryness, making up to a volume in 1-butanol and analyzing the sample by inductively coupled plasma optical emission spectroscopy (ICP- OES).

The initial results (Figure 2.16) show that **L3** (NO_2) and **L4** (Br) start to extract copper(II) at lower pH than the other ligands, suggesting that they are stronger extractants. The results also indicate that **L2** (Me) is the weakest extractant. The dependence of $pH_{0.5}$ values on 3-substitutions follows the order $NO_2 \leq Br < H <$ OMe < Me, which is comparable with that obtained for the oxime analogues (see section 2.1.3).

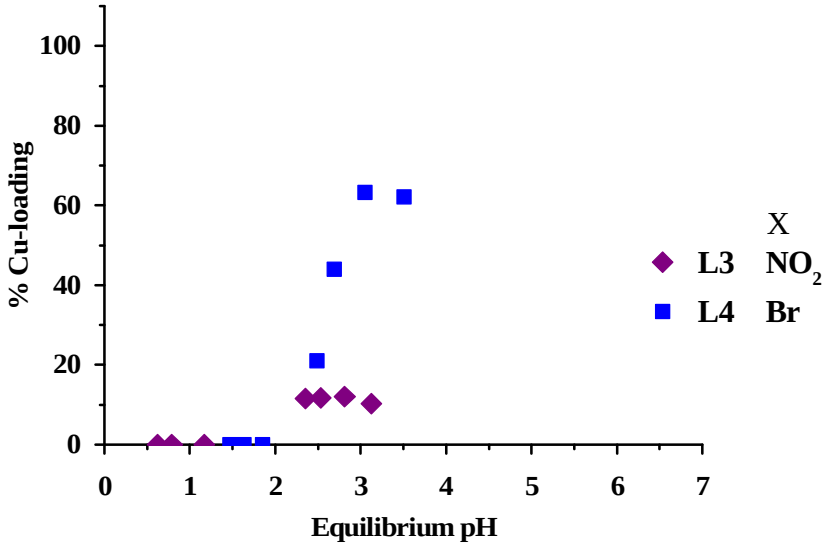

(a)

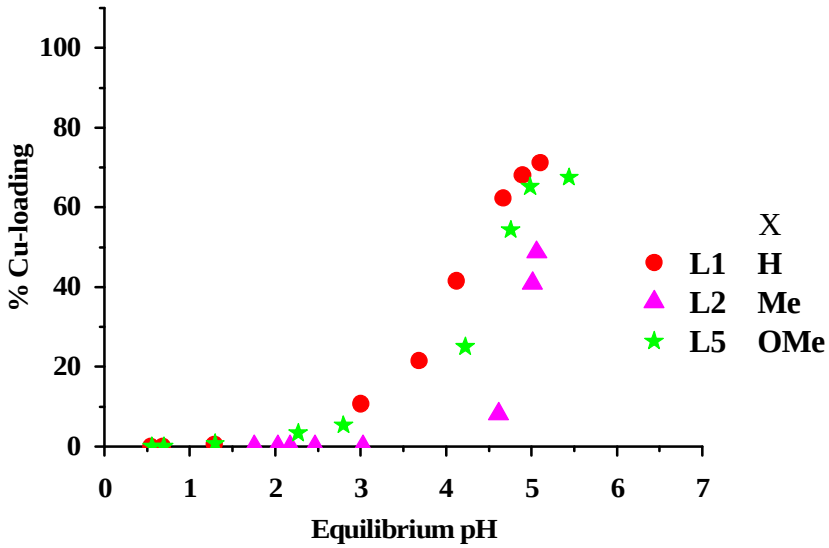

(b)

Figure 2.16 Copper loadings of 0.01 M chloroform solutions of **L1**-**L5** from equal volume 0.01 M $CuSO_4$ solutions. The copper contents were measured by ICP-OES in 1-butanol.

However, the determination of $pH_{0.5}$ values for **L1-L5** by the standard loading protocol is associated with problems. The solubility of the copper complex

[Cu(**L3**-H)$_2$] in chloroform is too low to generate a reliable loading curve. The formation of the precipitate could be observed by eye and explains the maximum loading of *ca.* 15% for **L3** (Figure 2.16 (a)). Also the complexes [Cu(**L2**-H)$_2$], [Cu(**L3**-H)$_2$], and [Cu(**L4**-H)$_2$] have limited solubilities in 1-butanol, the solvent used to make up samples for analysis by ICP-OES. This may account for the apparent loading limit of *ca.* 60% for **L2**. Since **L1**, **L2** and **L5** have relatively high $pH_{0.5}$ values, the pH in the aqueous $CuSO_4$ solution need to be raised to *ca.* pH 7 to obtain a whole set of extraction data. A part of the copper cation precipitated under these conditions, and the suspension in the aqueous phase had not redissolved at the end of the solvent extraction experiment. Consequently it is difficult to obtain reliable loading data at pH values above 5 (Figure 2.16 (b)).

The above problems result in the incomplete loading plots with *ca.* 70% maximum uptakes (Figure 2.16). As it was known (section 2.4) that the bishydrazonato complexes could be readily prepared and characterized, it was decided to investigate the $pH_{0.5}$ values for copper extraction by conducting stripping experiment, in which a chloroform solution of the prepared complex was contacted with aqueous solutions with a fixed total sulfate concentration and various pH values (see section 2.5.2). A reliable method of analyzing the copper content of the organic phase also required the identification of a suitable solvent for making up solutions for ICP-OES analysis (see section 2.5.3).

2.5.2 Stripping Experiment

The stripping experiment was carried out under a very similar condition to that of the loading experiment. Na_2SO_4 was added to the aqueous solution to ensure that the sulfate concentration remains the same as in the loading experiment (0.01 M) in section 2.5.1. The advantage of the stripping experiment is that it starts with a

solution of copper complex in a known concentration. For the complex with limited solubility, such as [Cu(**L3**-H)$_2$], the stock solution was properly diluted (0.0005 M) to avoid the formation of a third phase in solvent extraction. Also the stripping experiment can provide extraction data over a wider pH range. For pH values up to 7 or higher, there are no copper cations in the aqueous phase to begin with and no copper will be stripped from the organic phase at these high pH values, so no copper precipitate has been found.

2.5.3 A New Approach to ICP-OES Analysis

ICP-OES is a powerful technique to measure the concentration of most elements in an aqueous or organic solution. The instrument uses an ICP source to dissociate the sample into its constituent atoms or ions, exciting them to a level where they emit light of a characteristic wavelength. The intensity of analyte emission is proportional to analyte concentration, so initial calibration of the spectrometer with known standard samples makes it possible to detect accurate concentrations of up to 60 elements in less than one minute.[81] The detection limits of low-parts-per-billion[81] can be achieved. It is desirable to dissolve the amount of 1 to 5 mg inorganic constituents in 5 ml solution due to concerns about homogeneity.[81] As a routine analysis done in the group for solvent extraction, the organic phase is evaporated to dryness and redissolved in 1-butanol to measure the metal content. Under standard condition, this gives the concentration in the range 0-100 ppm, which is close to the recommended value above. However, the limited solubilities of some of the [Cu(L-H)$_2$] complexes in 1-butanol made this protocol impracticable. Two options for an alternative approach to ICP-OES analysis in the stripping experiment are to identify a new solvent system for making up samples from the organic phase or to carry out the analysis of the aqueous phase.

Several factors should be considered when defining a new solvent system. It can be a single solvent or a mixture, but must dissolve the copper complexes. It must not be highly volatile because this tends to extinguish the plasma. Finally, in this work it is helpful if the new solvent system has similar properties to 1-butanol, because the optimized parameters on the ICP-OES equipment could be reproduced. 1-Butanol has been commonly used in ICP-OES analysis because it has relatively high boiling point and high viscosity. When the organic phase is nebulized in the plasma channel, the transport efficiency of the analyte depends on the evaporation rate of the solvent and the surface tension of the aerosol droplet.[82] For a solvent of low volatility, the latter is the dominant effect. Consequently the slow evaporation rate of 1-butanol results in desirable plasma stability, and the high viscosity achieves enhanced sensitivity because of the smaller aerosol droplets produced.[83]

Fortunately, after screening a few solvents, it was found that nitrobenzene matches all the requirements above. All the copper complexes of **L1**-**L5** are soluble in nitrobenzene, and it has high boiling point and high viscosity as 1-butanol.[83] The behaviour of these two solvents as ICP-OES media is fairly similar.[83] Calibration and dummy solutions prepared from purchased copper standards were tested to give good consistency. Thus ICP-OES analysis of the organic phase using nitrobenzene as the new solvent proved to be a valid method. The copper contents in the stripping experiment of **L3** and **L4** were successfully measured in this way, while the others were done conventionally in 1-butanol.

As mentioned above, an alternative approach is to analyse copper in the aqueous phase. Assuming all the copper cations stripped from organic phase transfers to aqueous phase, the summation of the copper contents in both phases should equal the original copper content in the organic phase. The copper content remaining in the organic phase can be calculated. The analysis of the aqueous phase in the stripping

experiment was carried out for **L1**-**L5**. The results were consistent with those of the organic phase analysis, and showed a good material balance of copper (see Appendix 6.2.3). This indicates no third phase containing copper was formed at any applied pH value. For simplicity, the extraction results displayed below are based on the analysis of the organic phase.

2.5.4 Extraction Results

The results shown in Figure 2.17 were obtained using the methodology just outlined. It can be seen that complete S-curves were achieved in all cases. No third phase was formed and the $pH_{0.5}$ values were successfully measured from the S-curves. The dependence of ligand strength on the 3-substituites (NO_2 > Br > H ≥ OMe > Me) is similar to that obtained in the loading experiment (see section 2.5.1).

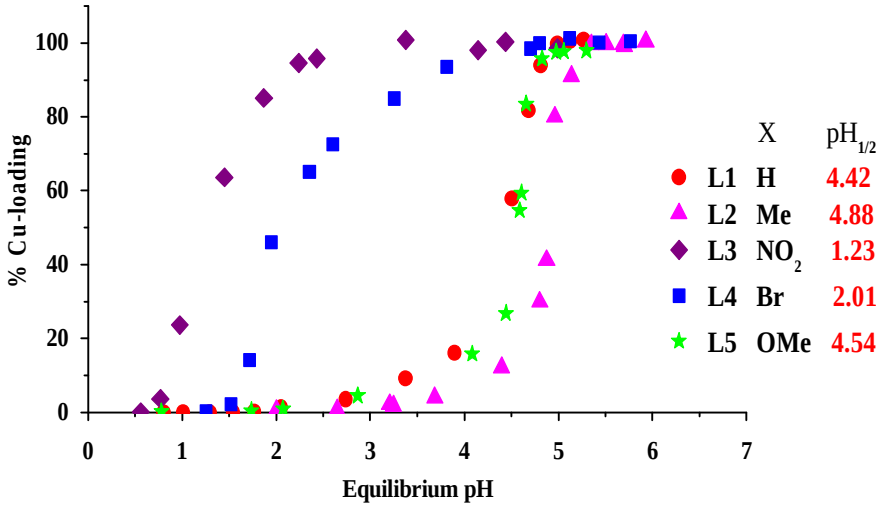

Figure 2.17 Copper loading of **L1**-**L5** after contacting 0.005 M chloroform solutions of $[Cu(L\text{-}H)_2]$ with equal volume 0.01 M Na_2SO_4 aqueous solutions of various acidities. For $[Cu(\mathbf{L3}\text{-}H)_2]$, 0.0005 M chloroform solutions were used due to the limited solubility. The copper contents of **L3** and **L4** solutions were measured by ICP-OES in nitrobenzene, the rest in 1-butanol.

2.6 Methylhydrazones as Copper Extractants

Clearly 3-substitution significantly affects the strength of the methylhydrazone extractants **L1**-**L5**. The distribution coefficient for copper extraction varies by more than three orders of magnitude across the series: NO_2 > Br > H ≥ OMe > Me. This arises from both the electronic and buttressing effect of the 3-substituent. The electron-drawing and H-bond acceptor nature of nitro and bromo groups combine to make **L3** and **L4** much stronger extrants, whilst **L2** is the weakest because the methyl group reduces K_a due to its electron-donating property and it has little effect on intermolecular hydrogen bonding. The importance of the buttressing effect is best indicated by **L5**. Despite the electron-donating effect of its methoxy group which decreases the K_a value, **L5** turns out to be stronger than **L2** as a result of its bifurcated hydrogen bonds which stabilise the intracomplex hydrogen bonding motif.

The strength of **L1**-**L5** can be compared with their oxime analogues **O1**-**O5**[22] using the $pH_{0.5}$ values in Table 2.6. The methylhydrazones are much weaker extractants than salicylaldoximes. For the unsubstituted methylhydrazone and its 3-methyl and 3-methoxy derivatives, the distribution coefficients for copper extraction are approximately three orders of magnitude smaller than the related oximes. There is a smaller difference in strength between the nitro- and bromo-substituted methylhydrazones and oximes. This could be because the beneficial effect of 3-substitution in lowering the pK_a value is less obvious in pH regions where proton acidity is influenced by buffering from sulfate

$$H^+ + SO_4^{2-} \rightleftharpoons HSO_4^- \qquad \textbf{Equation 2.5}$$

The most striking observation is that a 3-substituent such as NO_2 or Br can make the methylhydrazones (**L3** and **L4**) comparably strong extractants to the unsubstituted

oximes. This emphasizes the importance of the substitution effects.

Although the $pH_{0.5}$ values of the methylhydrazones (NO_2 < Br < H ≤ OMe < Me) are not in the exact same order as the oximes (Br < NO_2 < OMe < H ≤ Me), the trend is nevertheless similar. Strength is increased by substitution of groups with electron-withdrawing or hydrogen bond acceptor properties.

Substituent	Oxime	$pH_{0.5}$	Hydrazone	$pH_{0.5}$
H	**O1**	1.68	**L1**	4.42
Me	**O2**	1.67	**L2**	4.88
NO_2	**O3 (O9)**	n/a[a] (0.70[b])	**L3**	1.23
Br	**O4**	0.42	**L4**	2.01
OMe	**O5**	1.09	**L5**	4.54

Table 2.6 The $pH_{0.5}$ values of **L1**-**L5** and their oxime analogues **O1**-**O5**[22]. [a]Not measurable due to poor solubility of the Cu^{II} complex. [b]The analogue **O9** has a *t*-octyl group instead of a *t*-butyl group.

2.7 Phenylhydrazones as Copper Extractants

The phenylhydrazone extractants **L6**-**L10** were found to be much weaker than their methylhydrazone analogues. **L8** (NO_2) and **L9** (Br) shows some copper(II) uptakes above pH 4, but **L6**, **L7** and **L10** did not load copper(II) from aqueous solutions with pH values up to 7. As copper(II) precipitates in such pH ranges, it proved impossible to determine $pH_{0.5}$ values for the phenylhydrazone extractants and it is clear that they have little potential as copper extractants. However, the observation that the nitro- and bromo-substituted ligands **L8** and **L9** are the strongest in the series is consistent

with the results obtained for the methylhydrazones (section 2.6) and oximes[22].

2.8 Substitution Effects on the Hydrazones and Oximes

The results presented above demonstrate that the strength as copper(II) extractants decreases in the order: salicylaldoximes > salicylaldehyde methylhydrazones > salicylaldehyde phenylhydrazones, and it has been confirmed (see section 2.6) that both the acidity of the phenolic group and the interligand hydrogen bonding are important in defining extractant strength. The following discussion attempts to increase the understanding of the structure/activity relationship by focusing on how the nature of the substituent on the imino nitrogen atom (OH, NHMe or NHPh in Figure 2.18) influences the above properties of the ligands.

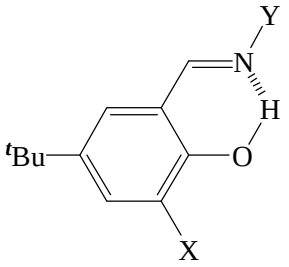

Y	Ligands
OH	Salicylaldoxime
NHMe	Salicylaldehyde Methylhydrazone
NHPh	Salicylaldehyde Phenylhydrazone

Figure 2.18 Substituents on the imino nitrogen atoms

2.8.1 Phenol Acidity

As discussed before, electronic properties of the substituents on the benzene ring affect the acidity of the phenolic hydroxyl group, and hence the strength of the extractant. In a way the imino group is simply a substituent and should have the same effect. Generally the imino group has an electron-withdrawing inductive effect and electron-donating conjugation effect.[29] The overall electronic property is determined by which is stronger, and usually the inductive effect results in that the imino group

shows electron-withdrawing property. However, this depends on the N-substituent. Oxygen is more electronegative than nitrogen, and hence the electron-withdrawing inductive effect is stronger in oximes than in hydrazones. Research has shown that the OH substituent in oxime group does not contribute as much to the conjugation of the system as the NHR substituent in hydrazone.[84] The methyl group in the methylhydrazone has an electron-donating effect, whilst the phenyl group in the phenylhydrazone shows an electron-withdrawing property. Taking all these factors into account, the conclusion is reached that the electronic-withdrawing effects of the imino groups decrease in the order: salicylaldoximes > salicylaldehyde phenylhydrazones > salicylaldehyde methylhydrazones. Consequently the phenol acidity and the extractant strength should decrease in that order.

The trend of this electronic effect is strongly supported by ^{1}H NMR spectra. Proton chemical shifts of **L1**, **L6** and **O1** with 4-*tert*-Butylphenol and those of **L2**, **L7** and **O2** with 4-*tert*-butyl-2-methyl-phenol were measured in DMSO-d_6 and listed in Table 2.7. The phenols without the imino groups are included as benchmarks, and the observed smaller chemical shifts suggest that the imino groups are electron-withdrawing, since the protons in hydrazones or oximes get deshielded and the chemical shifts move downfield. Further analysis of the chemical shifts, particularly those of the azomethine protons which vary the most, support that the electron-withdrawing properties decrease in the order: oximes > phenylhydrazones > methylhydrazones.

On the basis of solely the N-substituents and their effect on the acidity of the phenol group, the phenylhydrazones should be stronger extractants than the methylhydrazones, which is proved not to be the case by experiment (section 2.6). In the following sections the effects of the N-substituents on conformations and hydrogen bonding are examined.

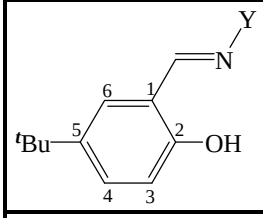	**L1** (Y = NHMe)	**L6** (Y = NHPh)	**O1** (Y = OH)	
C(C*H*$_3$)$_3$	1.25	1.27	1.24	1.22
Ar-*H* (3-position)	6.73	6.81	6.82	6.68[a]
Ar-*H* (4-position)	7.11	7.20	7.25	7.16[b]
Ar-*H* (6-position)	7.29	7.49	7.49	7.16[c]
C*H*N	7.70	8.16	8.34	/
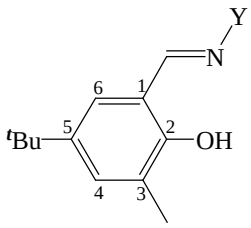	**L2** (Y = NHMe)	**L7** (Y = NHPh)	**O2** (Y = OH)	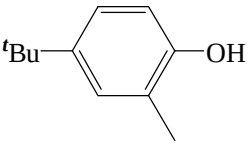
C(C*H*$_3$)$_3$	1.24	1.27	1.24	1.21
Ar-C*H*$_3$	2.16	2.22	2.18	2.10
Ar-*H* (4-position)	7.02	7.13	7.17	7.05[b]
Ar-*H* (6-position)	7.08	7.16	7.21	6.97[c]
C*H*N	7.69	8.12	8.36	/

Table 2.7 Chemical shifts (ppm) in DMSO-d_6 of **L1**, **L6** and **O1** compared with 4-*tert*-butylphenol and **L2**, **L7** and **O2** compared with 4-*tert*-butyl-2-methyl-phenol.

[a,b,c]These analogous protons are respectively in 2-, 3- and 5-positons.

2.8.2 Hydrogen Bonding Motif

The *pseudo*macrocyclic H-bonding arrangements in copper(II) complexes of methylhydrazones, phenylhydrazones and oximes are likely to greatly influence the strength of these extractants. The observation that phenylhydrazones are the weakest

extractants could be rationalized by steric effect on the hydrogen bond motif. As discussed in section 2.3.3, the free ligands of **L6**-**L10** adopt the E conformation in solid state. In case of the copper(II) complexes, the Z conformation will be favoured because it allows the intracomplex hydrogen bonds shown on the right in Figure 2.19. The E conformation (left in Figure 2.19) will experience an impossible steric clash between the phenyl group of the hydrazone and the phenolate part of the other ligand in the planar complexes. In the Z conformation, the repulsion between the azomethine hydrogen atom and the phenyl group of the hydrazone will cause the latter to move out of plane by twisting about the N-N or C-N bond (see Figure 2.19). A combination of the loss of conjugation on complex formation and the weaker hydrogen bond motif are likely to account for phenylhydrazones being the weakest extractants.

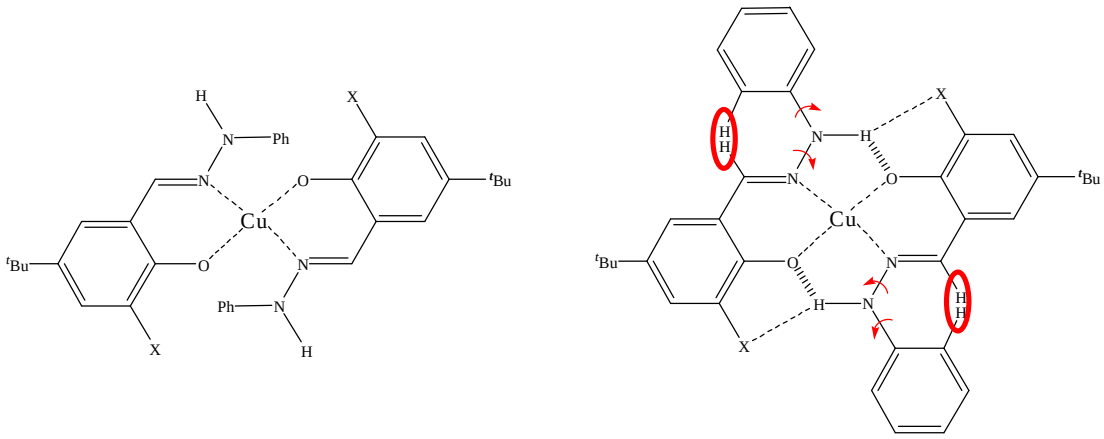

E conformation **Z** conformation

Figure 2.19 The phenylhydrazonato copper(II) complexes $[Cu(L\text{-}H)_2]$ with E or Z conformation about the N-N bond.

2.8.3 Intramolecular Hydrogen Bonding

Intramolecular hydrogen bonding between the phenolic proton and the imino

nitrogen (Figure 2.18) will result in charge redistribution among the nitrogen, hydrogen, oxygen and neighbouring atoms,[85, 86] which could affect the hydrogen bonding motif in the free ligand dimer. It also influences the acidity of the phenol because deprotonation involves breaking both the O-H and N···H bonds.[87] The strength of the intramolecular hydrogen bond will increase with stronger basicity of the imino nitrogen atom and stronger acidity of the phenol group, both of which are dependent on the nature of the N-substituents. The basicity of the imino nitrogen is expected to vary in the order: methylhydrazones > phenylhydrazones > oximes due to the increasing electron-withdrawing effect of the N-substituents. This is supported by ^{15}N chemical shifts in the literature.[88, 89] On the other hand, this electron-withdrawing property of the N-substituent will increase the acidity of the phenol proton in the inverse order as discussed in section 2.8.1. The balance between these two effects makes it difficult to predict the strength of the intramolecular hydrogen bonds in these extractants.

A systematic NMR study was carried out to further investigate the effects of the X and Y substituents (Figure 2.18) on the phenol acidity, hydrogen bonding and intermolecular association in solution, and is described in the following sections.

2.9 Systematic NMR Solution Studies

The NMR spectra of the ligands **L1**-**L10** and **O1**-**O5** were initially run in $CDCl_3$ which is consistent with the solvent used in extraction experiment. However, the phenol proton, hydrazone proton and oxime proton were not observed in most cases due to the existence of trace amount of D_2O and DCl. Consequently the NMR studies involving these groups were run in DMSO-d_6, and the solvent effect was taken into consideration.

2.9.1 Tautomerism

In theory salicylaldehyde methylhydrazones, phenylhydrazones and salicylaldoximes exist as the imino-enol tautomers shown in Figure 2.20 in solution due to the substantial advantage of aromaticity,[29] which is well established in the literature.[90]

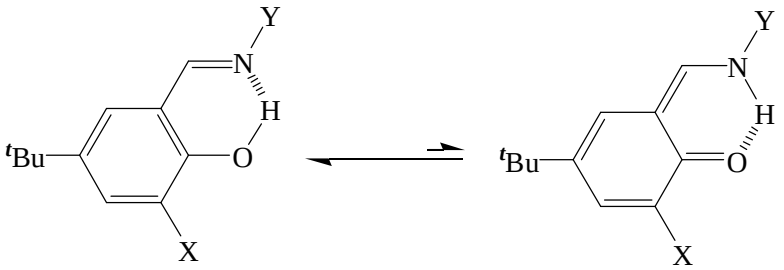

Imino-enol tautomer Amino-keto tautomer

Figure 2.20 Imino-enol and amino-keto tautomeric forms of **L1**-**L10** and **O1**-**O5**

The ^{1}H NMR spectra confirm this by:

- only one tautomer appears in the spectra,
- the aromatic protons can be assigned with the chemical shifts and coupling constants in all cases, which are consistent with the aromatic form of the benzene ring,
- in the methylhydrazones (Y = NHMe in Figure 2.20) a 1H singlet is assigned to the phenol proton, and a 1H quartet is assigned to the N*H*CH_3 group,
- in the phenylhydrazones (Y = NHPh) two 1H singlets are assigned to the phenol proton and hydrazone proton, and
- in the oximes (Y = OH) two 1H singlets are assigned to the phenol proton and oxime proton.

2.9.2 Conformation and Dimerization

In this chapter the methylhydrazones **L1**-**L5** are of greatest interest in term of their metal extraction properties. Consequently the conformation and aggregation of the free ligand in solution were investigated in order to unveil its relationship with the extractant strength. So far there is not much known about whether **L1**-**L5** adopt the E or Z conformation and whether they form dimers in solution. Nuclear Overhauser Effect Spectroscopy (NOESY) experiment provides a useful approach to examine these problems.

The nuclear Overhauser effect (NOE) refers to the phenomenon that when one of two nuclei in close proximity is irradiated, the NMR signal of the other nucleus becomes more intense or weaker.[91, 92] This is because the two nuclei relax each other over the short distance and spin polarization of the observed nucleus from one spin population to another is achieved via the cross-relaxation of the irradiated nucleus.[91, 92] The NOE is distance dependent through space and hence provides information of the molecular geometry. A NOESY spectrum is a two-dimensional spectrum which records all the proton-proton NOEs occurring in a molecule in a single experiment.[91] The NOESY spectrum of **L2** in $CDCl_3$ is shown in Figure 2.21. Each orthogonal is of the proton chemical shifts and the normal spectrum appears on the diagonal.[91] The cross-peak indicates that the two involved protons show the NOE, i.e. are close in space.[91]

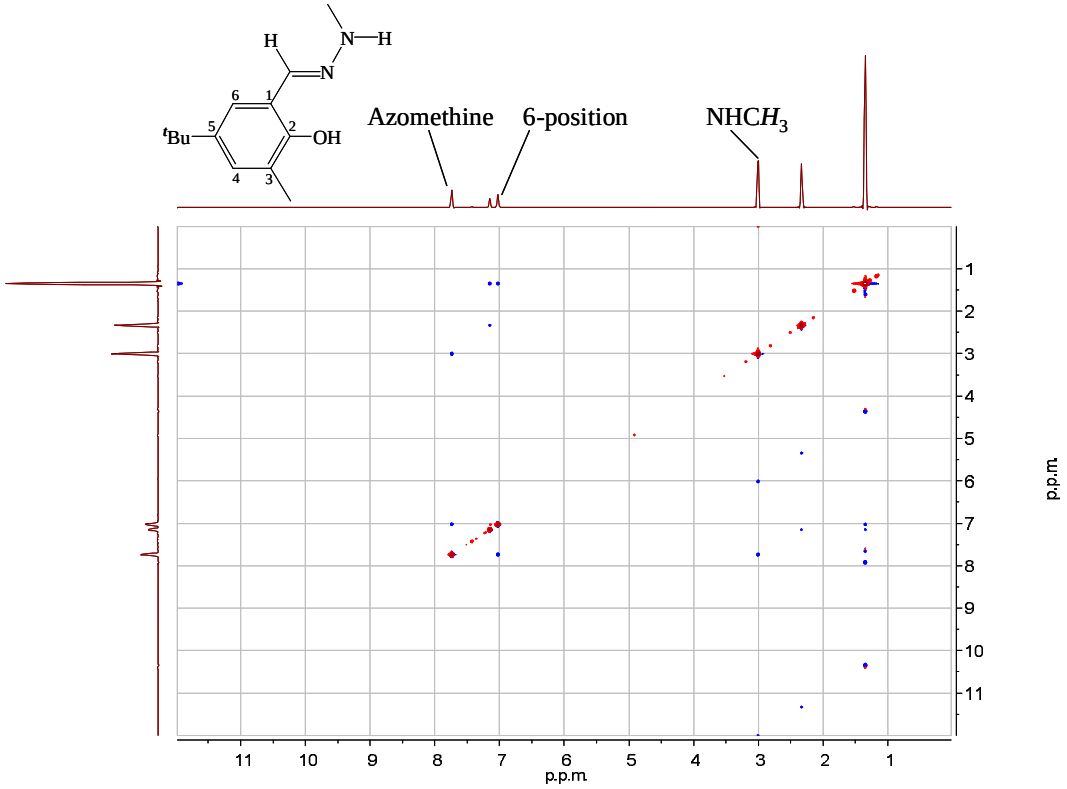

Figure 2.21 NOESY spectrum of **L2** in $CDCl_3$

All the NOESY spectra of **L1**-**L5** were run in $CDCl_3$ to make sure that the conditions are comparable with those of the solvent extraction experiment. The NOESY spectrum of **L2** in Figure 2.21 demonstrates that the N-substituted methyl group is close to the azomethine proton. In theory the N-N bond is free to rotate. However, as discussed in section 2.3.3, the conjugation of the molecule makes it partiallly double bond, which is supported by the shortened N-N bond length. Hence it is highly possible to adopt the E or Z conformation (defined in section 2.3.3) in solution as shown in Figure 2.22. The Z rather than E conformation fits the NOESY spectrum, which allows the dimer to be readily formed in solution. The spectrum also indicates that the azomethine proton and the proton at 6-position of the benzene ring are close to each other. It is not surprising given the conjugation effect and the potential intramolecular hydrogen bond as shown in Figure 2.22.

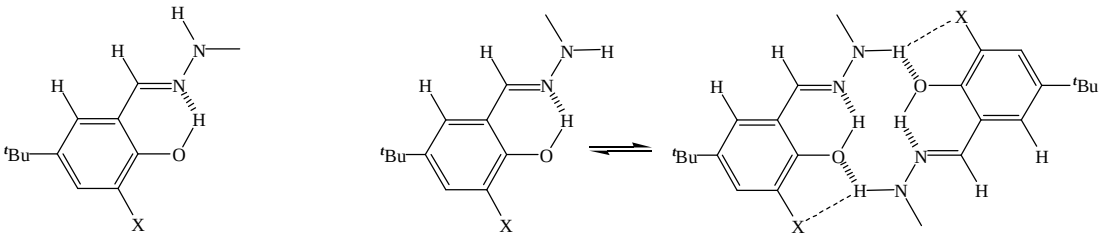

Figure 2.22 E and Z conformation (defined in section 2.3.3) of salicylaldehyde methylhydrazones

The other methylhydrazones **L1** and **L3**-**L5** showed similar NOESY spectra (see Appendix 6.2.5). However, in the spectrum of the nitro-substituted ligand **L3**, the intensity of the cross-peak between the azomethine proton and the 6-position proton of the benzene ring is weaker than those of the other ligands. It is known that the related oxime **O3** adopts a different conformation in the solid state from the other oximes as shown in Figure 2.23. An intramolecular hydrogen bond is formed between the phenol and the nitro group, and the molecular dimerizes by association of the oxime groups.[22] Consequently the azomethine proton is far away from the 6-position proton. Such an arrangement is likely to be present in the monomeric form B or dimer C of **L3** (Figure 2.23), and could explain the weaker NOE observed.

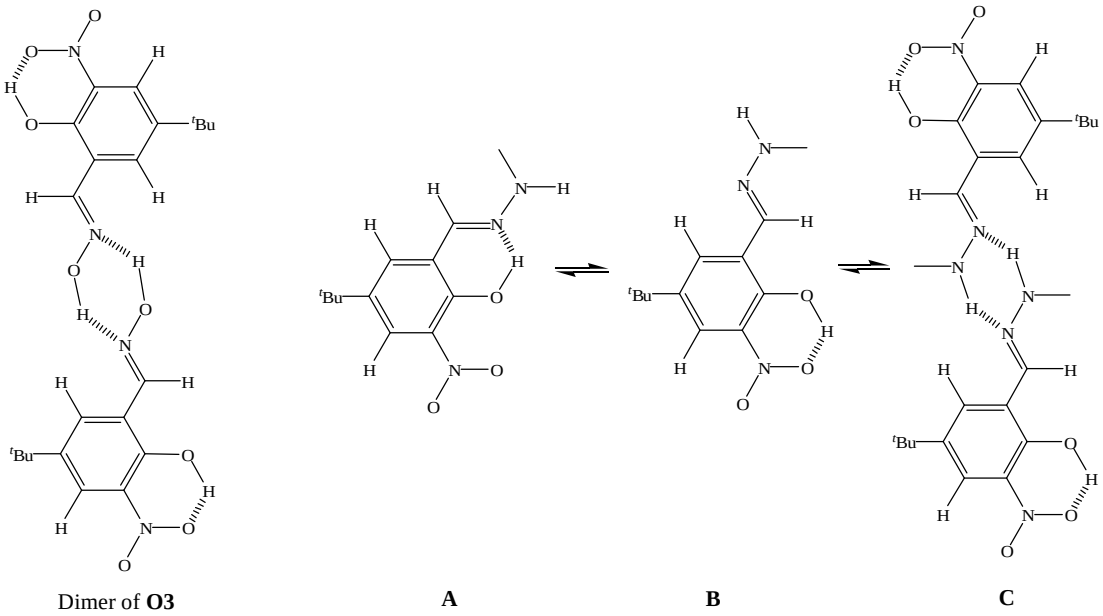

Figure 2.23 The conformation of the nitro-substituted oxime **O3** in the solid state[22] and possible conformations of **L3**

In order to investigate the conformation of **L3** further in solution, the 1D NOE difference spectra were run in $CDCl_3$ for **L1** and **L3**. The spectrum is achieved by subtracting the normal spectrum from a spectrum taken with the irradiating signal on, and hence showing only the difference between the two spectra.[91] Figure 2.24 shows the NOE difference spectrum of **L1** when the 3-position proton on the benzene ring is irradiated. An intense signal appears at the irradiating frequency, and the integrations of the other peaks simply indicate the NOEs. All the unaffected signals have integration values of zero. An advantage of the NOE difference experiment is that it provides a method to calculate the distance between the involved protons in solution from the value of their NOE. It is very sensitive since the NOE has a $1/r^6$ dependence on the distance r between the protons.[91] To calculate the distances, a pair of protons giving rise to the NOE need be used as the standard, which ideally is internal, not undergoing a lot of motion, showing the maximal NOE and of a known distance. The protons on 3- and 4- position of the benzene ring of **L1** are chosen. As

shown in Figure 2.24, the integration of the irradiated 3-position proton is normalized to the value -100.000, and the NOE of the 4-position proton is 1.603. The distance between these two protons in the crystal structure of **L6** is measured as 2.312 Å. When protons other than the 3-position proton are irradiated, the integration unit is kept unchanged by normalizing the integrations of the irradiated peaks according to the number of protons irradiated. In case of **L3**, the NOE between the 6-position proton on the benzene ring and the *tert*-butyl protons is monitored, and gives a consistent value with that of **L1**. Thus the standard obtained from **L1** is applied to **L3**.

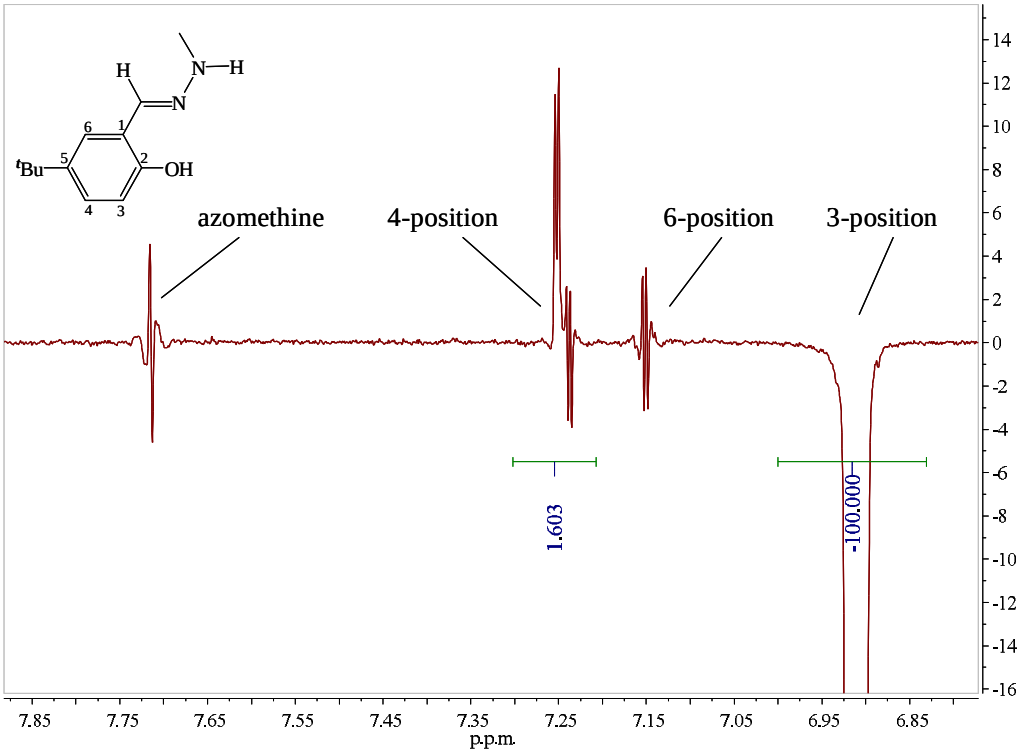

Figure 2.24 NOE difference spectrum of **L1** when the 3-position proton on the benzene ring is irradiated.

The key NOE values and distances calculated from the NOE difference spectra are listed in Table 2.8. In **L3** the azomethine proton and the 6-position proton are further

apart compared to **L1**, but still fairly close to each other. This suggests that a small portion of the ligands possibly adopt the conformation in Figure 2.23, but the Z conformation could remain to be predominant. The azomethine proton and the NCH_3 protons are closer in **L3** than in **L1**, which suggests that dimers of both potential conformations are more likely to form from **L3** resulting in the more rigid geometry.

Protons involved	**L1**		**L3**	
	NOE	**Distance**/Å	**NOE**	**Distance**/Å
Azomethine↔6-position	2.578	2.136	1.982	2.232
Azomethine↔NC*H*$_3$	4.053	1.981	5.042	1.910

Table 2.8 NOE values and calculated distances in **L1** and **L3**

2.9.3 3-Substituent Effect on Phenol Acidity

Research in the literature[93, 94] has shown that there is a good linear correlation between the pK_a values of phenols in aqueous solution and the chemical shift of their phenol protons at infinite dilution in DMSO. The ^{1}H NMR spectra of **L1-L10** and **O1-O5** in DMSO-d_6 were obtained to investigate the effect of the 3-substituents on the phenol acidity. First, the phenol proton needed to be correctly assigned, which in principle could be difficult because the hydrazone or the oxime protons occurs at similar chemical shifts and could be also exchangable.

For the methylhydrazones, the hydrazone proton shows a spin-spin coupling with the NC*H*$_3$ protons and appears as a quartet at 7-8 ppm. The ^{1}H NMR spectrum of **L1** is shown as an example in Figure 2.25. All the protons in **L1-L5** can be unambiguously assigned and the phenol proton appears as a singlet above 10 ppm.

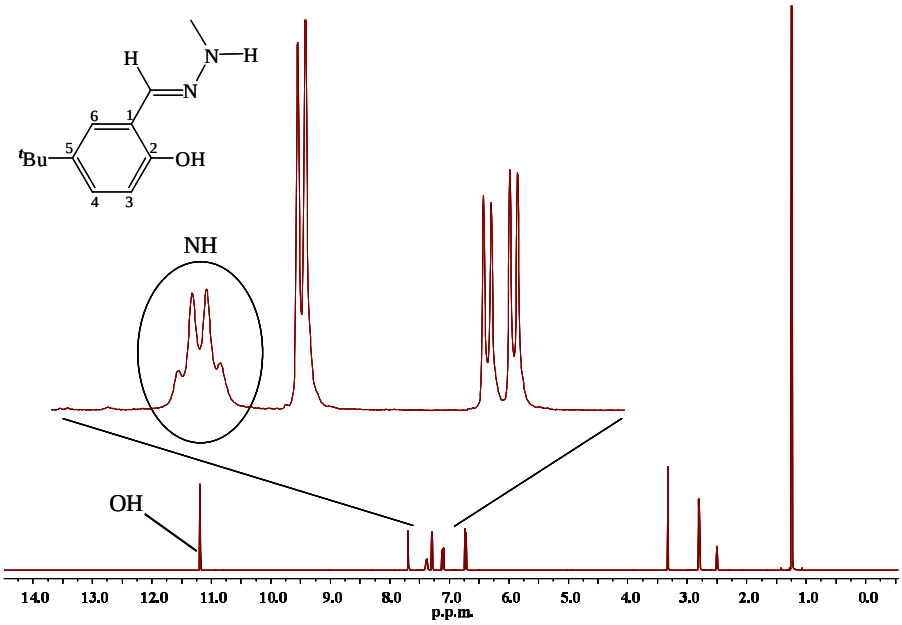

Figure 2.25 ^{1}H NMR spectrum of **L1** in DMSO-d_6

For the phenylhydrazones, both the phenol proton and the hydrazone proton show as singlets above 10 ppm. In order to distinguish them, Correlated Spectroscopy (COSY) experiment was carried out. The COSY spectrum is a two-dimensional NMR spectrum which indicates all the spin-spin coupled protons.[91] The COSY spectrum of the methyl-substituted ligand **L7** in DMSO-d_6 is shown in Figure 2.26. Each orthogonal is of the proton chemical shifts and the normal spectrum appears on the diagonal.[91] The cross-peak indicates that the two involved protons are mutually spin-spin coupled.[91] The COSY spectrum in Figure 2.26 demonstrates spin-spin coupling between the azomethine proton around 8 ppm and one of the protons above 10 ppm which is therefore assigned as the hydrazone proton. The two protons involved are four bonds apart, and hence the coupling is too weak to appear in 1D ^{1}H NMR spectrum. However, given the conjugation in the molecule, the COSY spectrum is not surprising, and suggests that the terminal nitrogen could influence the electron density in the conjugated system. All the protons in **L6-L10** can be unambiguously assigned and the phenol proton appears more downfield than the

hydrazone proton, with only the exception being the methoxy-substituted ligand **L10**.

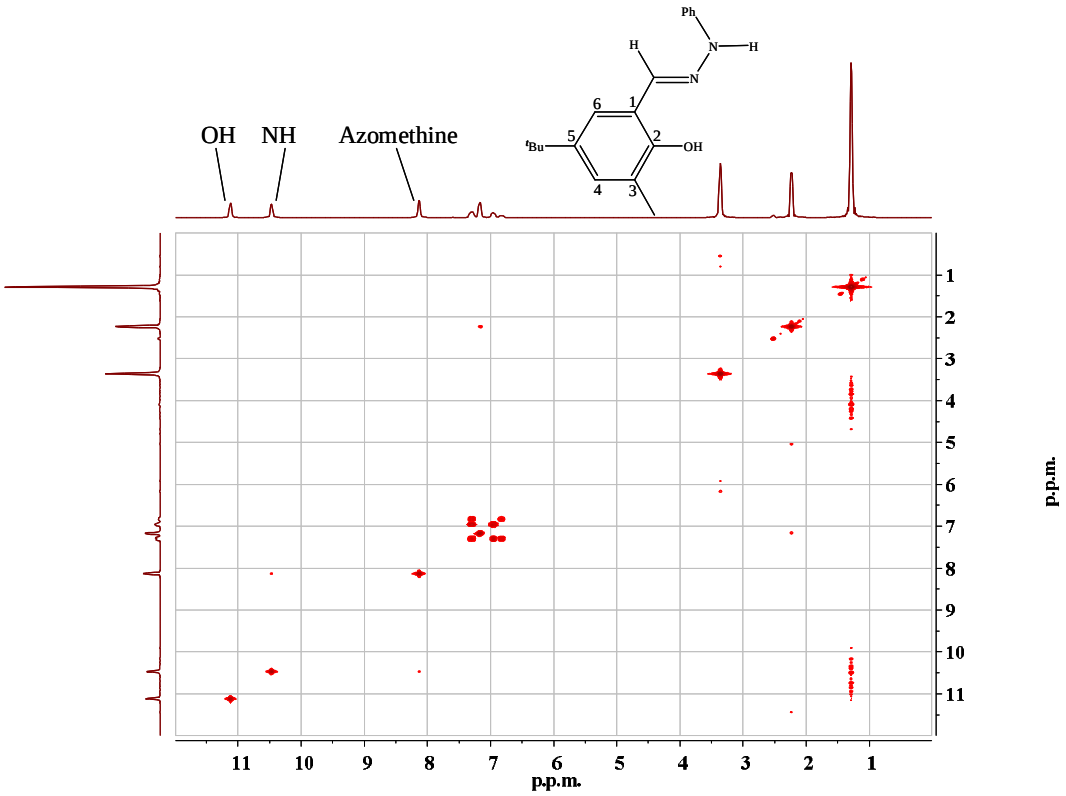

Figure 2.26 The COSY spectrum of the methyl-substituted phenylhydrazone **L7** in DMSO-d_6

For the oximes, the situation is similar to the phenylhydrazones, with both the phenol proton and the oxime proton showing as singlets above 9 ppm. However, the COSY experiment did not show spin-spin coupling between the azomethine and the oxime protons, which suggests that the oxime oxygen is not much involved in the conjugation of the molecule as discussed in section 2.8.1. Heteronuclear Multiple Bond Connectivity (HMBC, also known as long-range ^{1}H-^{13}C COSY) experiment was carried out to distinguish the phenol and oxime protons. The HMBC spectrum is a two-dimensional spectrum with ^{13}C chemical shifts on one axis and ^{1}H chemical shifts on the other.[91] Figure 2.27 shows the HMBC spectrum of the unsubstituted

oxime **O1** in DMSO-d_6. The cross-peak indicates a correlation between the ^{13}C nucleus and the proton which are separated by two or three bonds.[91] The atoms in between are usually carbons with the occasional exception of other nuclei, which are oxygen and nitrogen in the case of salicylaldoximes. Fortunately the HMBC spectrum in Figure 2.27 demonstrates the correlation between the azomethine ^{13}C at 148.95 ppm and the proton at 11.25 ppm, which confirms the latter to be the oxime proton. Consequently all the protons in **O1**-**O5** are unambiguously assigned and the phenol proton appears more upfield than the oxime proton, which is different from most of the hydrazones.

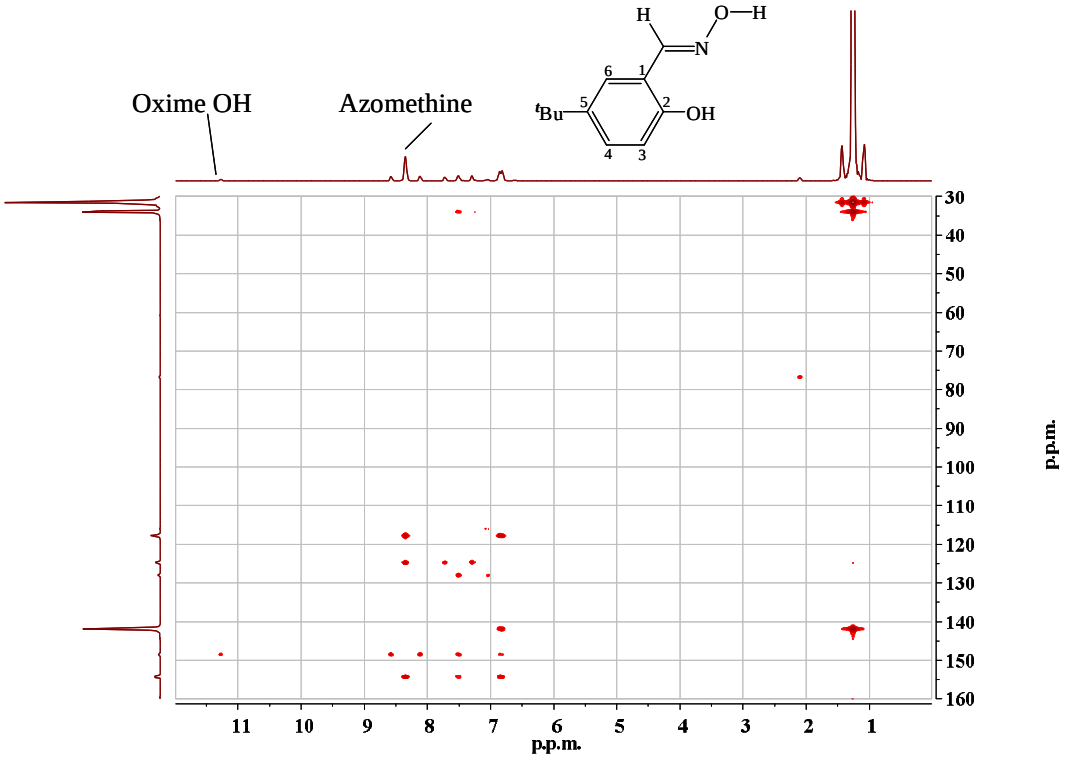

Figure 2.27 The HMBC spectrum of the unsubstituted oxime **O1** in DMSO-d_6.

The chemical shifts of the phenol, hydrazone and oxime protons of **L1**-**L10** and **O1**-**O5** in DMSO-d_6 are listed in Table 2.9. The results suggest that the 3-substituent effects on the chemical shifts of the phenol protons in salicylaldehyde

methylhydrazones, phenylhydrazones and salicylaldoximes are consistent, and hence should increase the phenol acidities in the order: OMe < H < Me < Br < NO_2.

3-Substituent	Methylhydrazone		Phenylhydrazone		Oxime	
H	**L1**		**L6**		**O1**	
	Ar-O*H*	**N*H*CH$_3$**	**Ar-O*H***	**N*H*Ph**	**Ar-O*H***	**NO*H***
	11.19	7.38	10.40	10.37	9.88	11.25
CH$_3$	**L2**		**L7**		**O2**	
	Ar-O*H*	**N*H*CH$_3$**	**Ar-O*H***	**N*H*Ph**	**Ar-O*H***	**NO*H***
	11.57	7.36	11.09	10.44	10.12	11.42
NO$_2$	**L3**		**L8**		**O3**	
	Ar-O*H*	**N*H*CH$_3$**	**Ar-O*H***	**N*H*Ph**	**Ar-O*H***	**NO*H***
	12.94	7.89	11.76	10.76	11.13	11.80
Br	**L4**		**L9**		**O4**	
	Ar-O*H*	**N*H*CH$_3$**	**Ar-O*H***	**N*H*Ph**	**Ar-O*H***	**NO*H***
	12.26	7.67	11.64	10.68	10.69	11.71
OCH$_3$	**L5**		**L10**		**O5**	
	Ar-O*H*	**N*H*CH$_3$**	**Ar-O*H***	**N*H*Ph**	**Ar-O*H***	**NO*H***
	11.08	7.39	9.99	10.36	9.48	11.25

Table 2.9 Chemical shifts of the phenol, hydrazone and oxime protons of **L1**-**L10** and **O1**-**O5** in DMSO-d_6

2.9.4 Intramolecular and Intermolecular Hydrogen Bonding

The formation of hydrogen bonds between ligands and the potential assembly of dimers are of great relevance to the properties of these ligands as metal extractants. The phenol, hydrazone and oxime protons appear as sharp peaks at quite low field in

the ^{1}H NMR spectra in DMSO-d_6, which indicates their involvement in hydrogen bonds[91] and provides the possibility of investigating these hydrogen bonds by NMR spectroscopy. However, the pronounced tendency of DMSO to act as a strong hydrogen bond acceptor complicates the situation and could break hydrogen bonds in or between the ligands. Despite this complication, temperature dependent and concentration dependent ^{1}H NMR experiment was carried out to elucidate aggregation of the ligands.

2.9.4.1 Temperature Dependence

Although the resonance position of most signals is generally little affected by temperature, OH and NH protons resonate at a higher field at higher temperature because the degree of hydrogen bonding is reduced.[91] It is also well established in the literature[95-98] that intramolecular hydrogen bonds are much less sensitive to temperature change than intermolecular hydrogen bonds, and hence the temperature dependent NMR study could discriminate these two types of hydrogen bonds. For the phenol and hydrazone protons of **L1**-**L5**, the temperature dependence of the chemical shifts is shown in Figure 2.28. All the chemical shifts are recorded relative to the TMS peak at the respective temperature.

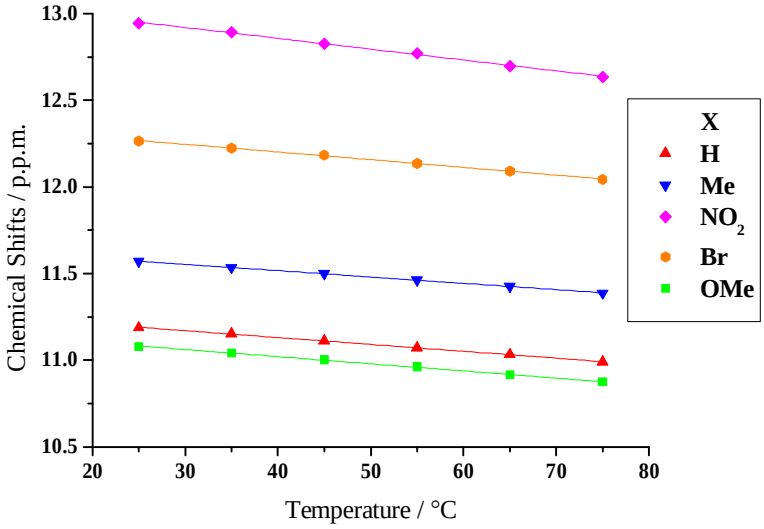

(a) Phenol protons

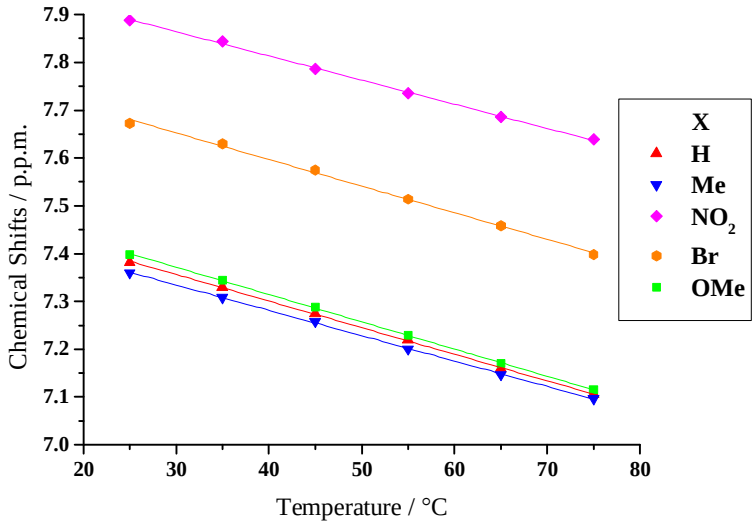

(b) Hydrazone protons

Figure 2.28 The temperature dependence of chemical shifts of the OH and NH protons in **L1**-**L5**

The chemical shifts of the phenol, hydrazone and oxime protons in **L1**-**L10** and **O1**-**O5** all show an excellent linear correlation with the temperature, while the peaks

of other protons barely move. The plots for the phenol and hydrazone protons of **L1**-**L5** (Figure 2.28) indicate that the phenol proton peaks are less temperature dependent than the hydrazone proton peaks. In order to demonstrate the difference, the Δδ/ΔT values were calculated for **L1**-**L10** and **O1**-**O5** as shown in Table 2.10.

3-Substituent	Methylhydrazone		Phenylhydrazone		Oxime	
H	**L1**		**L6**		**O1**	
	Ar-O*H*	**N*H*CH$_3$**	**Ar-O*H***	**N*H*Ph**	**Ar-O*H***	**NO*H***
	3.94	5.52	1.66	5.54	3.40	4.70
CH$_3$	**L2**		**L7**		**O2**	
	Ar-O*H*	**N*H*CH$_3$**	**Ar-O*H***	**N*H*Ph**	**Ar-O*H***	**NO*H***
	3.62	5.26	3.64	6.30	3.08	5.70
NO$_2$	**L3**		**L8**		**O3**	
	Ar-O*H*	**N*H*CH$_3$**	**Ar-O*H***	**N*H*Ph**	**Ar-O*H***	**NO*H***
	6.18	4.98	3.54	5.56	2.94	5.30
Br	**L4**		**L9**		**O4**	
	Ar-O*H*	**N*H*CH$_3$**	**Ar-O*H***	**N*H*Ph**	**Ar-O*H***	**NO*H***
	4.42	5.50	4.16	6.08	3.68	5.58
OCH$_3$	**L5**		**L10**		**O5**	
	Ar-O*H*	**N*H*CH$_3$**	**Ar-O*H***	**N*H*Ph**	**Ar-O*H***	**NO*H***
	4.10	5.66	0.94	5.40	3.40	4.86

Table 2.10 The Δδ/ΔT values (10^{-3} ppm/K) of the phenol, hydrazone and oxime protons of **L1**-**L10** and **O1**-**O5** in DMSO-d_6

In all cases the phenol protons are much less sensitive than the hydrazone or oxime protons to temperature change. This suggests that the phenol protons form intramolecular hydrogen bonds to the azomethine nitrogen atoms even in DMSO-d_6.

The Δδ/ΔT values of **L6**-**L10** are generally smaller, particularly **L6** and **L10**, which could suggest that the intramolecular hydrogen bonds are extremely strong in salicylaldehyde phenylhydrazones. Thus the deprotonation of the phenol group is more difficult and this could be another reason why the phenylhydrazones are the weakest extractants.

2.9.4.2 Concentration Dependence

Concentration also affects the chemical shifts of the OH and NH protons via hydrogen bonding.[91, 99] They appear at lower field at higher concentrations because the degree of intermolecular hydrogen bonding increases and stronger deshielding occurs.[91, 99] However, the protons involved in the intramolecular hydrogen bonds should be unaltered by varying concentration.[91, 99] The hydrogen bonds in DMSO solutions could be complicated because the solvent itself is a hydrogen bond acceptor. The concentration dependence NMR study was attempted by diluting a NMR sample containing 40 mg compound in 0.6 ml to respectively 1.2 ml, 1.6 ml and 2.4 ml in the same NMR tube. The results for **L1**-**L5** are shown in Figure 2.29, and the other extractants **L6**-**L10** and **O1**-**O5** behave similarly. All the chemical shifts barely change, which suggests that the OH and NH protons are involved in either intramolecular hydrogen bonding or hydrogen bonding with the solvent DMSO.

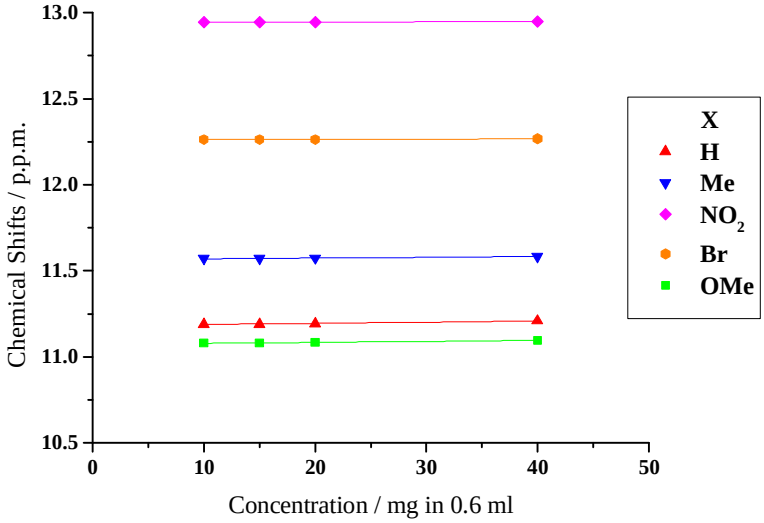

(a) Phenol protons

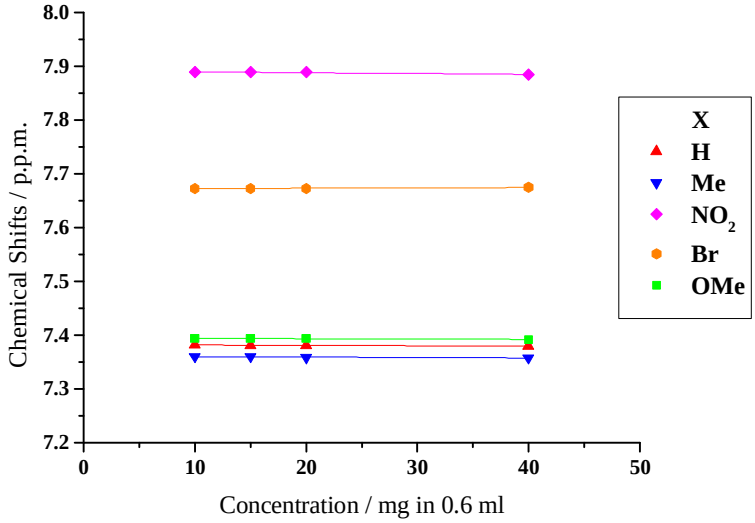

(b) Hydrazone protons

Figure 2.29 Concentration dependence of chemical shifts of the OH and NH protons in **L1**-**L5**

The combination of the temperature dependence and concentration dependence ^{1}H NMR experiment in DMSO demonstrates that the phenol protons in **L1**-**L10** and

O1-**O5** form intramolecular hydrogen bonds in solution, while the dimerization is less likely to happen due to the strong solvating effect of DMSO.

2.10 Experimental

2.10.1 Chemicals and Instrumentation

Unless otherwise specified a reagent or solvent was used as obtained from Aldrich, Fisher or Acros. Standards for inductively coupled plasma optical emission spectroscopy (ICP- OES) were purchased from Alfa Asar.

^{1}H and ^{13}C NMR spectra in section 2.3 were run on a Bruker ARX250 at ambient temperature. ^{1}H NMR spectra in section 2.9 were recorded on a Bruker DPX360 spectrometer at 298 K (unless stated otherwise), and chemical shifts (δ) are reported in parts per million (ppm) relative to TMS. CHN analytical data were obtained by the University of St Andrews Microanalytical Service. Mass spectrometry was performed on a Micromass ZMD instrument with a z-spray ESI source. Melting points were measured on a Gallenkamp melting point apparatus. ICP-OES analysis was performed on a Perkin Elmer Optima 5300DV spectrometer. The measurement of pH was carried out using a Sartorius PP-50 pH-meter. X-ray crystal structure determination was obtained by the University of Edinburgh Crystallography Service.

2.10.2 Ligand Synthesis

5-*tert*-Butyl-2-hydroxybenzaldehyde (1) Magnesium turnings (0.175 g, 7.20 mmol) were added to anhydrous methanol (10 ml) to form an 8% w/w methanol solution of magnesium methoxide. Magnesium turnings (20.0 g, 0.822 mol), methanol (360 ml), toluene (160 ml) and the solution of magnesium methoxide were stirred and refluxed

until all the magnesium was dissolved and H_2 evolution ceased. 4-*tert*-Butylphenol (203 g, 1.35 mol) was added and refluxed for a further hour. Toluene (330 ml) was added and the mixture was distilled under vacuum to remove the methanol-toluene azeotrope. Paraformaldehyde (120 g) in toluene (200 ml) was added slowly with concurrent removal of solvent by distillation. After cooling to room temperature, H_2SO_4 (20%, 800 ml) was added slowly with stirring and heated to 50 °C to dissolve all solids. The product was extracted with toluene (2 × 350 ml), washed with H_2SO_4 (10%, 2 × 150 ml) and water (150 ml), dried over $MgSO_4$, concentrated *in vacuo* and purified by silica-60 wet flash column chromatography (eluting with 2% ethyl acetate in hexane) to yield a bright yellow oil (141 g, 59%). (Anal. Calc. for $C_{11}H_{14}O_2$: C, 74.13; H, 7.92. Found: C, 73.85; H, 8.14%); ^{1}H NMR ($CDCl_3$, 250 MHz): δ 1.33 (s, 9H, C(C*H*$_3$)$_3$), 6.92 (d, 1H, Ar-*H*), 7.52 (d, 1H, Ar-*H*), 7.58 (dd, 1H, Ar-*H*), 9.88 (s, 1H, C*H*O), 10.88 (s, 1H, O*H*); ^{13}C NMR ($CDCl_3$, 250 MHz): δ 31.5 (3C, C(*C*H$_3$)$_3$), 34.4 (1C, *C*(CH$_3$)$_3$), 117.5 (1C, Ar-*C*), 120.4 (1C, Ar-*C*), 130.0 (1C, Ar-*C*), 134.9 (1C, Ar-*C*), 143.0 (1C, Ar-*C*), 159.8 (1C, Ar-*C*), 197.1 (1C, *C*HO). ESIMS *m/z* 179 (MH^+). Melting Point N/A (oil).

5-*tert*-Butyl-2-hydroxy-3-methylbenzaldehyde (2) Hexamethylenetetramine (30.9 g, 220 mmol) and 4-*tert*-butyl-2-methylphenol (7.45 g, 45 mmol) were mixed and heated in trifluoroacetic acid (110 ml) to 90 °C for 16 h under reflux. The mixture was poured still hot into 1 M HCl (200 ml), stirred for 6 h and extracted with DCM (3 × 150 ml). The combined organic phases were washed with water, dried over $MgSO_4$ and the solvent removed *in vacuo*. Chromatography (5% ethyl acetate in hexane eluent) was carried out to yield a pale yellow solid (6.07 g, 70%). (Anal. Calc. for $C_{12}H_{16}O_2$: C, 74.97; H, 8.39. Found: C, 74.72; H, 8.78%); ^{1}H NMR ($CDCl_3$, 250 MHz): δ 1.33 (s, 9H, C(C*H*$_3$)$_3$), 2.28 (s, 3H, C*H*$_3$), 7.36 (m, 1H, Ar-*H*), 7.45 (m, 1H, Ar-*H*), 9.88 (s, 1H, C*H*O), 11.12 (s, 1H, O*H*); ^{13}C NMR ($CDCl_3$, 250 MHz): δ 15.7 (1C, *C*H$_3$) 31.7 (3C, C(*C*H$_3$)$_3$), 34.4, (1C, *C*(CH$_3$)$_3$), 119.8 (1C, Ar-*C*), 126.6 (1C,

Ar-*C*), 127.7 (1C, Ar-*C*), 136.1 (1C, Ar-*C*), 142.6 (1C, Ar-*C*), 158.3 (1C, Ar-*C*), 197.3 (1C, *C*HO). ESIMS *m/z* 193 (MH^+). Melting Point 37-38 °C.

5-*tert*-Butyl-2-hydroxy-3-nitrobenzaldehyde (3) Nitric acid (4.17 ml, 95.2 mmol) was added dropwise to a solution of **(1)** (15.0 g, 84.2 mmol) in glacial acetic acid (15 ml) at 0 °C. The mixture was stirred at 55 °C for 20 h and then allowed to cool to room temperature. The orange solution was extracted with DCM (150 ml) and washed with water (2 x 100 ml) and tried over $MgSO_4$. The solvent was removed *in vacuo*. Purification by silica-60 wet flash column chromatography (2 % ethyl acetate in hexane eluent) yielded an orange solid (7.66 g, 41 %). (Anal. Calc. for $C_{11}H_{13}N_1O_4$: C, 59.19; H, 5.87; N, 6.27. Found: C, 59.00; H, 5.95; N, 6.33%); ^{1}H NMR ($CDCl_3$, 250 MHz): δ 1.36 (s, 9H, C(C*H*$_3$)$_3$), 8.15 (d, 1H, Ar-H), 8.34 (d, 1H, Ar-*H*), 10.43 (s, 1H, C*H*O), 11.25 (s, 1H, O*H*); ^{13}C NMR ($CDCl_3$, 250 MHz): δ 31.3 (3C, C(*C*H$_3$)$_3$), 35.0 (1C, *C*(CH$_3$)$_3$), 125.4 (1C, Ar-*C*), 128.3 (1C, Ar-*C*), 134.7 (1C, Ar-*C*), 135.2 (1C, Ar-*C*), 143.9 (1C, Ar-*C*), 154.9 (1C, Ar-*C*), 189.8 (1C, *C*HO). ESIMS *m/z* 224 (MH^+). Melting Point 86-87 °C.

3-Bromo-5-*tert*-butyl-2-hydroxybenzaldehyde (4) Bromine (29.1 g, 0.180 mol) in glacial acetic acid (300 ml) was added to a solution of **(1)** (31.27 g, 0.177 mol) and sodium acetate (26.83 g, 0.326 mol) in glacial acetic acid (500 ml) via a dropping funnel over 50 min. The yellow solution was stirred at 50 °C for 12 h. The solvent was removed *in vacuo* and water (400 ml) and DCM (250 ml) were added to the precipitate. After separation the aqueous phase was extracted again with DCM (2 x 100 ml). The combined organic phases were washed with $Na_2S_2O_5$ solution (300 ml, 10 % w/w), saturated $NaHCO_3$ solution (400 ml) and dried over $MgSO_4$. After removing the solvent *in vacuo* the solid was recrystallized from light petroleum spirits (bp 40-60 °C) to give yellow crystals (33.93 g, 75 %). (Anal. Calc. for $C_{11}H_{13}BrO_2$: C, 51.38; H, 5.10. Found: C, 51.32; H, 5.22%); ^{1}H NMR ($CDCl_3$, 250

MHz): δ 1.33 (s, 9H, C(C*H*$_3$)$_3$), 7.52 (d, 1H, Ar-*H*), 7.82 (d, 1H, Ar-*H*), 9.86 (s, 1H, C*H*O), 11.42 (s, 1H, O*H*). ^{13}C NMR ($CDCl_3$, 250 MHz): δ 31.6 (3C, C(*C*H$_3$)$_3$), 34.7 (1C, *C*(CH$_3$)$_3$), 111.2 (1C, Ar-*C*), 121.1 (1C, Ar-*C*), 129.8 (1C, Ar-*C*), 138.0 (1C, Ar-*C*), 144.6 (1C, Ar-*C*), 156.2 (1C, Ar-*C*), 196.6 (1C, *C*HO). ESIMS *m/z* 257 (MH^+). Melting Point 82-83 °C.

5-*tert*-Butyl-2-hydroxy-3-methoxybenzaldehyde (5) Sodium (3.20 g, 139 mmol) was added to anhydrous methanol (42 ml) to prepare a 4 M $NaOCH_3$/MeOH solution. **(4)** (5.40 g, 20.0 mmol) was dissolved in the minimum anhydrous methanol and poured into a refluxing mixture of the 4 M $NaOCH_3$/MeOH solution (35 ml), ethyl acetate (2.5 ml) and Cu(I)Br (1.0 g, 7 mmol) under nitrogen. The resulting solution was refluxed overnight. After the solvent was removed *in vacuo*, the solid was dissolved in 3 M HCl (100 ml) and extracted with ethyl acetate (3 x 100 ml). The combined organic phases were dried with $MgSO_4$, evaporated *in vacuo* and purified by silica-60 wet flash column chromatography (9 % diethyl-ether in petrolether eluent) to yield a yellow solid (2.23 g, 54 %). (Anal. Calc. for $C_{12}H_{16}O_3$: C, 69.21; H, 7.74. Found: C, 69.29; H, 7.69%); ^{1}H NMR ($CDCl_3$, 250 MHz): δ 1.34 (s, 9H, C(C*H*$_3$)$_3$), 3.94 (s, 3H, OC*H*$_3$), 7.15 (d, 1H, Ar-*H*), 7.18 (d, 1H, Ar-*H*), 9.92 (s, 1H, C*H*O), 10.96 (s, 1H, O*H*); ^{13}C NMR ($CDCl_3$, 250 MHz): δ 31.7 (3C, C(*C*H$_3$)$_3$), 34.8 (1C, *C*(CH$_3$)$_3$), 56.8 (1C, O*C*H$_3$), 116.9 (1C, Ar-*C*), 120.5 (1C, Ar-*C*), 121.0 (1C, Ar-*C*), 143.2 (1C, Ar-*C*), 148.2 (1C, Ar-*C*), 150.0 (1C, Ar-*C*), 197.2 (1C, Ar*C*HO). ESIMS *m/z* 209 (MH^+). Melting Point 56-57 °C.

Methylhydrazone Formation General Procedure. A solution of the appropriate precursor aldehyde in ethanol was slowly added to one equivalent of methylhydrazine in ethanol. The resulting mixture was stirred for 30 min and the solvent was removed *in vacuo* to yield the product which needs no further purification.

5-*tert*-Butyl-2-hydroxy-benzaldehyde methylhydrazone (L1) Combining ethanolic solutions of methylhydrazine (0.49 g, 10.6 mmol) and (1) (1.83 g, 10.3 mmol) as in the general procedure gave a yellow solid (2.08 g, 98%). (Anal. Calc. for $C_{12}H_{18}N_2O$: C, 69.87; H, 8.80; N, 13.58. Found: C, 70.48; H, 8.30; N, 13.94%); ^{1}H NMR ($CDCl_3$, 250 MHz): δ 1.34 (s, 9H, C(C*H*$_3$)$_3$), 2.97 (s, 3H, NHC*H*$_3$), 6.89 (d, 1H, Ar-*H*), 7.13 (d, 1H, Ar-*H*), 7.23 (dd, 1H, Ar-*H*), 7.69 (s, 1H, C*H*N); ^{13}C NMR ($CDCl_3$, 250 MHz): δ 31.9 (3C, C(*C*H$_3$)$_3$), 34.4 (1C, *C*(CH$_3$)$_3$), 35.0 (1C, NH*C*H$_3$), 116.3 (1C, Ar-*C*), 118.9 (1C, Ar-*C*), 126.1 (1C, Ar-*C*), 126.7 (1C, Ar-*C*), 140.5 (1C, *C*HN), 142.1 (1C, Ar-*C*), 155.3 (1C, Ar-*C*). ESIMS *m/z* 207 (MH^+). Melting Point 42-43 °C.

5-*tert*-Butyl-2-hydroxy-3-methylbenzaldehyde methylhydrazone (L2) Combining ethanolic solutions of methylhydrazine (0.50 g, 10.8 mmol) and **(2)** (1.92 g, 10.0 mmol) as in the general procedure gave a yellow solid (2.19 g, 99%). (Anal. Calc. for $C_{13}H_{20}N_2O$: C, 70.87; H, 9.15; N, 12.72. Found: C, 70.73; H, 9.56; N, 12.92%); ^{1}H NMR ($CDCl_3$, 250 MHz): δ 1.30 (s, 9H, C(C*H*$_3$)$_3$), 2.28 (s, 3H, C*H*$_3$), 2.98 (s, 3H, NHC*H*$_3$), 6.98 (d, 1H, Ar-*H*), 7.10 (d, 1H, Ar-*H*), 7.70 (s, 1H, C*H*N); ^{13}C NMR ($CDCl_3$, 250 MHz): δ 16.4 (1C, *C*H$_3$), 31.9 (3C, C(*C*H$_3$)$_3$), 34.3 (1C, *C*(CH$_3$)$_3$), 35.3 (1C, NH*C*H$_3$), 118.1 (1C, Ar-*C*), 123.9 (1C, Ar-*C*), 125.0 (1C, Ar-*C*), 128.3 (1C, Ar-*C*), 141.1 (1C, *C*HN), 141.6 (1C, Ar-*C*), 153.5 (1C, Ar-*C*). ESIMS *m/z* 221 (MH^+). Melting Point 95-96 °C.

5-*tert*-Butyl-2-hydroxy-3-nitrobenzaldehyde methylhydrazone (L3) Combining ethanolic solutions of methylhydrazine (0.62 g, 13.4 mmol) and **(3)** (3.01 g, 13.4 mmol) as in the general procedure yielded an orange solid (3.26 g, 97%). (Anal. Calc. for $C_{12}H_{17}N_3O_3$: C, 57.36; H, 6.82; N, 16.72. Found: C, 57.41; H, 6.72; N, 16.34%); ^{1}H NMR ($CDCl_3$, 250 MHz): δ 1.33 (s, 9H, C(C*H*$_3$)$_3$), 3.03 (s, 3H, NHC*H*$_3$), 7.64 (d, 1H, Ar-*H*), 7.72 (s, 1H, C*H*N), 7.90 (d, 1H, Ar-*H*); ^{13}C NMR ($CDCl_3$, 250 MHz): δ 31.5 (3C, C(*C*H$_3$)$_3$), 34.2 (1C, *C*(CH$_3$)$_3$), 34.7 (1C, NH*C*H$_3$), 121.4 (1C, Ar-*C*), 123.6

(1C, Ar-*C*), 131.1 (1C, Ar-*C*), 134.1 (1C, *C*HN), 136.5 (1C, Ar-*C*), 142.4 (1C, Ar-*C*), 150.4 (1C, Ar-*C*). ESIMS *m/z* 252 (MH^+). Melting Point 116-117 °C.

3-Bromo-5-tert-butyl-2-hydroxybenzaldehyde methylhydrazone (L4) Combining ethanolic solutions of methylhydrazine (0.75 g, 16.3 mmol) and **(4)** (4.12 g, 16.0 mmol) as in the general procedure gave a yellow solid (4.20 g, 92%). (Anal. Calc. for $C_{12}H_{17}BrN_2O$: C, 50.54; H, 6.01; N, 9.82. Found: C, 50.87; H, 5.85; N, 9.57%); ^{1}H NMR ($CDCl_3$, 250 MHz): δ 1.29 (s, 9H, C(CH_3)$_3$), 2.98 (s, 3H, NHCH_3), 7.07 (d, 1H, Ar-*H*), 7.43 (d, 1H, Ar-*H*), 7.60 (s, 1H, C*H*N); ^{13}C NMR ($CDCl_3$, 250 MHz): δ 31.8 (3C, C(*C*H$_3$)$_3$), 34.5 (1C, *C*(CH$_3$)$_3$), 34.8 (1C, NH*C*H$_3$), 110.3 (1C, Ar-*C*), 120.1 (1C, Ar-*C*), 125.4 (1C, Ar-*C*), 129.9 (1C, Ar-*C*), 138.7 (1C, *C*HN), 143.4 (1C, Ar-*C*), 151.8 (1C, Ar-*C*). ESIMS *m/z* 285 (MH^+). Melting Point 104-105 °C.

5-*tert*-Butyl-2-hydroxy-3-methoxybenzldehyde methylhydrazone (L5) Combining ethanolic solutions of methylhydrazine (0.28 g, 6.1 mmol) and **(5)** (1.25 g, 6.0 mmol) as in the general procedure yielded a yellow solid (1.34 g, 94%). (Anal. Calc. for $C_{12}H_{17}BrN_2O$: C, 66.07; H, 8.53; N, 11.85. Found: C, 65.71; H, 9.15; N, 11.55%); ^{1}H NMR ($CDCl_3$, 250 MHz): δ 1.31 (s, 9H, C(CH_3)$_3$), 2.97 (s, 3H, NHCH_3), 3.92 (s, 3H, OCH_3), 6.76 (d, 1H, Ar-*H*), 6.88 (d, 1H, Ar-*H*), 7.67 (s, 1H, C*H*N); ^{13}C NMR ($CDCl_3$, 250 MHz): δ 31.9 (1C, *C*(CH$_3$)$_3$), 34.7 (3C, C(*C*H$_3$)$_3$), 34.9 (1C, NH*C*H$_3$), 56.7 (1C, O*C*H$_3$), 110.3 (1C, Ar-*C*), 118.1 (1C, Ar-*C*), 118.9 (1C, Ar-*C*), 140.3 (1C, *C*HN), 142.1 (1C, Ar-*C*), 144.9 (1C, Ar-*C*), 147.7 (1C, Ar-*C*). ESIMS *m/z* 237 (MH^+). Melting Point 79-80 °C.

Phenylhydrazone Formation General Procedure. A solution of the appropriate precursor aldehyde in ethanol was slowly added to one equivalent of phenylhydrazine hydrochloride and three equivalents of sodium acetate in water. The resulting mixture was stirred and heated at 90 °C for 30 min. After cooling the

solvent was removed *in vacuo*. The solid was dissolved in DCM, washed with water twice, and dried over $MgSO_4$. The solvent was evaporated *in vacuo* to give the product which needs no further purification.

5-*tert*-Butyl-2-hydroxy-benzaldehyde phenylhydrazone (L6) Phenylhydrazine hydrochloride (10.21 g, 70.6 mmol) and **(1)** (12.38 g, 69.5 mmol) were combined as in the general procedure to give a pale yellow solid (15.79 g, 85%). Yellow block crystals suitable for XRD analysis were grown by slow cooling and evaporation of an ethanol solution. (Anal. Calc. for $C_{17}H_{20}N_2O$: C, 76.09; H, 7.51; N, 10.44. Found: C, 75.74; H, 7.88; N, 10.69%); ^{1}H NMR ($CDCl_3$, 250 MHz): δ 1.30 (s, 9H, C(C*H*$_3$)$_3$), 6.93 (m, 4H, Ar-*H*), 7.12 (d, 1H, Ar-*H*), 7.28 (m, 3H, Ar-*H*), 7.84 (s, 1H, C*H*N); ^{13}C NMR ($CDCl_3$, 250 MHz): δ 31.9 (3C, C(*C*H$_3$)$_3$), 34.4 (1C, *C*(CH$_3$)$_3$), 113.0 (2C, Ar-*C*), 116.5 (1C, Ar-*C*), 118.2 (1C, Ar-*C*), 121.1 (1C, Ar-*C*), 126.4 (1C, Ar-*C*), 127.7 (1C, Ar-*C*), 129.9 (2C, Ar-*C*), 142.2 (1C, *C*HN), 142.6 (1C, Ar-*C*), 144.0 (1C, Ar-*C*), 155.1 (1C, Ar-*C*). ESIMS *m/z* 269 (MH^+). Melting Point 172-173 °C.

5-*tert*-Butyl-2-hydroxy-3-methylbenzaldehyde phenylhydrazone (L7) Phenylhydrazine hydrochloride (0.75 g, 5.20 mmol) and **(2)** (1.00 g, 5.20 mmol) were combined as in the general procedure to give a yellow solid (1.17 g, 80%). (Anal. Calc. for $C_{18}H_{22}N_2O$: C, 76.56; H, 7.85; N, 9.92. Found: C, 76.69; H, 7.96; N, 9.97%); ^{1}H NMR ($CDCl_3$, 250 MHz): δ 1.32 (s, 9H, C(C*H*$_3$)$_3$), 2.34 (s, 3H, C*H*$_3$), 6.96 (m, 3H, Ar-*H*), 7.17 (d, 1H, Ar-*H*), 7.30 (m, 2H, Ar-*H*), 7.44 (d, 1H, Ar-*H*), 7.88 (s, 1H, C*H*N); ^{13}C NMR ($CDCl_3$, 250 MHz): δ 16.4 (1C, *C*H$_3$), 31.9 (3C, C(*C*H$_3$)$_3$), 34.3 (1C, *C*(CH$_3$)$_3$), 113.0 (2C, Ar-*C*), 117.4 (1C, Ar-*C*), 121.1 (1C, Ar-*C*), 124.1 (1C, Ar-*C*), 125.3 (1C, Ar-*C*), 129.2 (1C, Ar-*C*), 129.9 (2C, Ar-*C*), 142.1 (1C, *C*HN), 142.5 (1C, Ar-*C*), 144.0 (1C, Ar-*C*), 153.4 (1C, Ar-*C*). ESIMS *m/z* 283 (MH^+). Melting Point 104-105 °C.

5-*tert*-Butyl-2-hydroxy-3-nitrobenzaldehyde phenylhydrazone (L8)

Phenylhydrazine hydrochloride (0.65 g, 4.48 mmol) and **(3)** (1.00 g, 4.48 mmol) were combined as in the general procedure to give a yellow solid (1.31 g, 87%). (Anal. Calc. for $C_{17}H_{19}N_3O_3$: C, 65.16; H, 6.11; N, 13.41. Found: C, 65.12; H, 6.15; N, 13.13%); ^{1}H NMR ($CDCl_3$, 250 MHz): δ 1.37 (s, 9H, C(C*H*$_3$)$_3$), 6.94 (t, 1H, Ar-*H*), 7.09 (m, 2H, Ar-*H*), 7.32 (m, 2H, Ar-*H*), 8.01 (m, 1H, Ar-*H*), 8.04 (m, 1H, Ar-*H*), 8.05 (m, 1H, C*H*N); ^{13}C NMR ($CDCl_3$, 250 MHz): δ 31.5 (3C, C(*C*H$_3$)$_3$), 34.8 (1C, *C*(CH$_3$)$_3$), 113.2 (2C, Ar-*C*), 121.3 (1C, Ar-*C*), 121.9 (1C, Ar-*C*), 124.5 (1C, Ar-*C*), 129.9 (2C, Ar-*C*), 131.2 (1C, Ar-*C*), 134.0 (1C, *C*HN), 135.3 (1C, Ar-*C*), 143.3 (1C, Ar-*C*), 144.0 (1C, Ar-*C*), 150.5 (1C, Ar-*C*). ESIMS *m/z* 314 (MH^+). Melting Point 124-125 °C.

3-Bromo-5-*tert*-butyl-2-hydroxybenzaldehyde phenylhydrazone (L9)

Phenylhydrazine hydrochloride (1.69 g, 11.67 mmol) and **(4)** (3.00 g, 11.67 mmol) were combined as in the general procedure to give a white solid (3.25 g, 80%). (Anal. Calc. for $C_{17}H_{19}BrN_2O$: C, 58.80; H, 5.52; N, 8.07. Found: C, 58.26; H, 5.04; N, 7.69%); ^{1}H NMR ($CDCl_3$, 250 MHz): δ 1.31 (s, 9H, C(C*H*$_3$)$_3$), 6.95 (t, 1H, Ar-*H*), 7.02 (m, 2H, Ar-*H*), 7.10 (d, 1H, Ar-*H*), 7.31 (m, 2H, Ar-*H*), 7.51 (d, 1H, Ar-*H*), 7.84 (s, 1H, C*H*N); ^{13}C NMR ($CDCl_3$, 250 MHz): δ 31.7 (3C, C(*C*H$_3$)$_3$), 34.5 (1C, *C*(CH$_3$)$_3$), 110.5 (1C, Ar-*C*), 113.1 (2C, Ar-*C*), 119.3 (1C, Ar-*C*), 121.6 (1C, Ar-*C*), 125.7 (1C, Ar-*C*), 130.0 (2C, Ar-*C*), 130.9 (1C, Ar-*C*), 140.6 (1C, *C*HN), 143.4 (1C, Ar-*C*), 143.9 (1C, Ar-*C*), 151.6 (1C, Ar-*C*). ESIMS *m/z* 347 (MH^+). Melting Point 144-145 °C.

5-*tert*-Butyl-2-hydroxy-3-methoxybenzaldehyde phenylhydrazone (L10)

Phenylhydrazine hydrochloride (1.39 g, 9.60 mmol) and **(5)** (2.00 g, 9.60 mmol) were combined as in the general procedure to give a white solid (2.55 g, 90%). Colourless block crystals suitable for XRD analysis were grown by vapor diffusion

of DCM/Petrolether. (Anal. Calc. for $C_{18}H_{22}N_2O_2$: C, 72.46; H, 7.43; N, 9.39. Found: C, 72.31; H, 7.76; N, 9.44%); ^{1}H NMR ($CDCl_3$, 250 MHz): δ 1.33 (s, 9H, C(C*H*$_3$)$_3$), 3.96 (s, 3H, OC*H*$_3$), 6.79 (d, 1H, Ar-*H*), 6.97 (m, 4H, Ar-*H*), 7.29 (m, 2H, Ar-*H*), 7.88 (s, 1H, C*H*N); ^{13}C NMR ($CDCl_3$, 250 MHz): δ 31.9 (3C, C(*C*H$_3$)$_3$), 34.7 (1C, *C*(CH$_3$)$_3$), 56.7 (1C, O*C*H$_3$), 110.9 (1C, Ar-*C*), 113.0 (2C, Ar-*C*), 118.1 (1C, Ar-*C*), 118.3 (1C, Ar-*C*), 121.1 (1C, Ar-*C*), 129.9 (2C, Ar-*C*), 141.7 (1C, ArCHN), 142.6 (1C, Ar-*C*), 143.9 (1C, Ar-*C*), 144.9 (1C, Ar-*C*), 148.0 (1C, Ar-*C*). ESIMS *m/z* 299 (MH^+). Melting Point 132-133 °C.

2.10.3 Cu(II) Complex Syntheses

General Procedure A solution of the ligand in ethanol was added to 0.5 equivalents of copper(II) acetate in ethanol. Colour changes due to complex formation occurred immediately, along with precipitation. The resulting mixture was stirred for 3 h. The precipitation was filtered, washed with ethanol and dried *in vacuo* to give the pure product as a brownish solid.

[Cu(L1-H)$_2$]. $Cu(OAc)_2 \cdot H_2O$ (0.46 g, 2.29 mmol) and **L1** (0.94 g, 4.55 mmol) yielded a dark brown solid from the general procedure (1.04 g, 96%). (Anal. Calc. for $C_{24}H_{34}Cu\ N_4O_2$: C, 60.80; H, 7.23; N, 11.82. Found: C, 61.05; H, 7.45; N, 11.34%). ESIMS *m/z* 474 (MH^+).

[Cu(L2-H)$_2$]. $Cu(OAc)_2 \cdot H_2O$ (0.68 g, 3.40 mmol) and **L2** (1.49 g, 6.76 mmol) yielded a light brown solid from the general procedure (1.55 g, 91%). (Anal. Calc. for $C_{26}H_{38}Cu\ N_4O_2$: C, 62.19; H, 7.63; N, 11.16. Found: C, 62.66; H, 7.77; N, 10.73%). ESIMS *m/z* 502 (MH^+).

[Cu(L3-H)$_2$]. $Cu(OAc)_2 \cdot H_2O$ (0.24 g, 1.20 mmol) and **L3** (0.60 g, 2.39 mmol)

yielded a yellow solid from the general procedure (0.47 g, 70%). (Anal. Calc. for $C_{24}H_{32}CuN_6O_6$: C, 51.10; H, 5.72; N, 14.90. Found: C, 51.88; H, 5.52; N, 14.63%). ESIMS *m/z* 564 (MH^+).

[Cu(L4-H)$_2$]. $Cu(OAc)_2 \cdot H_2O$ (0.20 g, 1.00 mmol) and **L4** (0.57 g, 2.00 mmol) yielded a light brown solid from the general procedure (0.55 g, 87%). (Anal. Calc. for $C_{24}H_{32}Br_2CuN_4O_2$: C, 45.62; H, 5.10; N, 8.87. Found: C, 45.71; H, 4.90; N, 9.05%). ESIMS *m/z* 632 (MH^+).

[Cu(L5-H)$_2$]. $Cu(OAc)_2 \cdot H_2O$ (0.20 g, 1.00 mmol) and **L5** (0.47 g, 2.00 mmol) yielded a dark brown solid from the general procedure (0.52 g, 97%). (Anal. Calc. for $C_{26}H_{38}CuN_4O_4$: C, 58.46; H, 7.17; N, 10.49. Found: C, 57.98; H, 6.69; N, 9.61%). ESIMS *m/z* 534 (MH^+).

[Cu(L6-H)$_2$]. $Cu(OAc)_2 \cdot H_2O$ (0.10 g, 0.50 mmol) and **L6** (0.27 g, 1.00 mmol) yielded a light brown solid from the general procedure (0.27 g, 90%). (Anal. Calc. for $C_{34}H_{38}CuN_4O_2$: C, 68.26; H, 6.40; N, 9.37. Found: C, 65.25; H, 6.00; N, 8.79%). ESIMS *m/z* 598 (MH^+).

[Cu(L7-H)$_2$]. $Cu(OAc)_2 \cdot H_2O$ (0.10 g, 0.50 mmol) and **L7** (0.30 g, 1.00 mmol) yielded a light brown solid from the general procedure (0.27 g, 81%). (Anal. Calc. for $C_{36}H_{42}CuN_4O_2$: C, 69.04; H, 6.76; N, 8.95. Found: C, 69.08; H, 6.89; N, 8.97%). ESIMS *m/z* 626 (MH^+).

[Cu(L8-H)$_2$]. $Cu(OAc)_2 \cdot H_2O$ (0.10 g, 0.50 mmol) and **L8** (0.32 g, 1.00 mmol) yielded a dark brown solid from the general procedure (0.28 g, 82%). (Anal. Calc. for $C_{34}H_{36}CuN_6O_6$: C, 59.34; H, 5.27; N, 12.21. Found: C, 58.42; H, 4.77; N, 11.70%). ESIMS *m/z* 688 (MH^+).

[Cu(L9-H)$_2$]. $Cu(OAc)_2 \cdot H_2O$ (0.20 g, 1.00 mmol) and **L9** (0.69 g, 2.00 mmol) yielded a brown solid from the general procedure (0.68 g, 90%). (Anal. Calc. for $C_{34}H_{36}BrCuN_4O_2$: C, 54.01; H, 4.80; N, 7.41. Found: C, 53.94; H, 4.83; N, 7.41%). ESIMS *m/z* 756 (MH^+).

[Cu(L10-H)$_2$]. $Cu(OAc)_2 \cdot H_2O$ (0.34 g, 1.70 mmol) and **L10** (1.00 g, 3.40 mmol) yielded a brown solid from the general procedure (1.04 g, 91%). (Anal. Calc. for $C_{36}H_{42}CuN_4O_4$: C, 65.68; H, 6.43; N, 8.51. Found: C, 65.33; H, 6.61; N, 8.18%). ESIMS *m/z* 658 (MH^+).

2.10.4 Solvent Extraction

The loading experiment was carried out by contacting a chloroform solution of the ligand (5.00 ml, 0.010 M) with an aqueous solution of copper(II) sulfate (5.00 ml, 0.010 M) at different pH values in a tightly sealed, screw top glass jar. The aqueous solution was prepared by adding a H_2SO_4 solution (0.10 M for pH 1.5 and above, 1.00 M for lower pH) or a NaOH solution (0.10 M) to a $CuSO_4$ solution (3.00 ml, 0.0167 M) and adding water to make up to 5.00 ml. The two-phase system was stirred at 900 r.p.m. at room temperature for 18 h. A 1.00 ml aliquot was taken from the organic phase, dried *in vacuo* and redissolved in butan-1-ol (10.00 ml). The copper or sulfur content was then analysed by ICP-OES. The pH of the aqueous phase was measured by the pH meter. The calculated percentage of the copper(II) uptaken into the organic phase was plotted against the measured equilibrium pH to give the S-curve.

Stripping experiment was performed in a similar procedure to the loading experiment by using a chloroform solution of the copper(II) complex (5.00 ml, 0.005 M) and an aqueous solution of sodium sulfate (5.00 ml, 0.010 M). Due to the solubility issues, a

few changes were necessarily made as shown in Table 2.11.

Cu Complex	Organic Phase		Aqueous Phase		ICP-OES	
	Conc. / M	Volume / ml	Conc. / M	Volume / ml	Solvent	Dilution Times
[Cu(L1-H)$_2$]	0.005	5.00	0.010	5.00	butan-1-ol	10
[Cu(L2-H)$_2$]	0.005	5.00	0.010	5.00	butan-1-ol	**20**
[Cu(L3-H)$_2$]	**0.0005**	**10.00**	0.010	**10.00**	**nitrobenzene**	**2**
[Cu(L4-H)$_2$]	0.005	5.00	0.010	5.00	**nitrobenzene**	10
[Cu(L5-H)$_2$]	0.005	5.00	0.010	5.00	butan-1-ol	10

Table 2.11 Conditions applied for **L1**-**L5** in stripping experiment

2.10.5 NMR Solution Study

NMR samples were generally prepared by dissolving 10 mg the ligand in 0.6 ml $CDCl_3$ or DMSO-d_6. Samples for NOESY and 1D NOE difference spectra need to be concentrated, and hence 40 mg the ligand in 0.6 ml $CDCl_3$ were used. The concentration dependence NMR study was carried out by diluting a NMR sample containing 40 mg the ligand in 0.6 ml DMSO-d_6 to respectively 1.2 ml, 1.6 ml and 2.4 ml in the same NMR tube.

2.11 Conclusions

The aim of the work in this chapter was to establish whether salicylaldehyde hydrazones could function in a similar manner to their oxime analogues as copper extractants and to what extent variation of the 3-substituent (adjacent to the phenolic group) could tune extractant strength. Both of these objectives have been achieved.

The hydrazones are weaker extractants than the oximes, and the strength varies in the order: oximes > methylhydrazones > phenylhydrazones. This order probably arises from a combination of variations in the phenol acidities and the strength of the hydrogen bonding motifs (Figure 2.30). These were probed in the free ligands using NMR techniques.

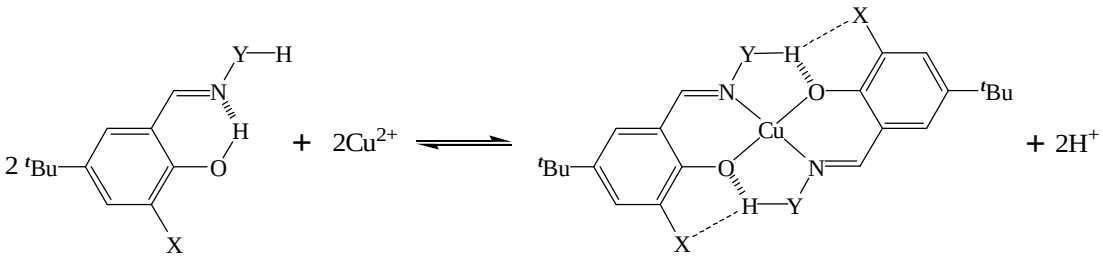

Figure 2.30 Copper extraction mechanisms of the hydrazones and oximes

Both the phenol acidity and intermolecular hydrogen bonding are significantly influenced by the 3-substituents. Electron-withdrawing groups also with the properties of hydrogen bond acceptors (X = NO_2 or Br) are particularly effective in lowering the $pH_{0.5}$ values of the methylhydrazones (Y = NMe), and make them reagents of similar strength to the commercial P50 extractant. The distribution coefficient for copper extraction can be increased by more than three orders of magnitudes along the series (X) Me < OMe ≤ H < Br < NO_2. The importance of the buttressing effect is best illuminated by **L5**. Despite the electron-donating effect of its 3-methoxy group, **L5** is a stronger extractant than its methyl analogue **L2**, and has a similar $pH_{0.5}$ value to the unsubstituted ligand **L1**. This can best be explained by the formation of bifurcated hydrogen bonds to stabilise the intracomplex hydrogen bonding motif (Figure 2.31).

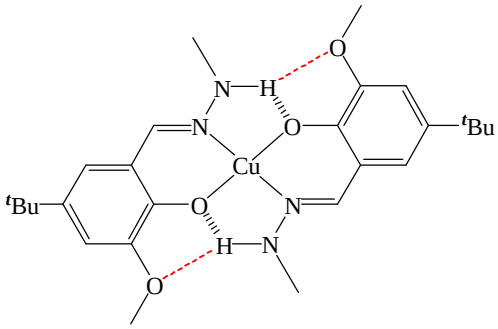

Figure 2.31 The intracomplex hydrogen bonding motif of [Cu(**L5**-H)$_2$]

All the hydrazone ligands studied in this chapter, **L1**-**L10**, can be prepared on the gram scale by facile and high yielding methods. The development of novel synthetic strategies minimized the number of starting materials and steps required, and it can be assumed that the industry can efficiently manufacture the analogues based on commercially available 4-nonylphenol which will have higher solubility in the kerosene used in industry.

In terms of commercial application, the phenylhydrazones are likely to be too weak, even when tuned with NO_2 or Br 3-substituition. The low solubilities of some of the copper complexes could limit mass transport efficiency in industry.

In the context of the work in this chapter, the weakness of the ligands as extractants and the solubility issue presented difficulties carrying out the extraction tests. The need to raise the pH of the aqueous phase to ensure high loading of some of the hydrazones led to the formation of a third phase. By contacting prepared [Cu(L-H)$_2$] chloroform solutions with aqueous solutions of varied pH values, much better material balances and smooth S-curves were obtained. A new approach to ICP-OES analysis of the organic phases had to be established to solve the issues of some of the copper complexes with low solubilities in 1-butanol, the solvent used for ICP-OES analysis in the group. Nitrobenzene was used to introduce samples into the plasma

after evaporation of chloroform aliquots.

NMR methods not previously used in the group were applied to the study of solution speciation. ^{1}H NMR spectra established that all the hydrazone and oxime ligands exist only as the imino enol tautomers in solution and the 3-substituents significantly varied the phenol acidities by the electronic effects of the substituents. The NOESY and 1D NOE difference spectra have suggested that the methylhydrazones adopt mainly the Z conformation in chloroform, which is needed for dimerization to form the 14-membered *pseudo*macrocyclic structures. The temperature dependent and concentration dependent NMR experiment in DMSO demonstrated that the phenol protons in all ligands form intramolecular hydrogen bonds in solution, and dimerization does not occur to any significant extent in highly polar solvent such as DMSO. The temperature dependent NMR experiment also indicated that the intramolecular hydrogen bonds are particularly strong in the phenylhydrazones, which is consistent with these being the weakest extractants.

The variation of the 3-substituent could have other effects on the hydrazone extractants and their copper complexes, *i.e.* the solubility, the distribution coefficient in two phases, the hydrolytic stability and so on. These effects can influence the extractant strength and be further investigated in the future work.

In summary, salicylaldehyde hydrazones could be used as copper(II) extractants for hydrometallurgical recovery. The substituent effects, particularly the buttressing effect, have proved effective in tuning extraction strength.

2.12 References

1. J. W. Laist, "Copper, Silver and Gold", Van Nostrand, New York, 1954.
2. T. E. Graedel, D. van Beers, M. Bertram, K. Fuse, R. B. Gordon, A. Gritsinin, A. Kapur, R. J.

Klee, R. J. Lifset, L. Memon, H. Rechberger, S. Spatari and D. Vexler, *Environmental Science and Technology*, 2004, **38**, 1242-52.

3. D. Nicholls, "Complexes and First-Row Transition Elements", MacMillan Press Ltd, London, 1974.
4. N. N. Greenwood and A. Earnshaw, "Chemistry of the Elements", Butterworth-Heinemann, 1997.
5. D. F. Shriver and P. W. Atkins, "Inorganic Chemistry", Oxford University Press, 1999.
6. M. Grayson and D. Eckroth, "Kirk-Othmer Encyclopaedia of Chemical Technology", John Wiley and Sons, New York, 1978.
7. S. Hong, J.-P. Candelone, M. Soutif and C. F. Boutron, *Science of the Total Environment*, 1996, **188**, 183-93.
8. R. B. Gordon, M. Bertram and T. E. Graedel, *Proceedings of the National Academy of Sciences of the United States of America*, 2006, **103**, 1209-14.
9. A. Cole, *Metal Bulletin Monthly supplement*, 2004, **copper**, 6-8.
10. P. J. Mackey, *CIM Magazine*, 2007, **2**, 35-42.
11. D. Cohen, *The New Scientist*, 2007, **194**, 34-41.
12. London Metal Exchange. www.lme.co.uk/dataprices.asp
13. P. A. Tasker, P. G. Plieger and L. C. West, "Comprehensive Coordination Chemistry II", Elsevier Ltd, Oxford, 2004.
14. G. A. Kordosky, International Solvent Extraction Conference, Cape Town, South Africa, 2002, 853-62.
15. J. Szymanowski, "Hydroxyoximes and Copper Hydrometallurgy", CRC Press, London 1993.
16. A. G. Smith, P. A. Tasker and D. J. White, *Coordination Chemistry Reviews*, 2003, **241**, 61-85.
17. P. O'Brien and J. R. Thornback, *Hydrometallurgy*, 1982, **8**, 331-9.
18. P. O'Brien, J. R. Thornback and J. Szymanowski, *Journal of Coordination Chemistry*, 1983, **13**, 11-15.
19. B. McCudden, P. Obrien and J. R. Thornback, *Journal of the Chemical Society-Dalton Transactions*, 1983, 2043-46.
20. H. Irving and R. J. P. Williams, *Journal of the Chemical Society*, 1953, 3192-210.
21. R. J. Gordon, PhD Thesis, University of Edinburgh, 2008.
22. R. S. Forgan, PhD Thesis, University of Edinburgh, 2008.
23. J. Szymanowski and A. Borowiak-Resterna, *Critical Reviews in Analytical Chemistry*, 1991, **22**, 519-66.
24. K. Burger and I. Egyed, *Journal of Inorganic and Nuclear Chemistry*, 1965, **27**, 2361-70.
25. K. Burger and I. Egyed, *Magyar Kemiai Folyoirat*, 1965, **71**, 143-9.
26. J. March and M. B. Smith, "March's Advanced Organic Chemistry, Reactions, Mechanisms and Structures", John Wiley's and Sons, New York, 2001.
27. R. S. Forgan, J. E. Davidson, S. G. Galbraith, D. K. Henderson, S. Parsons, P. A. Tasker and F. J. White, *Chemical Communications*, 2008, 4049-51.
28. B. B. N. Raj and P. M. R. Kurup, *Spectrochimica Acta, Part A*, 2007, **66**, 898-903.
29. J. Clayden, N. Greeves, S. Warren and W. Peter, "Organic Chemistry", Oxford University Press, Oxford, 2001.

30. X. Deng and N. S. Mani, *Organic Letters*, 2006, **8**, 3505-08.
31. X. Deng and N. S. Mani, *Journal of Organic Chemistry*, 2008, **73**, 2412-15.
32. V. Y. Korotaev, I. B. Kutyashev, V. Y. Sosnovskikh and M. I. Kodess, *Mendeleev Communications*, 2007, **17**, 52-53.
33. F. Risitano, G. Grassi and F. Foti, *Journal of Chemical Research, Synopses*, 1981, 65.
34. J. Jacq, C. Einhorn and J. Einhorn, *Organic Letters*, 2008, **10**, 3757-60.
35. R. B. Singh, P. Jain and R. P. Singh, *Talanta*, 1982, **29**, 77-84.
36. M. P. Jain and S. Kumar, *Indian Journal of Chemistry, Section A: Inorganic, Physical, Theoretical & Analytical*, 1978, **16A**, 464-5.
37. M. P. Jain and S. Kumar, *Talanta*, 1982, **29**, 52-3.
38. N. Guskos, V. Likodimos, S. Glenis, J. Typek, M. Wabia, D. G. Paschalidis, I. Tossidis and C. L. Lin, *Journal of Magnetism and Magnetic Materials*, 2004, **272-276**, 1067-69.
39. S. N. Rao, D. D. Mishra, R. C. Maurya and N. N. Rao, *Polyhedron*, 1997, **16**, 1825-29.
40. L. Larabi, Y. Harek, A. Reguig and M. M. Mostafa, *Journal of the Serbian Chemical Society*, 2003, **68**, 85-95.
41. F. Cariati, U. Caruso, R. Centore, W. Marcolli, A. De Maria, B. Panunzi, A. Roviello and A. Tuzi, *Inorganic Chemistry*, 2002, **41**, 6597-603.
42. P. G. Lacroix, *European Journal of Inorganic Chemistry*, 2001, 339-48.
43. U. Caruso, R. Centore, B. Panunzi, A. Roviello and A. Tuzi, *European Journal of Inorganic Chemistry*, 2005, 2747-53.
44. B.-D. Wang, Z.-Y. Yang, D.-W. Zhang and Y. Wang, *Spectrochimica Acta, Part A: Molecular and Biomolecular Spectroscopy*, 2006, **63A**, 213-19.
45. A. Majumder, G. M. Rosair, A. Mallick, N. Chattopadhyay and S. Mitra, *Polyhedron*, 2006, **25**, 1753-62.
46. Y. Xiang, Z. Li, X. Chen and A. Tong, *Talanta*, 2008, **74**, 1148-53.
47. M. Bakir and C. Gyles, *Journal of Molecular Structure*, 2005, **753**, 35-39.
48. D. R. Dabideen, K. F. Cheng, B. Aljabari, E. J. Miller, V. A. Pavlov and Y. Al-Abed, *Journal of Medicinal Chemistry*, 2007, **50**, 1993-97.
49. D. K. Johnson, T. B. Murphy, N. J. Rose, W. H. Goodwin and L. Pickart, *Inorganica Chimica Acta*, 1982, **67**, 159-65.
50. J. E. Dubois, H. Fakhrayan, J. P. Doucet and J. M. El Hage Chahine, *Inorganic Chemistry*, 1992, **31**, 853-9.
51. M. Mohan, A. Kumar, M. Kumar and N. K. Jha, *Inorganica Chimica Acta*, 1987, **136**, 65-74.
52. E. W. Ainscough, A. M. Brodie, A. J. Dobbs, J. D. Ranford and J. M. Waters, *Inorganica Chimica Acta*, 1998, **267**, 27-38.
53. H. Zhao, N. Neamati, S. Sunder, H. Hong, S. Wang, G. W. A. Milne, Y. Pommier and T. R. Burke, Jr., *Journal of Medicinal Chemistry*, 1997, **40**, 937-41.
54. L. R. Morgan, "Hydrazone Agents to Treat Cutaneous Lesions", Patent, 2007.
55. E. Massarani, D. Nardi, A. Tajana and L. Degen, *Journal of Medicinal Chemistry*, 1971, **14**, 633-5.
56. P. B. Sreeja, M. R. P. Kurup, A. Kishore and C. Jasmin, *Polyhedron*, 2004, **23**, 575-81.
57. J. K. Sears and J. R. Darby, "The Technology of Plasticizers", John Wiley and Sons, New York, 1982.

58. A. M. El-Hendawy, A. H. Al-Kubaisi and A. F. Shoair, *Monatshefte fuer Chemie*, 1995, **126**, 1291-302.
59. T. Mino, T. Ogawa and M. Yamashita, *Heterocycles*, 2001, **55**, 453-56.
60. T. Mino, Y. Shirae, M. Sakamoto and T. Fujita, *Journal of Organic Chemistry*, 2005, **70**, 2191-94.
61. M. F. Iskander, T. E. Khalil, R. Werner, W. Haase, I. Svoboda and H. Fuess, *Polyhedron*, 2000, **19**, 949-58.
62. N. M. Samus, V. I. Tsapkov and A. V. Kerner, *Russian Journal of General Chemistry (Translation of Zhurnal Obshchei Khimii)*, 2003, **73**, 1611-15.
63. N. M. Samus, V. I. Prisakar, V. I. Tsapkov, S. A. Buracheva and A. P. Gulya, *Pharmaceutical Chemistry Journal (Translation of Khimiko-Farmatsevticheskii Zhurnal)*, 2004, **38**, 373-75.
64. S. Das and S. Pal, *Journal of Molecular Structure*, 2005, **753**, 68-79.
65. L.-M. Wu, H.-B. Teng, X.-C. Feng, X.-B. Ke, Q.-F. Zhu, J.-T. Su, W.-J. Xu and X.-M. Hu, *Crystal Growth & Design*, 2007, **7**, 1337-42.
66. L. Hunter and J. A. Marriott, *Journal of the Chemical Society*, 1937, 2000-3.
67. T. V. Troepol'skaya, E. N. Munin, Z. S. Titova and Y. P. Kitaev, *Izvestiya Akademii Nauk SSSR, Seriya Khimicheskaya*, 1978, 898-905.
68. R. S. Mandal and L. Mishra, *Asian Journal of Chemistry*, 2007, **19**, 95-101.
69. T. A. Henry and T. M. Sharp, *Journal of the Chemical Society*, 1926, 2432-40.
70. M. Crawford and J. W. Rasburn, *Journal of the Chemical Society*, 1956, 2155-60.
71. R. Aldred, R. Johnston, D. Levin and J. Neilan, *Journal of the Chemical Society, Perkin Transactions 1: Organic and Bio-Organic Chemistry (1972-1999)*, 1994, 1823-31.
72. F. Lam, J. X. Xu and K. S. Chan, *Journal of Organic Chemistry*, 1996, **61**, 8414-18.
73. D. F. Taber, S. Patel, T. M. Hambleton and E. E. Winkel, *Journal of Chemical Education*, 2007, **84**, 1158.
74. L. F. Lindoy, G. V. Meehan and N. Svenstrup, *Synthesis*, 1998, 1029-32.
75. E. M. McGarrigle, D. M. Murphy and D. G. Gilheany, *Tetrahedron: Asymmetry*, 2004, **15**, 1343-54.
76. J. T. Hewitt, J. Kenner and H. Silk, *Journal of the Chemical Society*, 1904, **85**, 1225-30.
77. D. Nobel, *Journal of the Chemical Society, Chemical Communications*, 1993, 419-20.
78. P. Capdevielle and M. Maumy, *Tetrahedron Letters*, 1993, **34**, 1007-10.
79. R. G. Jesaitis, *Theoretica Chimica Acta*, 1973, **32**, 71-5.
80. J. O. Jarvie and A. Rauk, *Canadian Journal of Chemistry*, 1974, **52**, 2785-91.
81. F. A. Settle, "Handbook of Instrumental Techniques for Analytical Chemistry", Prentice Hall, New Jersey, 1997.
82. A. W. Boorn, M. S. Cresser and R. F. Browner, *Spectrochimica Acta, Part B: Atomic Spectroscopy*, 1980, **35B**, 823-32.
83. A. W. Boorn and R. F. Browner, *Analytical Chemistry*, 1982, **54**, 1402-10.
84. I. G. Adembri, P. Sarti-Fantoni and E. Belgodere, *Tetrahedron*, 1966, **22**, 3149-56.
85. P. A. Kollman and L. C. Allen, *Chemical Reviews*, 1972, **72**, 283-303.
86. H. Umeyama and K. Morokuma, *Journal of the American Chemical Society*, 1977, **99**, 1316-32.
87. D. Kanamori, A. Furukawa, T.-A. Okamura, H. Yamamoto and N. Ueyama, *Organic &*

Biomolecular Chemistry, 2005, **3**, 1453-59.

88. P. W. Westerman, R. E. Botto and J. D. Roberts, *Journal of Organic Chemistry*, 1978, **43**, 2590-6.
89. K. Neuvonen, F. Fueloep, H. Neuvonen, A. Koch, E. Kleinpeter and K. Pihlaja, *Journal of Organic Chemistry*, 2003, **68**, 2151-60.
90. V. A. Bren, T. M. Stul'neva, B. Y. Simkin and V. I. Minkin, *Zhurnal Organicheskoi Khimii*, 1976, **12**, 633-40.
91. D. H. Williams and I. Fleming, "Spectroscopic Methods in Organic Chemistry", McGraw-Hill Publishing Company, London, 1995.
92. R. J. Abraham, J. Fisher and P. Loftus, "Introduction of NMR Spectroscopy", John Wiley and Sons, New York, 1988.
93. G. Socrates, *Transactions of the Faraday Society*, 1970, **66**, 1052-7.
94. Y. Tsuno, M. Fujio, Y. Takai and Y. Yukawa, *Bulletin of the Chemical Society of Japan*, 1972, **45**, 1519-29.
95. J. B. Hyne, *Canadian Journal of Chemistry*, 1960, **38**, 125-30.
96. M. Onda, Y. Yamamoto, Y. Inoue and R. Chujo, *Bulletin of the Chemical Society of Japan*, 1988, **61**, 4015-21.
97. S. H. Gellman, G. P. Dado, G. B. Liang and B. R. Adams, *Journal of the American Chemical Society*, 1991, **113**, 1164-73.
98. G. T. Crisp and Y.-L. Jiang, *ARKIVOC*, 2001, **2**, 77-87.
99. W. Kemp, "Organic Spectroscopy", MacMillan Press Ltd, Basingstoke, 1991.

CHAPTER 3

POLYTOPIC SALICYLALDIMINE LIGANDS FOR ZINC CHLORIDE RECOVERY

Content

3.1 Introduction

This and the following chapter describe the development and investigation of polytopic ligands **L12** and **L13** in Figure 3.1 for the hydrometallurgical recovery of zinc chloride as compared to the monotopic analogue **L11**. Particular attention is paid to the unusually high $ZnCl_2$ loadings by **L12** and its possible mechanism in this chapter.

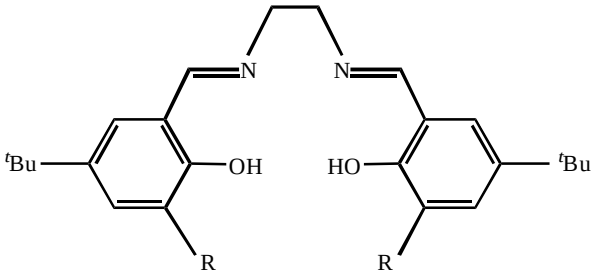

	R	
L11	H	**Mono**topic
L12	$CH_2N(n\text{-}C_6H_{13})_2$	**Di** or **tri**topic
L13	CH_2N	**Di** or **tri**topic

Figure 3.1 Polytopic ligands studied in this chapter

3.1.1 Zinc

Zinc is a blue-white lustrous metal of moderate ductility, strength and hardness.[1] It is about the 24th most abundant element[2] and presents at 76 ppm[3] in the Earth's crust. Zinc is a chalcophile,[3] which means that the element has a low affinity for oxygen and prefers to bond with sulfur. The major ore of zinc is sphalerite[3] (also known as zinc blende), which is a form of zinc sulfide and accounts for over 90% production from ore.[3] Zinc is the 30th element in the periodic table and a diamagnetic transition metal with electronic configuration $3d^{10}4s^2$. It has five stable isotopes ^{64}Zn (48.87%), ^{66}Zn (27.62%), ^{67}Zn (18.71%), ^{68}Zn (4.12%) and ^{70}Zn (0.69%).[1] Most of the isotopes have nuclear spin values 0 with the exception of ^{67}Zn being $-^5/_2$. The melting point (419.5 °C) and boiling point (907 °C)[3] are much lower than those of most transition metals. Zinc shows a dominant oxidation state of II.[1] It is quite electropositive with

the electronegativity coefficient 1.6 and the electrode potential (Zn^{2+}/Zn) -0.762 V.[3] Chemically zinc differs in most respects from transition metals due to a stable filled d-shell.[3] It shows more similarities with the main group metal magnesium, and many of their compounds are isomorphous.[3] However, zinc has a much greater tendency than magnesium to form covalent compounds, and resembles the transition metals in forming stable complexes not only with *O*-donor ligands but also with *N*- and *S*-donor ligands and with halides and CN^- as well.[3] Zinc can be alloyed with other metals. The main alloy is brass, which consists of zinc and copper as discussed in section 2.1.1. There is also nickel silver, typically with 20% zinc, 60% copper and 20% nickel.[2] The alloy prestal (78% zinc, 22% aluminium) is almost as strong as steel but as easy to mould as plastic.[2]

Zinc was not known as early as many of the other metals, though the use of its alloy brass could date back to 1400-1000 BC in Palestine,[3, 4] which contained about 23% zinc by the deliberate mixing of copper and zinc ores.[3, 4] Brass was similarly produced by the Romans in Cyprus and later in the Cologne region of Germany.[3, 4] The reason for the late discovery of zinc as a pure element is due to its low boiling point,[3, 4] as ancient metallurgists lost the volatile metal as vapour during the reduction process at a temperature of 1000 °C or more. It is believed that the art of smelting zinc with some form of condenser and the exclusion of air originated in India about the thirteenth century and then passed to China where zinc coins and ornaments were made in large scales during the Ming Dynasty (1368-1644 AD).[3, 4] In the seventeenth century, most of the zinc used in the western world was imported from China.[3, 4] Later the zinc industry started in the Bristol area of England and production quickly followed in Silesia and Belgium.[3, 4]

Nowadays zinc is the fourth commonest metal in use with an annual production of over 10 million tonnes,[5] exceeded only by iron, aluminium and copper. The most

important application of zinc is as an anti-corrosion agent.[1, 3] Galvanization, the coating of iron or steel as protection against corrosion, accounts for over 50% of the world's zinc consumption.[2, 5] The galvanized steel is used for roofing, fencing, car bodies, motorway guard rails, lighting posts, suspension bridges, *etc*.[2] The zinc coatings serve in two capacities, protective surface and sacrificial anode.[1, 2] As the zinc corrodes, a layer of oxide and carbonate ($Zn_5(OH)_6(CO_3)_2$)[6] forms to prevent oxygen and moisture from reaching the steel.[2] When the zinc layer is scratched or ruptured, the corrosion preferentially takes place on the zinc rather than the iron.[1] The iron is maintained in a cathodic condition since zinc stands above iron in the electrochemical series.[1] For a similar reason, a zinc disc bolted to an iron rudder protects the latter from the attack of sea water, and zinc is also used as a sacrificial anode for underground pipelines made of steel.[2] Metallic zinc makes a good material for an anode or negative terminus in batteries. The first dry battery had a zinc anode, a carbon cathode and an alkaline electrolyte of ammonium chloride paste.[2] Such batteries are still popular because they are cheap and considered as more environmentally friendly for containing no toxic metal.[2] Nearly one fourth of zinc is consumed as alloys,[5] including brass and zinc die casting alloys.[1-3] The remaining one fourth is used as zinc compounds,[5] of which zinc oxide is the most important both in commerce and research.[4] It has been extensively investigated in the areas of catalysis, ferromagnetism, semiconductor, luminescence, photoconductivity and photochemistry.[4] It is widely used in rubber, plastics, pigment, ceramics and other industries.[1, 2, 4]

In the past few years, the demand for zinc has significantly increased, which is driven by the emerging markets in China as well as Brazil and India.[7] The annual average price reached a record high of $1.48 per pound in 2006.[7] The supply deficit had led to huge increase in both mine production and refinery production worldwide,[8] and consequently the price has stabilised.[7]

The commercially exploitable zinc reserves exceed 100 million tonnes,[2] and the world mine production in 2007 alone was 10.94 million tonnes.[9] In order to maintain the production in a long term, low grade ores will need to be exploited to extend the lifetimes of the reserves, and more attention should be paid to recycling. Currently more than 30% of the world zinc production[2] is provided by recycling from galvanized products and wastes,[10] spent batteries,[11] *etc*. These secondary sources are usually in chloride-rich media. Also oxidative ferric chloride leaching[12] and other leaching technologies[13] employed for processing primary sources (see section 1.5) result in zinc chloride feed solutions. These are driving forces to develop novel and efficient reagents to recover zinc chloride in hydrometallurgical processes.

3.1.2 Solvent Extraction of Zinc

Approximately 90% of the world zinc production involves hydrometallurgy.[14] The conventional process employs roasting, leaching and electrowinning steps as shown in Figure 3.2.[14] Sphalerite is roasted to be converted into ZnO, which is then leached with sulfuric acid to produce zinc leachates. Further purification involves Fe(III) precipitation, cementation and electrolysis. This process causes undesirable economical and environmental problems associated with the roasting step and with the disposal or storage of very large volumes of iron wastes,[14] and it cannot be effectively applied for non-sulfidic ores, low-grade ores and secondary sources.[14] Selective solvent extraction can be used to overcome these problems and has gained more popularity for the zinc recovery lately.[14]

Figure 3.2 A simplified flowsheet of a conventional process for zinc recovery

As introduced in chapter 1, the SX process for primary sources generally employs leaching, extraction, stripping and electrowinning steps.[12] Some of the suggested extractants for Zn(II) are listed in Table 3.1.[14]

Reagent	Structure
D2EHPA	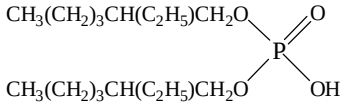
PC-88A	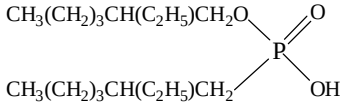
CYANEX 272	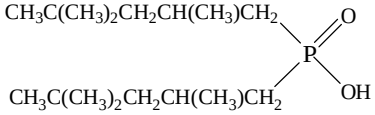
CYANEX 301	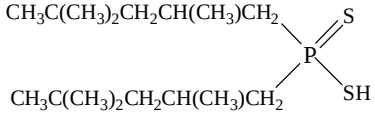
CYANEX 302	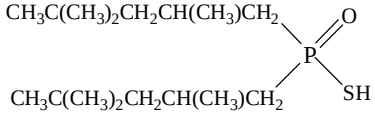
TBP	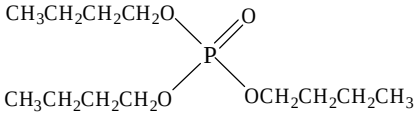
DBBP	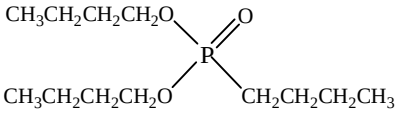
Aliquat 336	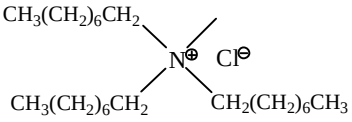

Table 3.1 Structures of some of the suggested extractants for Zn(II)[14, 15]

Zinc extraction from sulfate media has been extensively investigated because it can easily adopt the well-developed electrowinning technique from the conventional process to produce special high grade (SHG) electrolytic zinc. Di-(2-ethylhexyl) phosphoric acid (D2EHPA), 2-ethylhexyl phosphonic acid mono-2-ethylhexyl ester

(PC-88A), bis-(2,4,4-trimethylpentyl) phosphinic acid (CYANEX 272), and bis-(2,4,4-trimethylpentyl) dithiophosphinic acid (CYANEX 301) in Table 3.1 have shown great potential for zinc extraction from the sulfate media.[14] These organophosphorus extractants primarily behave as cation exchange reagents and the zinc extraction is pH dependent as discussed in chapter 1.[16-18] The stripping of Zn(II) can be simply achieved with sulfuric acid.[16-18] One of the biggest challenges is the separation of Zn(II) from Fe(III).[14] These extractants show a high affinity for the latter,[14] e.g. D2EHPA forms a strong complex with Fe(III) and the stripping requires concentrated HCl.[19] In order to avoid the continuous build-up of Fe(III) in organic phase and to regenerate the extractants, a few things can be done, including Fe(III) precipitation before the extraction step,[14] reduction of Fe(III) to Fe(II) in the organic phase,[14] mixing the extractant with modifiers such as tri-n-butyl phosphate (TBP) or tri-n-octyl phosphine oxide (TOPO) to allow easier stripping of Fe(III),[14] using octylphenyl acid phosphate (OPAP) as Fe(III) extractant from $ZnSO_4$-H_2SO_4 solutions,[20, 21] *etc*. One of the most successful applications is the Skorpion project in Namibia, Africa.[12, 14] The zinc silicate ore is leached with dilute sulfuric acid at 50 °C, and neutralized to pH 4.2 to precipitate iron, silica and aluminium.[22] Zn(II) is selectively extracted by D2EHPA and stripped with H_2SO_4 to give zinc sulfate electrolyte.[22] The Skorpion project produces about 150,000 tonnes SHG electrolytic zinc per annum.[22]

Zinc extraction from the chloride media has generated more and more interest because chloride leaching provides an effective recovery of zinc from sulfide or oxide ores and from secondary sources.[14] The disadvantage is the technical problems of electrowinning from chloride media, including chlorine- and chloride-resistant materials for construction, purification of electrolytes, separation of the anode and cathode compartments, handling of chlorine off-gas and the electrowinning deposit morphology.[23, 24] However, these problems can be overcome as evidenced by the

pilot and demonstration plant work that has been undertaken.[23, 24] The separation of Zn(II) from the chloride media is achievable by a variety of extractants,[14] including organophosphorus acids,[25, 26] chelating reagents,[27] and amines.[15] The mechanism of the extraction, and therefore the choice of the extractant depends on the formation of different zinc chloride species at different Cl^- activities.[14] Below 1 M Cl^-, the cationic species Zn^{2+} dominates, which is extractable by acidic extractants such as D2EHPA and bis-(2,4,4-trimethylpentyl) monothiophosphinic acid (CYANEX 302).[25, 26] Above about 1 M Cl^-, the main species are $ZnCl_4^{2-}$ and $ZnCl_3^-$, and these can be extracted by basic extractants, e.g. tricaprylmethylammonium chloride (Aliquat 336).[15] Neutral species at higher acidity are extractable by solvating reagents such as TBP and dibutyl butyl posphonate (DBBP).[15, 28] So far only a few industrial plants have used the extraction of zinc from chloride media, e.g. Técnicas Reunidas's ZINCLOR process as discussed in chapter 1. There is still much research needed in this field, and the project presented in this chapter focuses on developing novel reagents for zinc chloride extraction.

3.1.3 Polytopic Ligands

Earlier work at the University of Edinburgh has involved the development of metal salt reagents for copper sulfate.[29] As **II** shown in Figure 3.3, the tetradentate salicylaldimine ligands of the "salen" type bearing pendant tertiary amine groups undergo a zwitterionic transformation when binding metal salts, and form overall neutral assemblies in non-polar solvents in which the cations and anion(s) are bound in separated sites.[29]

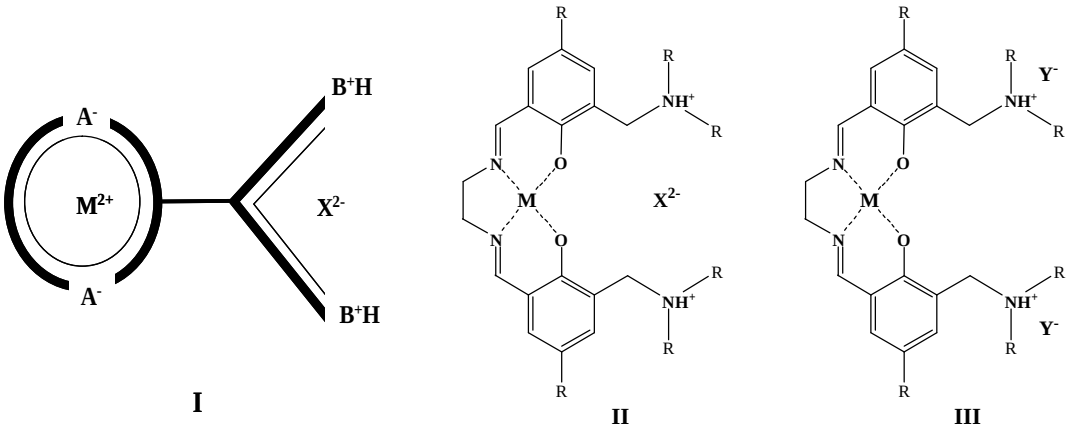

Figure 3.3 Ditopic systems **I** and **II** to recover divalent metal salts $M^{II}X$ and a tripotic arrangement, **III**, for salts of monoanions

A ditopic system of this type is displayed schematically as **I** in Figure 3.3 and an example based on a bis-salicylaldiminato unit to bind the metal cation and two pendant ammonium groups to carry the attendant dianion X^{2-} is shown as **II**. The overall neutral charge allows the cation and anion(s) to be stripped separately by adjustment of the pH of the aqueous phase.[29] It was hoped that the ligand design would achieve extraction selectivity of $CuSO_4$ over $CuCl_2$.[29] However, in two-phase solvent extraction the ligands showed selectivity for chloride over sulfate, although formation of the sulfato assembly [Cu**L**SO_4] was favoured over the chloride [Cu**L**Cl_2] in single phase system.

In screening tests for other metal salts, interesting results were observed for the extraction of zinc from chloride media.[30] These types of extractants yielded unusually high zinc loadings from chloride media in contrast to sulfate media as shown in Table 3.2.[30] The preliminary results indicated that 200% loadings of zinc by these extractants were possible from chloride media where 100% loading represents the "designed capacity" with a Zn^{2+} ion in the $N_2O_2^{2-}$ donor set of the bis-salicylaldiminato units and two chloride ions associated with the protonated pendant amine units as **III** in Figure 3.3. The results needed confirmation, but

provoked a lot of interest. When recovering metals from high tenor chloride streams, it is possible that the anion binding site could be loaded with a chlorometallate anion, MCl_x^{y-}, which would double the metal transport efficiency. In the case of zinc, two moles could be transported (M = Zn^{2+} and X = $[ZnCl_4]^{2-}$ in Figure 3.3 **II**) by one mole of extractant, and the extractants could function as "polytopic" ligands because they not only form ditopic or tritopic assemblies, but also possibly bind metal cations, simple counter anions and metallate anions. The polytopic ligands possess a great potential for zinc recovery from chloride media, and therefore are thoroughly investigated in the following chapters.

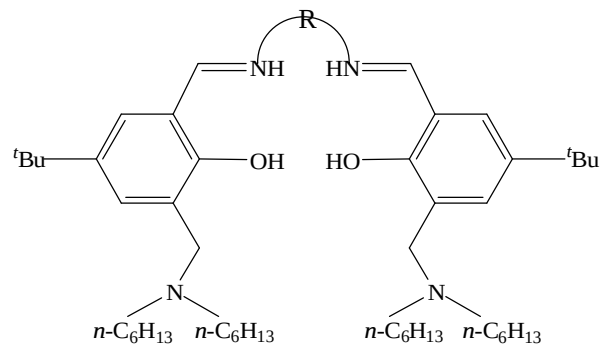

R	% Zn loading from	
	$ZnCl_2$	$ZnSO_4$
$-C_6H_{10}-$	187	13
$-C_6H_4-$	204	39
-biphenyl-	225	2
$-(CH_2)_2-$	269	7

Table 3.2 Preliminary results[30] for zinc extraction from 1 M $ZnCl_2$ or $ZnSO_4$ aqueous solutions by equivalent volume 0.01 M chloroform solutions of a series of salen type ligands bearing pendant tertiary amine groups. The 100% loading of Zn(II) is based on a Zn : L ratio of 1 : 1.

3.1.4 Aim of This Work

This project aims to develop polytopic ligands which achieve high transport efficiency of metal salts and high Cl^- over SO_4^{2-} selectivity for the hydrometallurgical recovery of $ZnCl_2$. The extraction mechanism is considered by carrying out a series of well-designed solvent extraction experiments and NMR studies. The research also

attempts to achieve an understanding of the benefits of combining cation and anion binding sites in the same molecule as in Figure 3.1, rather than using a mixture of the salen ligand and hydrophobic amines. The potential application for these extractants is evaluated by investigation of the $ZnCl_2$ transport achieved by solvent extraction and water stripping.

This chapter covers the syntheses and characterizations of the polytopic ligands, solvent extraction results, NMR studies and the proposed mechanisms for metal loading. Chapter 4 extends the work with a focus on anion analysis and anion selectivities of the polytopic ligands and their metal complexes.

3.2 Syntheses and Characterization of Polytopic Ligands

Polytopic and monotopic ligands have been developed for the hydrometallurgical recovery of zinc chloride as shown in Scheme 3.1.

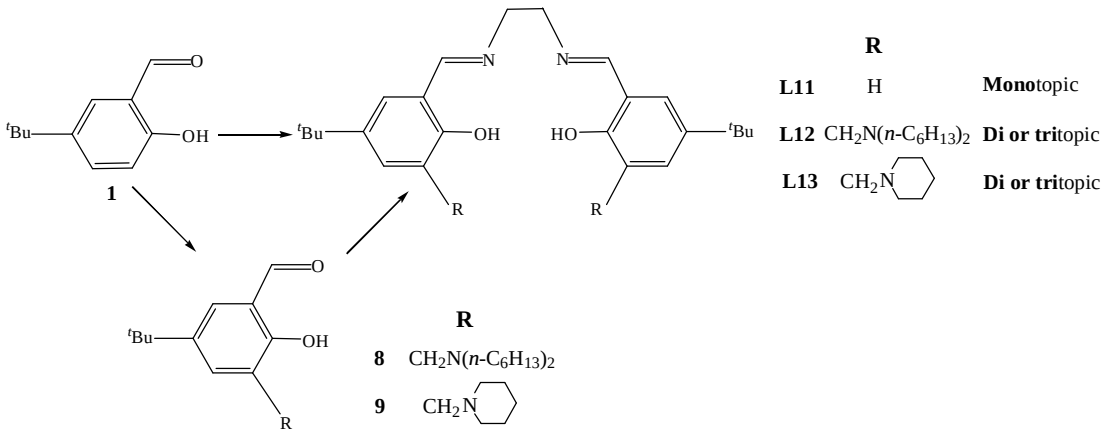

Scheme 3.1 Synthetic routes to extractants **L11**-**L13**

The *tert*-butyl derivative of the well-known tetradentate Schiff base ligand, **L11**, is a monotopic ligand and provides an $N_2O_2^{2-}$ donor set in a planar coordination

environment for a metal dication. Polytopic ligand **L12** has the salen unit substituted with dihexylaminomethyl units adjacent to the phenol groups to provide an anion binding site. It can form ditopic or tritopic assemblies as discussed in section 3.1.3. The dihexyl groups were incorporated to ensure good solubility in water-immiscible solvents. The piperidin-1-ylmethyl analogue **L13** was prepared to facilitate the isolation of crystalline complexes.

The syntheses of the extractants all start from the precursor **1** in Scheme 3.1, which can be readily prepared on a large scale by facile and high yielding methods as described in chapter 2. It is desirable for potential industrial application. The salicylaldehyde precursors can be easily transformed into the corresponding target ligands by one-step Schiff base condensation. For **L12** and **L13**, the incorporation of the pendant amine arm to the salicylaldehyde scaffold was achieved using a modified Mannich reaction.

3.2.1 Mannich Reaction

The Mannich reaction is the condensation of a compound having active hydrogen atoms (the substrate) with a carbonyl functionality (usually formaldehyde) and an amine as shown in Equation 3.1.[31, 32]

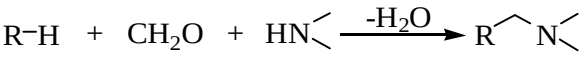

Equation 3.1

Phenol substrates have been well studied and give predominantly *ortho*-monosubstitution in the majority cases.[31, 33] Since the *para*-position and one of the *ortho*-positions of the phenolic group in **1** are blocked, Mannich reactions involving **1** should only give the desired products **8** and **9** (see Scheme 3.1). However, as the salicylaldehyde scaffold contains a carbonyl group, the possibility of an

unwanted side reaction between the amine and the salicylaldehyde may occur if a conventional, one-step Mannich reaction is carried out. Consequently a modified, two-step Mannich reaction was performed following a procedure reported by Fenton *et al.*[34]

The first step involves the preliminary formation of a Mannich base, either ethoxy-*N*-dihexylaminomethane (**6**) or 1-ethoxymethylpiperidine (**7**) in Figure 3.4, from the appropriate amine and formaldehyde to block the possible reaction with salicylaldehyde.[34, 35] By stirring the appropriate amine with paraformaldehyde in ethanol in the presence of potassium carbonate desiccant[34], **6** and **7** were produced in good yields after purification via vacuum distillation. A proposed mechanism for this step[32, 35] is shown in Figure 3.4.

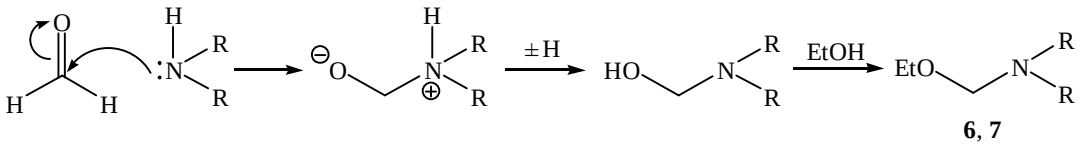

Figure 3.4 Proposed mechanism[32, 35] for the formation of the N-ethoxymethyldialkylamines **6** and **7**.

Subsequent attachment of the pendant amine groups to the salicylaldehyde was readily achieved by refluxing the Mannich base **6** or **7** with **1** in acetonitrile under nitrogen atmosphere. A mechanism involving a hydrogen-bonded complex[32] has been invoked to explain the preferred *ortho*-substitution of the phenolic group shown in Figure 3.5. The precursors **8** and **9** were obtained after purification by column chromatography.

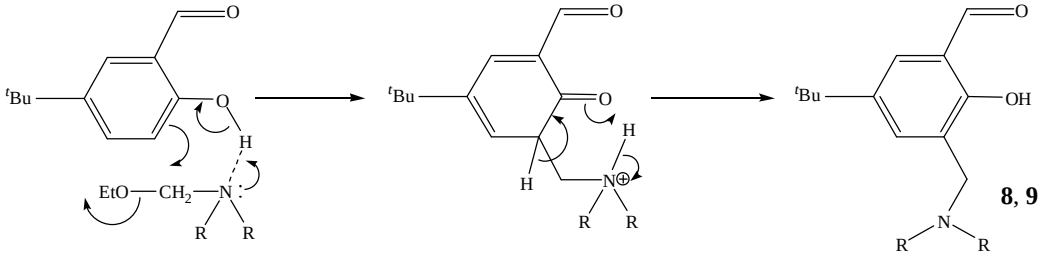

Figure 3.5 Proposed mechanism[32] for the substitution of the pendant amine groups to the salicylaldehyde scaffold to give precursors **8** and **9**.

3.2.2 Schiff Base Condensation

Schiff base condensations of the salicylaldehyde precursors **1**, **8** and **9** with ethylenediamine were carried out at room temperature in non-aqueous solvents as shown in Figure 3.6. The target ligands **L11**-**L13** were obtained in high yields.

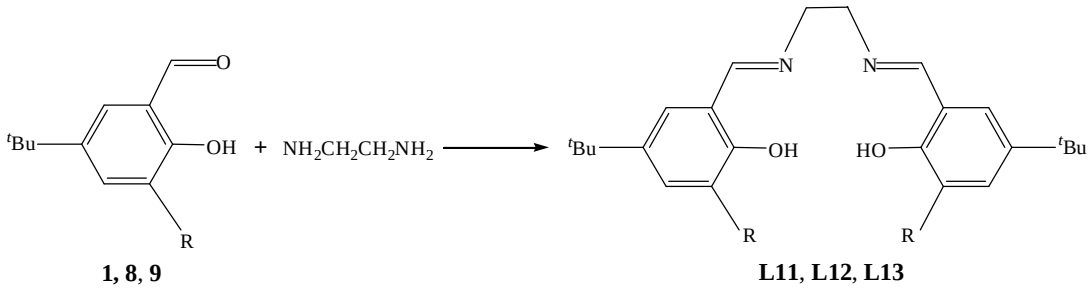

Figure 3.6 The Schiff base condensation reaction employed to produce ligands **L11**-**L13**.

3.2.3 Synthesis of an Auxiliary Amine

A tertiary amine with similar structure to the pendant amine group of **L12**, 1-*tert*-butyl-4-(dihexylamino)methylbenzene (**L14**), was synthesized for the solvent extraction studies. The synthesis was carried out via nucleophilic substitution of dihexylamine on 4-*tert*-butylbenzylbromide (see Figure 3.7).[36] The reactants were

mixed in dichloromethane at 0 °C, and stirred overnight at room temperature. The product was obtained in a good yield after washing with 4 M NaOH aqueous solution and purifying by column chromatography.

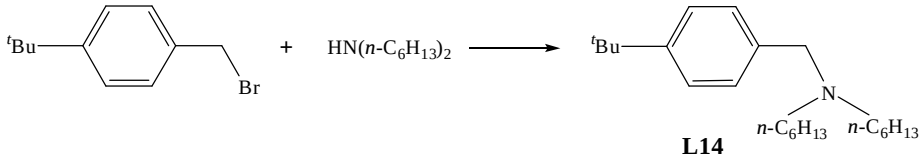

Figure 3.7 Synthesis of the auxiliary amine **L14**.[36]

3.2.4 Ligand Characterization

All ligands and precursors were fully characterized by ^{1}H and ^{13}C NMR spectroscopy and mass spectrometry. ^{1}H NMR spectra of the extractants **L11**-**L13** showed that the conversion of aldehyde to Schiff base was complete as indicated by the appearance of an azomethine signal and the absence of a carbonyl signal. ESI MS indicated the formation of the desired product by the presence of the expected parent ion (MH^{+}). The elemental microanalysis and melting points of ligands **L11**-**L14** confirmed their respective purities.

3.3 Initial Extraction Experiment

Two-phase solvent extraction experiments were carried out by contacting 0.01 M chloroform solutions of extractants **L11**, **L12** or **L13** with equal volumes of 1 M $ZnCl_2$ or $ZnSO_4$ aqueous solutions under stirring overnight. After completion of each experiment the Zn content of the organic phase was measured by evaporating an aliquot to dryness, making up to known volume in 1-butanol and analyzing the sample via ICP-OES. The results are shown in Figure 3.8, where 100% Zn-loading corresponds to one mole of zinc per mole of extractant.

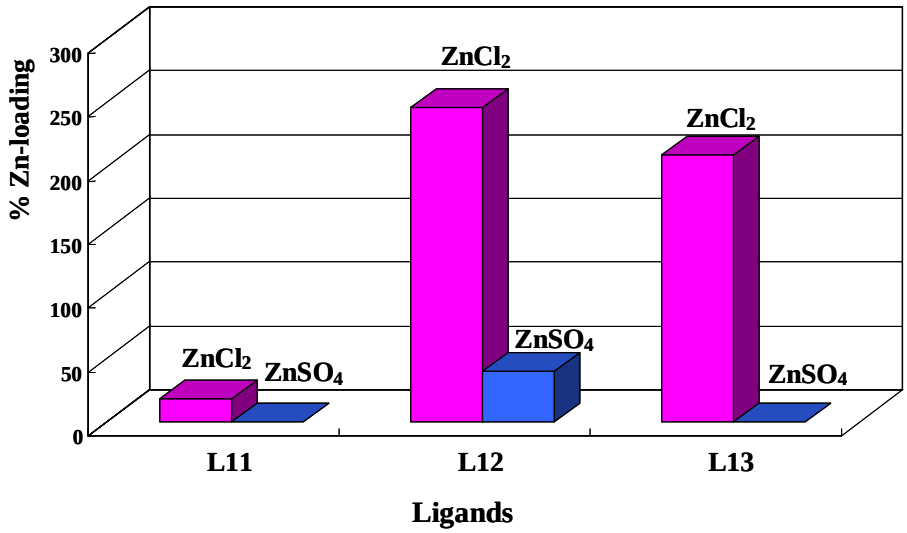

Figure 3.8 Equilibrium uptake of zinc by 0.01 M chloroform solutions of extractants **L11**-**L13** from an equal volume of 1 M aqueous $ZnCl_2$ or $ZnSO_4$ solution. The 100% loading corresponds to a 1:1 Zn:L ratio.

The uptake of zinc by **L11**-**L13** is much greater from chloride solution than from sulfate solution under comparable conditions. In the cases of **L11** and **L13** the Zn loadings from sulfate media are zero within experimental error. This indicates that the loading efficiency of the metal value is very dependent on the nature of the anion present. In particular, the polytopic ligands **L12** and **L13** show high selectivity for $ZnCl_2$ over $ZnSO_4$. In order to maintain the favoured overall neutral charge of the complexes in non-polar solvents, the anion is co-extracted by the polytopic ligands in their zwitterionic forms (see Figure 3.9). Consequently the ease of transferring the anion from the aqueous phase to the organic phase has a great effect on the efficiency of metal extraction. According to the Hofmeister bias[37], SO_4^{2-} is more strongly hydrated than Cl^- and prefers to stay in an aqueous environment, which is consistent with the observed selectivity. A more detailed discussion of the above phenomena along with the results of further research will be addressed in the next chapter.

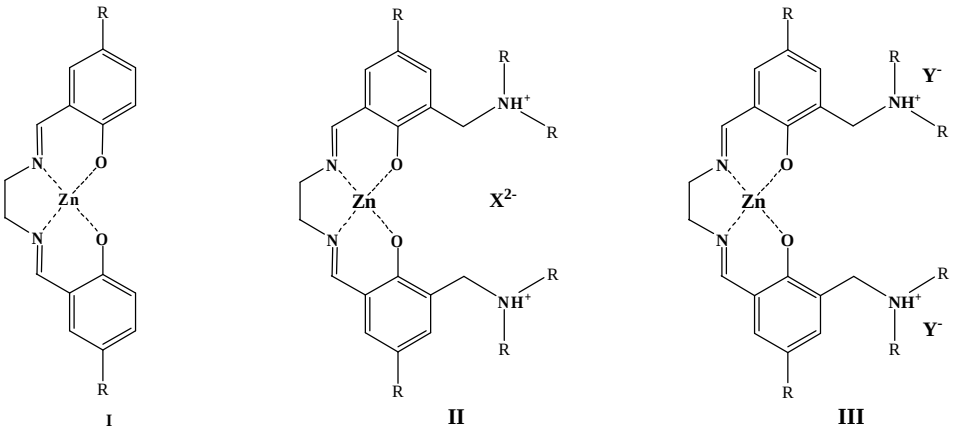

Figure 3.9 Possible structures for **I**, the monotopic complex of **L11**, **II,** the ditopic complex and **III**, the tritopic complex of **L12** and **L13**

The polytopic ligands **L12** and **L13** show much higher zinc uptakes from chloride media than the monotopic analogue **L11** (Figure 3.8). The inclusion of the pendant amine groups on the polytopic ligands has greatly improved the Zn loadings. The observation that 246% and 209% loadings were achieved by **L12** and **L13** respectively, suggests 2:1 (Zn:**L**) complexes were formed by these polytopic ligands. An attempt was made to grow crystals of the zinc complexes from the organic solutions of **L12** and **L13** after extraction. Unfortunately no single crystals were obtained. Some white amorphous solid was isolated from the solution of **L12** and subjected to elemental analysis, which indicated a molecular formula of [Zn**L12**($ZnCl_4$)] (Anal. Calc. for $C_{50}H_{86}Cl_4N_4O_2Zn_2$: C, 57.31; H, 8.27; N, 5.35. Found: C, 56.94; H, 8.45; N, 5.34%). All the above results confirm the preliminary results described in section 3.1.3 and support the supposition that the presence of the pendant amine groups in **L12** and **L13** promotes the uptake of both Zn^{2+} and $[ZnCl_4]^{2-}$ (see **II** in Figure 3.9, $X^{2-} = [ZnCl_4]^{2-}$).

Extractant **L12** shows considerable potential for zinc chloride recovery since it has achieved remarkably high transport efficiency and excellent $ZnCl_2$ over $ZnSO_4$ selectivity. Most of the currently available reagents discussed in section 3.1.2

requires one or two moles of ligands to extact one mole of zinc,[14, 15] while **L12** has shown to take up two zinc ions per ligand. Also it recovers both metal values and counter anions as a metal salt reagent, which is desirable for achieving overall material balance from an industry perspective. Consequently further detailed studies were undertaken for the polytopic ligand **L12**.

3.4 Polytopic Ligands Compared with Dual Host Systems

A key issue in the development of new polytopic reagents is whether they are more effective than the sum of their parts, i.e. dual host systems[38, 39] in which a *mixture* of cation and anion exchange reagents is used to transport a metal salt.

3.4.1 Dual Host Systems

The use of dual host systems as a strategy for achieving metal salt extraction in two-phase systems has been of increasing interest over recent years.[38-41]

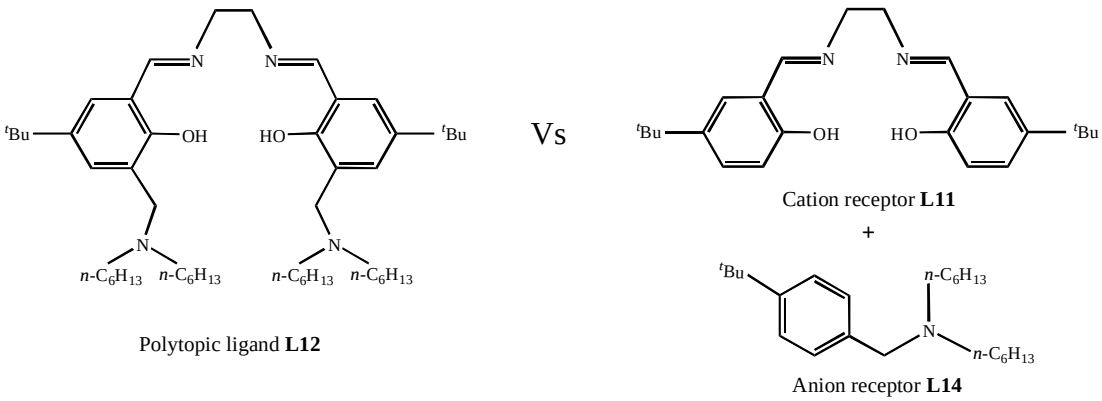

Polytopic ligand **L12**

Anion receptor **L14**

Figure 3.10 Polytopic ligand **L12** compared with dual host system **L11** + **L14**.

The most relevant dual host system for the present study is the combination of **L11** and **L14** which provide structurally similar cation and anion binding sites to the

polytopic ligand **L12** (see Figure 3.10). A series of related dual host systems listed in Table 3.3 were also studied. Solvent extraction experiments for these systems were carried out by contacting chloroform solutions of 0.01 M cation receptors and 0.02 M anion receptors with equal volumes of 1 M $ZnCl_2$ solutions under overnight stirring. For comparison, extractions using only the respective cation receptors or the anion receptors were also performed.

Dual host systems	% Zn loading from 1 M $ZnCl_2$ solution		
	Cation receptor only	Anion receptor only	Dual host system
L11 + **L14**	18	15	160
L11 + $N(C_2H_5)_3$	18	0	26
L11 + $N(n\text{-}C_4H_9)_3$	18	27	162
L11 + $N(n\text{-}C_6H_{13})_3$	18	31	163
L11 + 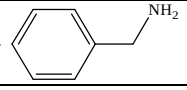	18	0	24
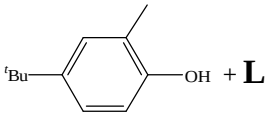 + **L14**	0	15	22

Table 3.3 The extraction of $ZnCl_2$ by a series of dual host systems. Cation receptors (0.01 M) or/and anion receptors (0.02 M) in chloroform were employed. The 100% Zn loading is based on 0.01 M Zn being transferred into organic phase.

The results in Table 3.3 indicate a few interesting features. Each of **L11** and **L14** on its own did not extract much zinc content, but their combination as a dual host system achieved a significant synergistic enhancement of zinc uptake. This may be rationalized in terms of the extraction mechanism employed by these ligands. In order to extract, **L11** is deprotonated and **L14** is protonated. For either of the extractants alone, an interfacial reaction involving a proton being transferred between

aqueous and organic phases occurs. However, when both species co-exist in the organic phase, the protonation and deprotonation required could occur in a single phase as shown in Equation 3.2. Such a process is expected to be much more thermodynamically and kinetically favoured than an interfacial process and hence results in an observed synergistic effect.

$$\mathbf{L11} + 2\mathbf{L14} \rightleftharpoons [\mathbf{L11}\text{-}2H]^{2+} + 2[\mathbf{L14}H]^{+} \qquad \textbf{Equation 3.2}$$

This rationale also accounts for one of the benefits of combining cation and anion binding sites in the same molecule as a polytopic ligand, and will be further discussed in section 3.4.2.

Another intriguing trend shown in Table 3.3 is that the nature of the anion receptor greatly affects the synergistic enhancement of zinc uptake. Comparison between similar dual host systems **L11** with $N(C_2H_5)_3$, **L11** with $N(n\text{-}C_4H_9)_3$, and **L11** with $N(n\text{-}C_6H_{13})_3$ indicates that the synergistic effect is significantly intensified as the alkyl chain length of the amine increases at the beginning, but after a certain length, the enhanced zinc uptake becomes roughly the same. A similar conclusion can be drawn on comparison of dual host systems **L11** with **L14** and **L11** with benzylamine. The above trend supports the proposition that $[ZnCl_4]^{2-}$ interacts with the amines present in the dual host systems, since the longer alkyl-chained amine forms a better "cavity" to more readily hold a big anion such as chlorozincate. When the alkyl-chain of the amine reaches a certain length, the bulky group may inhibit anion extraction and compensate for any enhancement, which is consistent with the obtained results.

The nature of the cation receptor also has a influence on the synergistic enhancement of zinc uptake. Compared to **L11**, 4-*tert*-Butyl-2-methyl-phenol is a poor Zn^{2+}

extractant and there is no increased zinc uptake when it pairs with **L14**. Even though simultaneous proton exchange could occur between the phenol and **L14** as shown in Equation 3.3, this equilibrium is expected to be driven to the left because the phenolate ion is not effective in extracting the metal cation to form a neutral charge species in the non-polar organic solvent.

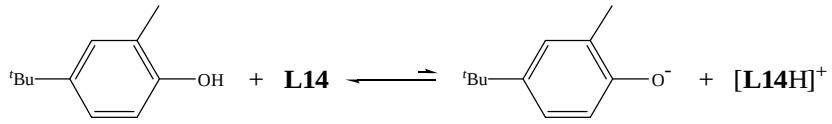

Equation 3.3

3.4.2 The Advantages of Polytopic Ligands

The solvent extraction results for polytopic ligand **L12** and dual host system **L11** with **L14** are compared in Figure 3.11. A chloroform solution as a blank was contacted with 1 M $ZnCl_2$ aqueous solution. No zinc uptake was obtained, which indicates that any observed enhancement was not due to solvation of zinc chloride by chloroform but rather due to the presence of the extractants. Neither **L11** nor **L14** on its own transports significant quantities of zinc into chloroform. The dual host formulation of **L11** and **L14** transports 1.60 moles zinc per mole of **L11** but is much less efficient than the polytopic reagent **L12** which loads 2.46 moles under the same conditions. This remarkable advantage of **L12** in term of transport efficiency demonstrates the success of polytopic approach to ligand design. The inclusion of the pendant amine groups at the *ortho*-position of the phenolic group in the same molecule makes proton exchange between them more facile than in the dual host system in Equation 3.2.

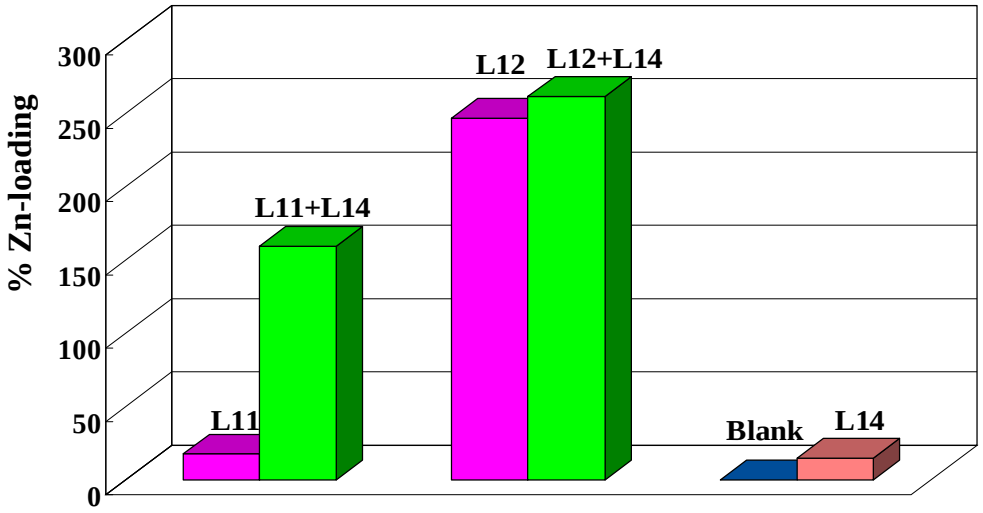

Figure 3.11 Equilibrium uptake of zinc by 0.01 M chloroform solutions of **L11** or **L12** or a blank chloroform solution in the presence or absence of **L14** (0.02 M) from an equal volume of 1 M aqueous $ZnCl_2$ solution. The 100% Zn loading is based on 0.01 M zinc being transferred into organic phase.

When the combination of **L12** and **L14** was used for extraction, no synergistic enhancement was observed (see Figure 3.11). The zinc uptake simply equals the sum of those by **L12** and **L14** on their own. This is consistent with the above discussion, because the phenolic groups in **L12** prefer to exchange protons with the pendant amine groups rather than with **L14**. Consequently **L14** will not be protonated to form a dual host system, and hence there is no synergistic effect.

More than 100% Zn loadings were achieved by both the polytopic ligand **L12** and the structurally similar combination of **L11** and **L14**. This implies that the anion binding sites are involved in the extraction and chlorozincate is loaded as the anion. Extraction experiments using 1 M $ZnSO_4$ solutions were carried out under comparable conditions. The results in Table 3.4 indicate that zinc uptakes were rather small and no synergistic effect was observed. This is not surprising because anionic sulfato complexes of zinc such as $[Zn(SO_4)_2]^{2-}$ are not stable and difficult to be

extracted as an anion. A comparison of the results from $ZnCl_2$ and $ZnSO_4$ media indicates that the zinc chloride species is important in solvent extraction and this aspect will be further investigated in the following sections.

Extractants	% Zn loading from 1 M $ZnSO_4$ solution
L11	0
L14	0
L11 + **L14**	0
L12	46
L12 + **L14**	48

Table 3.4 Zinc loadings from 1 M $ZnSO_4$ solutions by extractants **L11** (0.01 M), **L12** (0.01 M), **L14** (0.02 M) and their combinations respectively. The 100% Zn loading is based on 0.01 M zinc being transferred into organic phase.

3.5 Zinc Chloride Dependent Extraction

Solvent extraction experiments were carried out to study the dependence of zinc uptake on the concentration of the zinc chloride solution in order to unveil the extraction mechanism. Solutions of 0.01 M **L12** in chloroform were contacted with a series of $ZnCl_2$ aqueous solutions of varied concentrations ranging from 0.002 M to 2 M under overnight stirring. As shown in Figure 3.12, the zinc uptakes by **L12** are very dependent on the feed concentrations and greatly increase with the increasing $ZnCl_2$ concentrations in the aqueous solutions. However, this dependence is not linear, but much related with the zinc chloride speciation in the aqueous phase under different concentration.

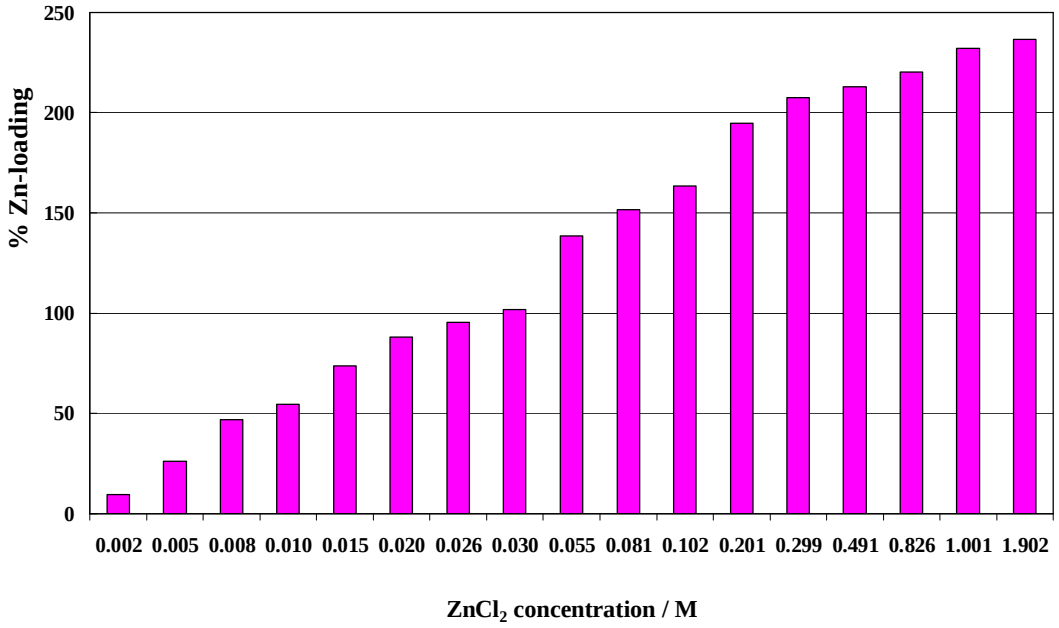

Figure 3.12 Zinc chloride dependent extraction by **L12** (0.01 M). The 100% loading is based on a 1:1 Zn:L ratio.

The speciation of aqueous $ZnCl_2$ solution has been investigated by X-ray diffraction, Raman spectroscopy, ^{67}Zn NMR and theoretical calculation studies.[42-49] At low concentration $[Zn(H_2O)_6]^{2+}$ is the dominant species;[45, 48] $[ZnCl(H_2O)_5]^{+}$ and $[ZnCl_2(H_2O)_4]$ start to form as the $ZnCl_2$ concentration is increased;[45, 48] $[ZnCl_3]^{-}$ and $[ZnCl_4]^{2-}$ exist at high $ZnCl_2$ concentrations and tend to be the dominant species in solutions of high chloride to zinc ratios.[43, 44, 46, 48] More importantly, $[ZnCl_4]^{2-}$ is unhydrated and $[ZnCl_3]^{-}$ is weakly hydrated,[43, 46, 49] which enables easy transfer from an aqueous phase to an organic phase. Given the existence of these species under different $ZnCl_2$ concentrations, it is reasonable to propose that the zinc cation is extracted from $ZnCl_2$ solutions of low concentrations and the $[ZnCl_4]^{2-}$ anion also becomes favourable for extraction as the $ZnCl_2$ concentration is increased. It is consistent with the results shown in Figure 3.12.

In order to probe the above proposition, another chloride dependent extraction was

performed in which a large excess of NaCl (0.94 M) was added to a 0.03 M $ZnCl_2$ solution. The results presented in Figure 3.13 show that the zinc uptake is dramatically increased from 100% to 200% loading on raising the concentration of chloride even with the concentration of zinc being unchanged in the aqueous phase. In the solution containing 0.03 M $ZnCl_2$ and 0.94 M NaCl, the dominant zinc species is $[ZnCl_4]^{2-}$.[46] Consequently the doubled zinc loading strongly supports the extraction of the $[ZnCl_4]^{2-}$ anion by **L12**.

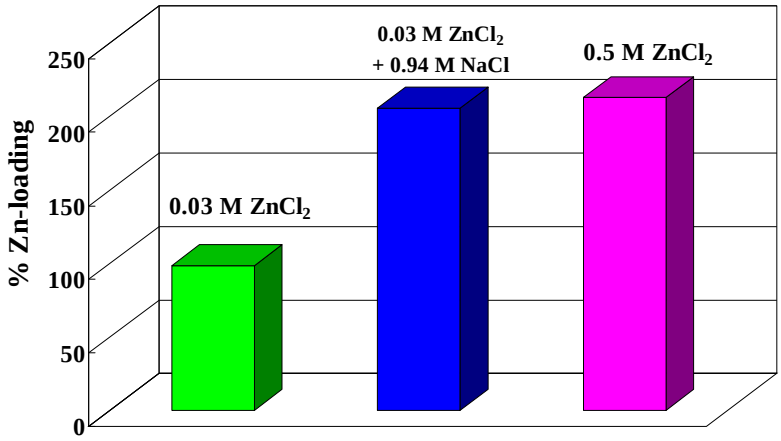

Figure 3.13 Chloride dependent extraction by **L12** (0.01 M). The 100% loading is based on a 1:1 Zn:L ratio.

The polytopic ligand **L12** shows excellent transport efficiency over a wide range of $ZnCl_2$ concentrations (see Figure 3.12), which is desirable for potential industrial applications. Comparable experiments were carried out for a dual host combination of **L11** and trihexylamine by contacting solutions of 0.01 M **L11** and 0.02 M trihexylamine in chloroform with a series of $ZnCl_2$ aqueous solutions of varied concentrations ranging from 0.002 M to 2 M under overnight stirring. The results are compared with those of **L12** in Figure 3.14. The dual host system only performs well over a rather narrow range of $ZnCl_2$ concentrations in contrast to the polytopic ligand

L12. For instance, **L12** achieved 100% and 200% Zn loadings respectively from 0.03 M and 0.2 M $ZnCl_2$ feed solutions, while the mixture of **L11** and trihexylamine loaded only 21% and 61% Zn under similar conditions. Also the zinc uptake by the dual host system was observed to decrease when contacted with high tenor $ZnCl_2$ feed solutions, while the polytopic ligand **L12** maintained its high transport efficiency.

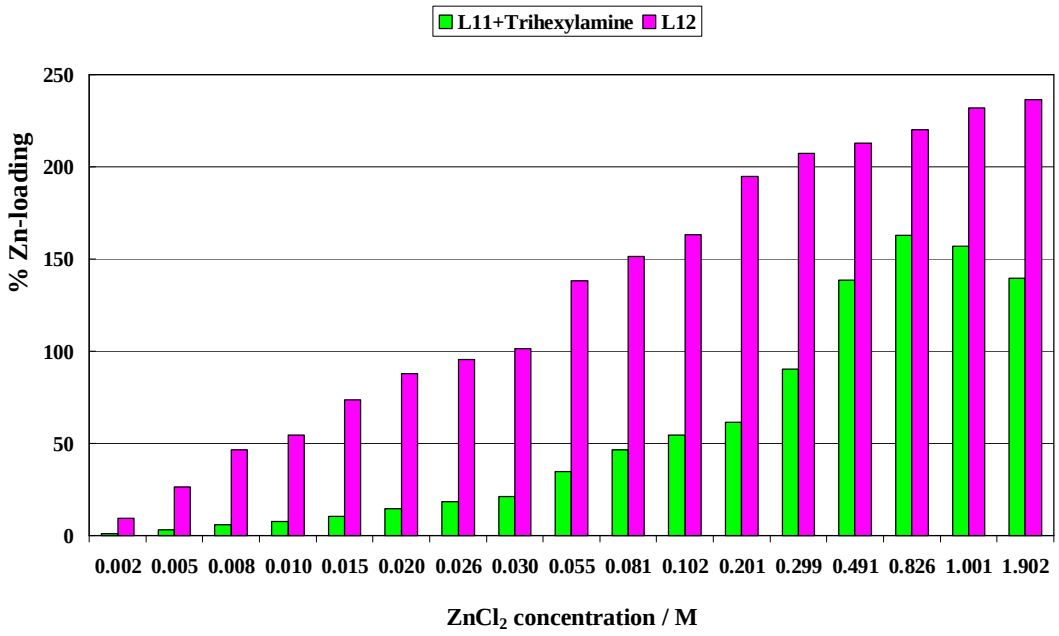

Figure 3.14 Zinc chloride dependent extraction by a dual host combination of **L11** (0.01 M) and trihexylamine (0.02 M) compared to **L12** (0.01 M). The 100% Zn loading is based on 0.01 M zinc content transferred into organic phase.

A possible rationale for the observed advantage of polytopic ligands is that the inclusion of the pendant amine groups on the phenol moiety makes the "salen" component a stronger cation exchange reagent, as is reflected by the much higher Zn loadings at low $ZnCl_2$ concentrations and stronger binding of the metal cation at high acidity caused by the high tenor $ZnCl_2$ (see Figure 3.14).

3.6 Stripping Experiment

The zinc chloride dependent extraction using the polytopic ligand **L12** indicates a potential "chloride swing" process in which the extraction and stripping are controlled by the activity of Cl^- in the aqueous solution as discussed in chapter 1. Consequently, water stripping experiments were carried out by contacting the organic phase separated from the $ZnCl_2$ dependent extraction with an equivalent volume of water under overnight stirring. The zinc contents in the chloroform solutions after equilibrium had been reached were then compared with those before the stripping as shown in Figure 3.15.

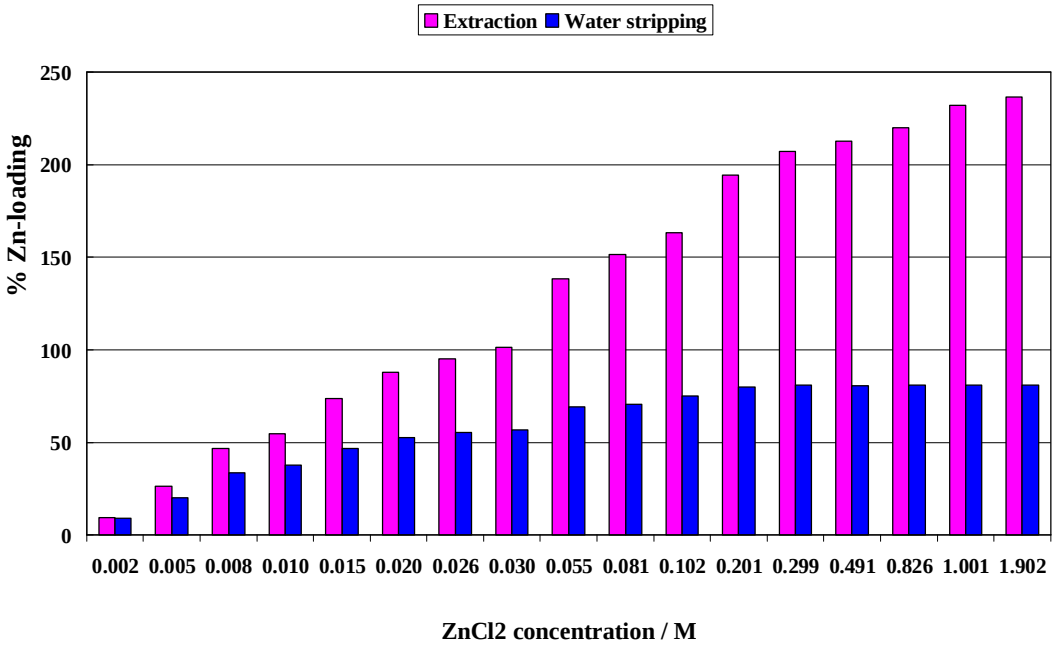

Figure 3.15 Extraction and water stripping by **L12** (0.01 M) from $ZnCl_2$ solutions of varied concentrations. The 100% Zn loading is based on 0.01 M zinc content in the organic phase.

The simple water stripping procedure is fairly effective, particularly for extraction solutions involving high zinc uptakes, which achieves a remarkable recovery of

160% $ZnCl_2$ per ligand at maximum. The mechanism of the stripping can be hypothetically considered to consist of two steps. First the loaded zinc chloride is fully stripped into the aqueous solution which forms a new feed solution for extraction. Then some of the zinc chloride is extracted back into the organic solution. This is consistent with the observed results. For instance, the extractions with about 200% Zn loadings would give rise to roughly 0.02 M $ZnCl_2$ aqueous solutions from which 80% should be and indeed is back extracted by **L12** (see Figure 3.15).

The water stripping results indicate that solvent extraction and stripping by **L12** from zinc chloride media could form the basis of a chloride-swing process which gives a recovery of 160% $ZnCl_2$ from one cycle of extraction and water stripping. In the industry more effective stripping methods such as acid stripping are applied and a full $ZnCl_2$ recovery is possible.

3.7 ^{1}H NMR Solution Studies

As zinc is diamagnetic, ^{1}H NMR spectroscopy was used to study **L12** and its complexes at different levels of $ZnCl_2$ loadings. In order to simulate the speciation during solvent extraction, all spectra were run in two-phase systems. Each NMR sample consisted of a stock solution of 0.01 M **L12** in $CDCl_3$ contacted with an equivalent volume of $ZnCl_2$ solution in D_2O with varied concentrations which corresponded to those used for the zinc chloride dependent extractions in section 3.5. Each NMR tube was shaken until equilibrium was established before the spectrum was obtained. Key spectra are shown in Figure 3.16.

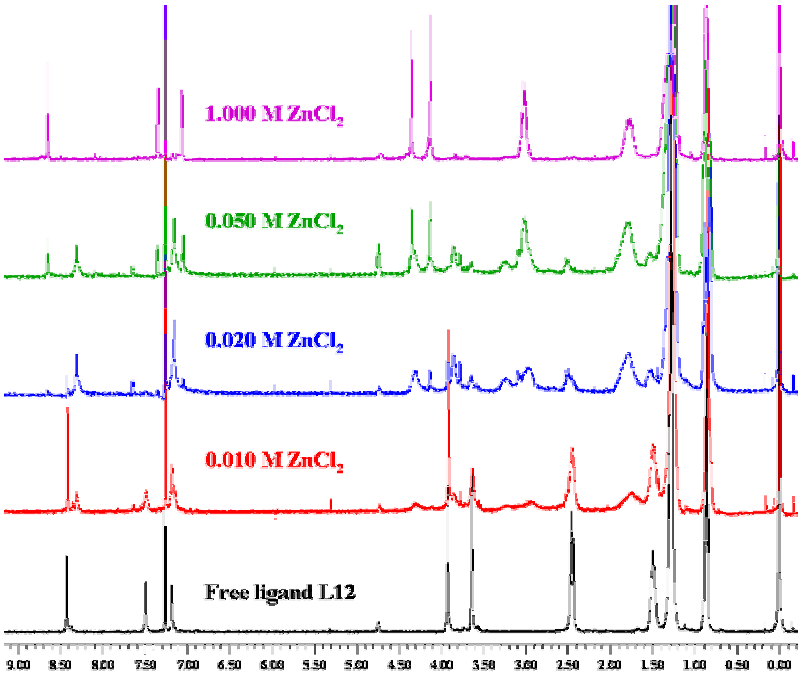

Figure 3.16 ^{1}H NMR spectra of **L12** (0.01 M) in $CDCl_3$ after extractions from $ZnCl_2$ solutions of varied concentrations in D_2O. The chemical shifts were recorded relative to the TMS peak.

Fortunately the ligand exchange is slow on the NMR timescale and hence chemical shifts from the same proton in different species are distinct instead of being the weighted average peaks. The spectra in Figure 3.16 reveal that two different complexes are successively formed as the ligand to zinc stoichiometry is increased to 1**L12** : 2$ZnCl_2$. The azomethine proton signal is chosen to follow the speciation since its chemical shifts are readily visible in the low field as shown in Figure 3.17. The Zn loadings at the respective concentrations are obtained by the corresponding zinc chloride dependent extractions in section 3.5. As shown in Figure 3.17 the azomethine proton appears at δ 8.42 in a 0.01 M solution of the free ligand in $CDCl_3$. A new signal appears at δ 8.31 when $ZnCl_2$ is loaded, reaching a maximum intensity at 100% Zn-loading, along with complete disappearance of the signal at δ 8.42. Higher zinc loadings are accompanied by the loss of the peak at δ 8.31, which is

replaced by a new signal at δ 8.65, reaching a maximum intensity at 200% $ZnCl_2$ loading. No further changes to the azomethine signal are observed when $CDCl_3$ solutions are contacted with very large excesses of $ZnCl_2$ in D_2O.

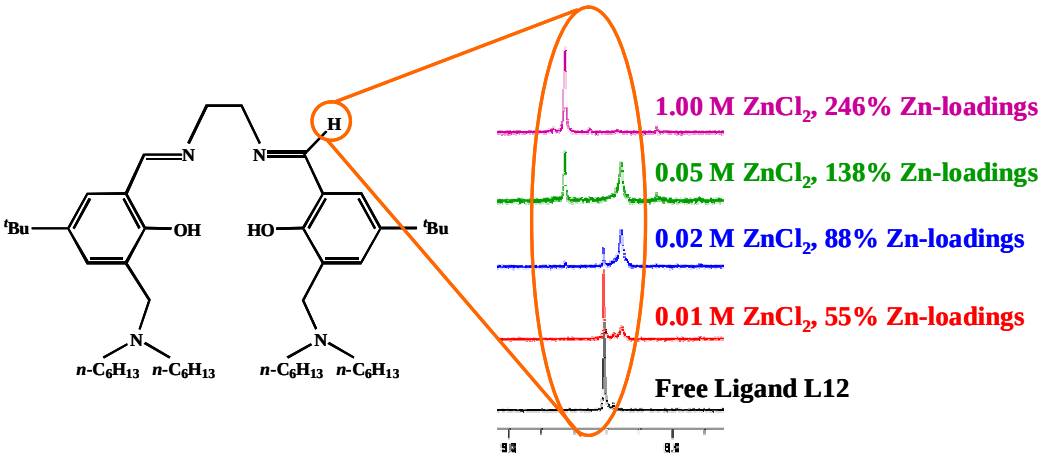

Figure 3.17 The variation in the chemical shift of the azomethine proton in **L12** resulting from the zinc loadings

The ^1H NMR data can be rationalized by the supposition that the first complex is formed by extracting the zinc cation at low $ZnCl_2$ concentrations and this is then converted to a second complex by the extraction of chlorozincate at high $ZnCl_2$ concentrations. In order to further investigate this proposition, a dual host pair, **L11** and trihexylamine, were used to carry out comparable experiments. The results are shown in Figure 3.18.

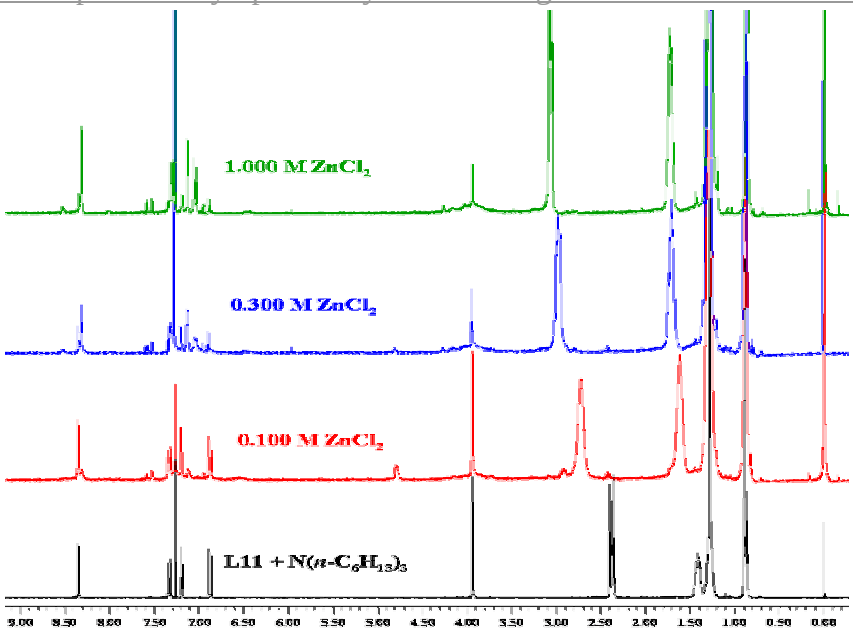

Figure 3.18 ^{1}H NMR spectra of **L11** (0.01 M) and trihexylamine (0.02 M) in $CDCl_3$ after extractions from $ZnCl_2$ solutions of varied concentrations in D_2O

Since the dual host system consists of two separate extractants for the respective cation and anion binding, the ^{1}H NMR spectra of **L11** should only show the complexing of the zinc cation while the spectra of trihexylamine demonstrate the extraction of chlorozincate. As shown in Figure 3.19, the azomethine proton of **L11** appears at δ 8.35 in the initial solution of 0.01 M **L11** and 0.02 M trihexylamine in $CDCl_3$. A new signal appears at δ 8.31 on zinc uptake, and corresponds to the disappearance of the signal at δ 8.35. No further change to the azomethine signal is observed at the presence of very large excesses of $ZnCl_2$ in D_2O. The changing chemical shifts in **L11** are very consistent with those of **L12** when the first complex is formed, and therefore confirm that the first complex results from the extraction of the zinc cation.

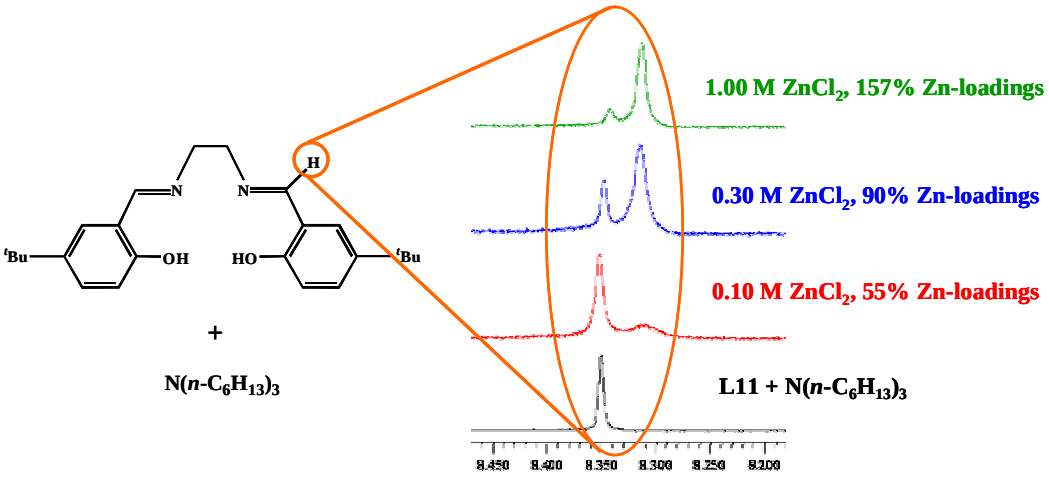

Figure 3.19 The variation in the chemical shifts of the azomethine proton in a dual host system **L11** and trihexylamine resulting from the zinc loadings

^{67}Zn NMR spectroscopy was attempted in the hope that the zinc nuclei in different coordination environments would be observed. However, only one peak is observed, which could represent either the weighted average peak or the peak with the highest symmetry.[49] The main difficulty in performing ^{67}Zn NMR is that ^{67}Zn is a quadrupolar nuclide (natural abundance 4.1%, nuclear spin quantum number I = 5/2, nuclear quadrupole moment Q = 0.15 × 10^{-28} m^2) with a width factor (a measure of typical line width) about 35 times larger than that of ^{17}O.[49-51] The ^{67}Zn line is usually very broad for Zn environments with symmetries lower than tetrahedral or octahedral and consequently with non-zero electric field gradients at the Zn nuclei.[49] Consequently no further attempts to obtain ^{67}Zn spectra were carried out.

3.8 Proposed Mechanism

A proposed mechanism for the solvent extraction from zinc chloride media by the polytopic ligands is shown in Figure 3.20. This is based on the above results, including the observation of multiple Zn-loadings by **L12** and **L13**, the elemental

analysis of the formed complex [Zn**L12**($ZnCl_4$)], the comparison of the polytopic ligand **L12** with the monotopic ligand **L11** as well as the dual host system **L11** and **L14**, the zinc chloride dependent extraction and stripping results and the ^1H NMR solution studies. Chloride analysis of the species formed in the organic phase will be discussed in chapter 4, which indicates that two moles of Cl^- are present per mole of zinc, confirming the uptake as $ZnCl_2$. The proposed mechanism shows that the tritopic assembly [Zn**L**Cl_2] forms when extracting from low concentrated $ZnCl_2$ feed solutions and then the ditopic assembly [Zn**L**($ZnCl_4$)] forms as the $ZnCl_2$ loading is increased with the increasing concentration of feed solution.

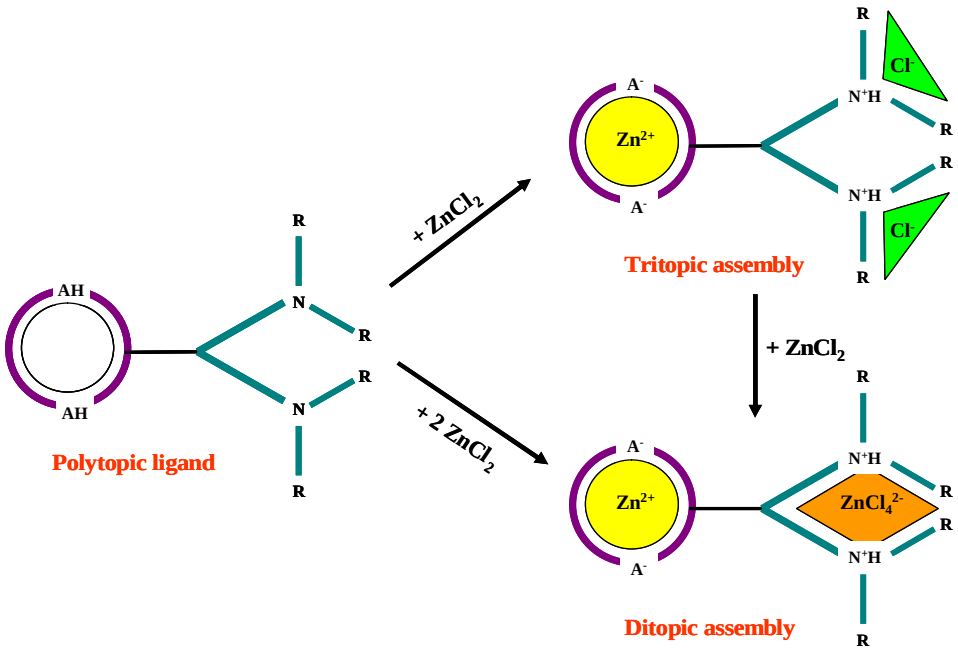

Figure 3.20 Proposed tritopic and ditopic assemblies involved in the extraction mechanism of $ZnCl_2$ by the polytopic ligand **L12**

The above mechanism for uptakes of $ZnCl_2$ can be adapted to account for cases where more than two moles of $ZnCl_2$ are loaded per mole of **L12**. When the zinc content of the aqueous feed is very high, some $[ZnCl_3]^-$ monoanions may replace the chloride ions in the tritopic assembly giving rise to neutral species [Zn**L**($ZnCl_3$)$_2$].

Consequently it achieves the overall transport efficiency of more than 200%. This rationale is reasonable considering that the $[ZnCl_3]^-$ species indeed exists in high tenor $ZnCl_2$ feed solutions and is known to be weakly hydrated.[43, 44, 46, 48, 49] Also ESI MS spectra of the species formed in the organic phase from concentrated $ZnCl_2$ feed solutions showed peaks for $[Zn\mathbf{L12}(ZnCl_3)]^+$ and $[Zn\mathbf{L13}(ZnCl_4)]H^+$. This provides further support for the proposed mechanism, though the possibility of generating such species in the MS capillary cannot be excluded.

3.9 Experimental

3.9.1 Chemicals and Instrumentation

Unless otherwise specified a reagent or solvent was used as obtained from Aldrich, Fisher or Acros. Standards for inductively coupled plasma optical emission spectroscopy (ICP- OES) were purchased from Alfa Asar.

^1H and ^{13}C NMR spectra were run on a Bruker ARX250 at ambient temperature. Chemical shifts (δ) are reported in parts per million (ppm) relative to internal standards. CHN analytical data were obtained by the University of St Andrews Microanalytical Service. Mass spectrometry was performed on a Micromass ZMD instrument with a z-spray ESI source. Melting points were measured on a Gallenkamp melting point apparatus. ICP-OES analysis was performed on a Perkin Elmer Optima 5300DV spectrometer.

3.9.2 Ligand Synthesis

Ethoxy-*N*-dihexylaminomethane (6) Dihexylamine (342 g, 1.84 mol) was added dropwise to a stirred suspension of paraformaldehyde (68.8 g, 2.29 mol) and

potassium carbonate (516 g, 3.73 mol) in ethanol (900 ml) at 0 °C. The mixture was allowed to warm to room temperature and continually stirred for 72 h. The product was filtered and the potassium carbonate was washed with ethanol (200 ml). The combined solution was concentrated *in vacuo* and then purified by vacuum distillation (2mm Hg, b.p. 160 °C) to afford the product as a colourless liquid (285 g, 63%). ^{1}H NMR ($CDCl_3$, 250 MHz): δ 0.80 (t, 6H, $N(CH_2)_5CH_3$), 1.09 (t, 3H, $CH_2OCH_2CH_3$), 1.20 (m, 12H, $NCH_2CH_2(CH_2)_3CH_3$), 1.37 (m, 4H, $NCH_2CH_2(CH_2)_3CH_3$), 2.53 (t, 4H, $NCH_2(CH_2)_4CH_3$), 3.35 (q, 2H, $CH_2OCH_2CH_3$), 4.06 (s, 2H, $CH_2OCH_2CH_3$); ^{13}C NMR ($CDCl_3$, 250 MHz): δ 14.3 (2C, $N(CH_2)_5CH_3$), 15.5 (1C, OCH_2CH_3), 23.0 (2C, $N(CH_2)_4CH_2CH_3$), 27.4 (2C, $N(CH_2)_2CH_2(CH_2)_2CH_3$), 28.5 (2C, $NCH_2CH_2(CH_2)_3CH_3$), 32.1 (2C, $N(CH_2)_3CH_2CH_2CH_3$), 52.3 (2C, $NCH_2(CH_2)_4CH_3$), 63.4 (1C, OCH_2CH_3), 85.5 (1C, NCH_2O). ESIMS *m/z* 244 (MH^+). Melting Point N/A (oil).

1-Ethoxymethylpiperidine (7) The same method was employed as for the synthesis of **6**, using piperidine (85.4 g, 1.00 mol) as the amine, paraformaldehyde (37.6 g, 1.25 mol) and potassium carbonate (276 g, 2.00 mol) to afford the product as a colourless oil (73.7 g, 52%). ^{1}H NMR ($CDCl_3$, 250 MHz): δ 0.99 (t, 3H, CH_3), 1.25 (m, 2H, $NCH_2CH_2CH_2$), 1.37 (m, 4H, $NCH_2CH_2CH_2$), 2.44 (t, 4H, $NCH_2CH_2CH_2$), 3.29 (q, 2H, OCH_2CH_3), 3.85 (s, 2H, NCH_2O); ^{13}C NMR ($CDCl_3$, 250 MHz): δ 15.3 (1C, OCH_2CH_3), 24.3 (2C, $NCH_2CH_2CH_2$), 26.1 (1C, $NCH_2CH_2CH_2$), 50.8 (2C, $NCH_2CH_2CH_2$), 64.1 (1C, OCH_2CH_3), 89.2 (1C, NCH_2O). ESIMS *m/z* 144 (MH^+). Melting Point N/A (oil).

5-*tert*-Butyl-3-dihexylaminomethyl-2-hydroxybenzaldehyde (8) A mixture of **1** (22.6 g, 0.12 mol) and **6** (30.4 g, 0.12 mol) in acetonitrile (200 ml) was heated to reflux under a nitrogen atmosphere for 90 h. After cooling to room temperature, the solvent was removed *in vacuo*. The crude product was dissolved in dichloromethane

(150 ml) and extracted with water (3 × 50 ml). The organic fraction was dried over $MgSO_4$, concentrated *in vacuo* and purified by silica-60 wet flash column chromatography (hexane: ethyl acetate, 20:1) to afford the product as a yellow oil (23.7 g, 53%). ^{1}H NMR ($CDCl_3$, 250 MHz): δ 0.84 (t, 6H, $N(CH_2)_5CH_3$), 1.25 (m, 12H, $NCH_2CH_2(CH_2)_3CH_3$), 1.26 (s, 9H, $C(CH_3)_3$), 1.53 (m, 4H, $NCH_2CH_2(CH_2)_3CH_3$), 2.51 (t, 4H, $NCH_2(CH_2)_4CH_3$), 3.77 (s, 2H, $ArCH_2N$), 7.26 (d, 1H, Ar-*H*), 7.63 (d, 1H, Ar-*H*), 10.40 (s, 1H, C*H*O), 12.01 (s, 1H, O*H*); ^{13}C NMR ($CDCl_3$, 250 MHz): δ 14.3 (2C, $N(CH_2)_5CH_3$), 22.9 (2C, $N(CH_2)_4CH_2CH_3$), 26.6 (2C, $N(CH_2)_2CH_2(CH_2)_2CH_3$), 27.3 (2C, $NCH_2CH_2(CH_2)_3CH_3$), 31.6 (3C, $C(CH_3)_3$), 32.0 (2C, $N(CH_2)_3CH_2CH_2CH_3$), 34.4 (1C, $C(CH_3)_3$), 53.8 (1C, $CH_2N(CH_2)_5CH_3$), 57.7 (2C, $NCH_2(CH_2)_4CH_3$), 122.7 (1C, Ar-*C*), 123.8 (1C, Ar-*C*), 124.0 (1C, Ar-*C*), 132.5 (1C, Ar-*C*), 141.7 (1C, Ar-*C*), 160.5 (1C, Ar-*C*), 191.4 (1C, *C*HO). ESIMS *m/z* 376 (MH^+). Melting Point N/A (oil).

5-*tert*-Butyl-3-piperidin-1-ylmethyl-2-hydroxybenzaldehyde (9) 1 (10.0 g, 57 mmol) and **7** (8.88 g, 62 mmol) were refluxed in acetonitrile (200 ml) under a nitrogen atmosphere for 90 h. After cooling to room temperature, the solvent was removed *in vacuo* and the resulting sticky solid was recrystallized from hexane to give a light yellow solid (7.53 g, 48%). ^{1}H NMR ($CDCl_3$, 250 MHz): δ 1.28 (s, 9H, $C(CH_3)_3$), 1.52 (m, 2H, $NCH_2CH_2CH_2$), 1.66 (m, 4H, $NCH_2CH_2CH_2$), 2.54 (m, 4H, $NCH_2CH_2CH_2$), 3.71 (s, 2H, NCH_2Ar), 7.25 (d, 1H, Ar-*H*), 7.65 (d, 1H, Ar-*H*), 10.42 (s, 1H, C*H*O), 11.30 (s, 1H, O*H*); ^{13}C NMR ($CDCl_3$, 250 MHz): δ 24.2 (2C, $NCH_2CH_2CH_2$), 26.1 (1C, $NCH_2CH_2CH_2$), 31.7 (3C, $C(CH_3)_3$), 34.4 (1C, $C(CH_3)_3$), 54.3 (1C, $CH_2NCH_2CH_2CH_2$), 61.8 (2C, $NCH_2CH_2CH_2$), 122.7 (1C, Ar-*C*), 123.2 (1C, Ar-*C*), 124.1 (1C, Ar-*C*), 132.7 (1C, Ar-*C*), 141.8 (1C, Ar-*C*), 160.4 (1C, Ar-*C*), 191.5 (1C, *C*HO). ESIMS *m/z* 276 (MH^+). Melting Point 96-97 °C.

4,4'-Di-*tert*-butyl-2,2'-(ethylenedinitrilodimethylidyne)diphenol (L11) A solution

of ethylenediamine (0.54 g, 8.9 mmol) in acetonitrile (25 ml) was added to a stirred solution of **1** (3.09 g, 17 mmol) in ethanol (50 ml). The mixture was stirred overnight and the solvents were removed *in vacuo*. The product was dissolved in dichloromethane (50 ml) and extracted with water (3 × 25 ml). The organic fraction was dried with $MgSO_4$, filtered and the solvent removed *in vacuo* to afford a viscous yellow solid which was recrystallized from ethanol to afford the product as a light yellow solid (3.12 g, 96%). (Anal. Calc. for $C_{24}H_{32}N_2O_2$: C, 75.75; H, 8.48; N, 7.36. Found: C, 75.90; H, 8.45; N, 7.35%); ^{1}H NMR ($CDCl_3$, 250 MHz): δ 1.29 (s, 18H, C(CH_3)$_3$), 3.94 (s, 4H, N(CH_2)$_2$N), 6.90 (d, 2H, Ar-*H*), 7.21 (d, 2H, Ar-*H*), 7.35 (dd, 2H, Ar-*H*), 8.37 (s, 2H, N=C*H*); ^{13}C NMR ($CDCl_3$, 250 MHz): δ 31.8 (6C, C(*C*H_3)$_3$), 34.3 (2C, *C*(CH_3)$_3$), 60.3 (2C, N(*C*H_2)$_2$N), 116.8 (2C, Ar-*C*), 118.3 (2C, Ar-*C*), 128.3 (2C, Ar-*C*), 130.1 (2C, Ar-*C*), 141.7 (2C, Ar-*C*), 159.0 (2C, Ar-*C*), 167.2 (2C, *C*=N). ESIMS *m/z* 381 (MH^+). Melting Point 161-162 °C.

4,4'-Di-*tert*-butyl-6,6'-bis(dihexylaminomethyl)-2,2'-(ethylenedinitrilodimethylidyne)diphenol (L12) The same method was employed as for the synthesis of **L11**, using **8** (6.44 g, 17 mmol) instead of **1** to afford the product as a viscous yellow oil (6.54 g, 99%), which was used without further purification. (Anal. Calc. for $C_{50}H_{86}N_4O_2$: C, 77.46; H, 11.18; N, 7.23. Found: C, 77.25; H, 11.89; N, 7.74%); ^{1}H NMR ($CDCl_3$, 250 MHz): δ 0.87 (t, 12H, N(CH_2)$_5$C*H*$_3$), 1.27 (m, 24H, NCH_2CH_2(C*H*$_2$)$_3$CH_3), 1.30 (s, 18H, C(C*H*$_3$)$_3$), 1.50 (m, 8H, NCH_2C*H*$_2$(CH_2)$_3$CH_3), 2.46 (t, 8H, NC*H*$_2$(CH_2)$_4$CH_3), 3.65 (s, 4H, ArC*H*$_2$N), 3.92 (s, 4H, N(C*H*$_2$)$_2$N), 7.19 (d, 2H, Ar-*H*), 7.51 (d, 2H, Ar-*H*), 8.43 (s, 2H, N=C*H*); ^{13}C NMR ($CDCl_3$, 250 MHz): δ 14.4 (4C, N(CH_2)$_5$*C*H_3), 23.0 (4C, N(CH_2)$_4$*C*H_2CH_3), 27.4 (4C, N(CH_2)$_2$*C*H_2(CH_2)$_2$CH_3), 27.6 (4C, NCH_2*C*H_2(CH_2)$_3$CH_3), 31.8 (6C, C(*C*H_3)$_3$), 32.2 (4C, N(CH_2)$_3$*C*H_2CH_2CH_3), 34.4 (2C, *C*(CH_3)$_3$), 53.0 (2C, *C*H_2N(CH_2)$_5$CH_3), 54.6 (4C, N*C*H_2(CH_2)$_4$CH_3), 60.6 (2C, N(*C*H_2)$_2$N), 118.3 (2C, Ar-*C*), 125.9 (2C, Ar-*C*), 126.9 (2C, Ar-*C*), 130.4 (2C, Ar-*C*), 141.1 (2C, Ar-*C*), 157.3 (2C, Ar-*C*), 166.4 (2C,

C=N). ESIMS *m/z* 776 (MH^+). Melting Point N/A (oil).

4,4'-Di-*tert*-butyl-6,6'-bis(piperidin-1-ylmethyl)-2,2'-(ethylenedinitrilodimethylidyne)diphenol (L13) A solution of ethylenediamine (0.44 g, 7.3 mmol) in ethanol (40 ml) was added to a stirred solution of **9** (4.05 g, 14.7 mmol) in diethyl ether (40 ml). The mixture was stirred overnight and concentrated *in vacuo* to yield a yellow solid, which was recrystallized from hexane/diisopropyl ether (3.66 g, 87%). (Anal. Calc. for $C_{36}H_{54}N_4O_2$: C, 75.22; H, 9.47; N, 9.75. Found: C, 75.42; H, 9.80; N, 9.76%); ^{1}H NMR ($CDCl_3$, 250 MHz): δ 1.30 (s, 18H, $C(CH_3)_3$), 1.45 (m, 4H, $NCH_2CH_2CH_2$), 1.61 (m, 8H, $NCH_2CH_2CH_2$), 2.46 (t, 8H, $NCH_2CH_2CH_2$), 3.59 (s, 4H, NCH_2Ar), 3.92 (s, 4H, $N(CH_2)_2N$), 7.21 (d, 2H, Ar-*H*), 7.37 (d, 2H, Ar-*H*), 8.42 (s, 2H, N=C*H*); ^{13}C NMR ($CDCl_3$, 250 MHz): δ 24.7 (4C, $NCH_2CH_2CH_2$), 26.4 (2C, $NCH_2CH_2CH_2$), 31.8 (6C, $C(CH_3)_3$), 34.3 (2C, $C(CH_3)_3$), 54.8 (2C, $CH_2NCH_2CH_2CH_2$), 57.8 (4C, $NCH_2CH_2CH_2$), 60.5 (2C, $N(CH_2)_2N$), 118.5 (2C, Ar-*C*), 125.0 (2C, Ar-*C*), 126.4 (2C, Ar-*C*), 131.0 (2C, Ar-*C*), 141.0 (2C, Ar-*C*), 157.5 (2C, Ar-*C*), 166.3 (2C, *C*=N). ESIMS *m/z* 575 (MH^+). Melting Point 112-113 °C.

1-*tert*-Butyl-4-(dihexylamino)methylbenzene (L14) An excess of dihexylamine (30.0 g, 162 mmol) was added to a solution of 4-*tert*-butylbenzylbromide (11.9 g, 52.5 mmol) in dichloromethane (150 ml) at 0 °C. The mixture was stirred overnight at room temperature and the solvents then removed *in vacuo*. The product was washed with 4 M NaOH aqueous solution (150 ml), extracted with diethyl ether (2 × 50 ml), dried over $MgSO_4$, concentrated *in vacuo* and purified by silica-60 wet flash column chromatography (eluting with 10% methanol in dichloromethane) to yield a brown oil (10.8 g, 62%). (Anal. Calc. for $C_{23}H_{41}N$: C, 83.31; H, 12.46; N, 4.22. Found: C, 83.17; H, 12.24; N, 4.59%); ^{1}H NMR ($CDCl_3$, 250 MHz): δ 0.89 (t, 6H, $N(CH_2)_5CH_3$), 1.28 (m, 12H, $NCH_2CH_2(CH_2)_3CH_3$), 1.33 (s, 9H, $C(CH_3)_3$), 1.52 (m,

4H, $NCH_2CH_2(CH_2)_3CH_3$), 2.48 (t, 4H, $NCH_2(CH_2)_4CH_3$), 3.62 (s, 2H, $ArCH_2N$), 7.29 (d, 2H, Ar-*H*), 7.35 (d, 2H, Ar-*H*); ^{13}C NMR ($CDCl_3$, 250 MHz): δ 14.4 (2C, $N(CH_2)_5CH_3$), 23.0 (2C, $N(CH_2)_4CH_2CH_3$), 26.9 (2C, $N(CH_2)_2CH_2(CH_2)_2CH_3$), 27.4 (2C, $NCH_2CH_2(CH_2)_3CH_3$), 31.8 (3C, $C(CH_3)_3$), 32.1 (2C, $N(CH_2)_3CH_2CH_2CH_3$), 34.8 (1C, $C(CH_3)_3$), 53.8 (2C, $NCH_2(CH_2)_4CH_3$), 58.3 (1C, $CH_2N(CH_2)_5CH_3$), 125.4 (2C, Ar-*C*), 129.2 (2C, Ar-*C*), 136.1 (1C, Ar-*C*), 150.2 (1C, Ar-*C*). ESIMS *m/z* 332 (MH^+). Melting Point N/A (oil).

3.9.3 Solvent Extraction

All extractions were performed by the same general procedure. A solution of L (L= **L11**, **L12**, **L13**) in chloroform (10 ml, 0.01 M) was contacted with an aqueous ZnX_2 ($X= Cl^-$, $1/2SO_4^{2-}$) solution (10 ml, 1 M or specific concentration) in a tightly sealed, screw top glass jar. The two-phase system was stirred at 500 r.p.m at room temperature for 18 h. A 0.50 ml aliquot was taken from the organic phase, dried *in vacuo*, redissolved in butan-1-ol (10 ml), and the zinc content analysed by ICP-OES.

For experiments involving dual host systems, the same method was employed, but 0.02M **L14** or the appropriate amine was added to the organic phase.

For the water stripping experiment, the organic phase was separated from the original extraction and contacted with H_2O (10 ml) in a tightly sealed, screw top glass jar. The new two-phase system was stirred at 500 r.p.m. at room temperature for 18 h. The same analysis method was employed.

3.9.4 ^{1}H NMR Solution Study

In NMR tubes, stock solutions of 0.01 M **L12** (or the dual host pair 0.01 M **L11** and

0.02 M trihexylamine) in 1.00 ml $CDCl_3$ were contacted with 1.00 ml $ZnCl_2$ solutions of varied concentrations in D_2O. The tubes were vigorously shaken for 10 min and stood still for 5 min. The NMR spectra were run on a Bruker DPX360 spectrometer at 298 K and the chemical shifts were recorded relative to the TMS peak.

3.10 Conclusions

The work in this chapter aimed to develop polytopic salicylaldimine ligands with high transport efficiency of metal salts and high $ZnCl_2$ over $ZnSO_4$ selectivity for the hydrometallurgical $ZnCl_2$ recovery, to investigate the extraction mechanism of these ligands and to understand the ligand design features such as the benefits of combining cation and anion binding sites in the same molecule. All these objectives have been achieved.

The polytopic ligands bearing the pendant amine groups, **L12** and **L13**, were readily prepared on a large scale by facile and high yielding methods and were tested in solvent extraction experiments to show multiple zinc loadings from chloride media (246% by **L12** and 209% by **L13**). The transport efficiency was much higher than that obtained for the monotopic ligand **L11** (18% Zn-loadings) as well as the dual host combination of **L11** and the auxiliary amine **L14** (160% Zn-loadings) with the latter having a related structure to the pendant amine groups of **L12**. The polytopic ligands also showed much higher zinc uptakes from chloride media than sulfate media, which corresponds to a high $ZnCl_2$ over $ZnSO_4$ selectivity.

The multiple loading of $ZnCl_2$ by **L12** suggested the extraction of chlorozincate as anions given that $[ZnCl_4]^{2-}$ and $[ZnCl_3]^-$ ions are weakly hydrated species existing in highly concentrated $ZnCl_2$ feed solutions.[43, 44, 46, 48, 49] For the species formed in the

organic phase under high tenor $ZnCl_2$ feed, the elemental analysis confirmed the formula of the complex as [Zn**L12**($ZnCl_4$)], and the ESI MS spectra showed the peaks of [Zn**L12**($ZnCl_3$)]$^+$ and [Zn**L13**($ZnCl_4$)]H^+. The zinc chloride dependent extraction and stripping experiments further indicated that the extraction by **L12** proceeds as a chloride-swing process which is controlled by the Cl^- activities in the aqueous solutions. The corresponding ^{1}H NMR solution studies showed that two different complexes are successively formed as the ligand to zinc stoichiometry is increased to 1**L12** : 2$ZnCl_2$. The first complex is formed by extracting the zinc cation at low $ZnCl_2$ concentrations, supported by the comparable studies of the dual host system **L11** and trihexylamine, and the second complex could result from the extraction of chlorozincate at high $ZnCl_2$ concentrations. Based on all these results, the proposed mechanism concludes that a tritopic assembly [Zn**L12**Cl_2] forms from low concentrated $ZnCl_2$ feed solutions by binding the Zn^{2+} cation with the $N_2O_2^{2-}$ site and two Cl^- anions with the protonated pendant amine groups and then a ditopic assembly [Zn**L12**($ZnCl_4$)] forms on extracting the $[ZnCl_4]^{2-}$ anion when the $ZnCl_2$ loading is increased under high tenor $ZnCl_2$ feed. The possible formation of the tritopic assembly [Zn**L12**($ZnCl_3$)$_2$] is able to account for the observed Zn-loading of more than 200%.

The dual host pair **L11** and **L14** along with a series of other dual host systems provided a comparison to the polytopic ligands in term of ligand design. Combining both the cation and anion binding sites in the same molecule **L12** results in many benefits. One is that the deprotonation of the phenolic group and the protonation of the amine group can occur as a simultaneous intramolecular proton exchange instead of an interfacial reaction or a reaction between two separate reagents. This is expected to be much thermodynamically and dynamically favoured, and therefore significantly increases the transport efficiency. Another advantage is that the inclusion of the pendant amine groups on the phenol moiety makes the “salen”

component a stronger cation exchange reagent. This is indicated by the results of the zinc chloride dependent extractions. **L12** achieved much higher Zn loadings than the combination of **L11** and trihexylamine at low $ZnCl_2$ concentrations and stronger binding of the metal cation at high acidity caused by the high tenor $ZnCl_2$.

The above properties of the polytopic ligands indicate their potential for industrial application in the hydrometallurgical $ZnCl_2$ recovery. In particular, **L12** achieved a recovery of 160% $ZnCl_2$ from one cycle of extraction and simple water stripping, which makes it promising in this regard.

Some of the results presented in this chapter showed that the loading efficiency of the metal value was dependent on the nature of the counter anion, and the polytopic ligands achieved anion selectivity of chlorozincate over chloride. These interesting aspects are further investigated in the following chapter.

3.11 References

1. H. M. Cyr, T. D. O'Brien, M. C. Sneed and R. C. Brasted, "Comprehensive Inorganic Chemistry", Princeton, New Jersey, 1955.
2. J. Emsley, "Nature's Building Blocks: An A-Z Guide to the Elements", Oxford University Press, Oxford, 2001.
3. N. N. Greenwood and A. Earnshaw, "Chemistry of the Elements", Butterworth-Heinemann Ltd, Oxford, 1984.
4. M. Farnsworth, C. H. Kline and J. G. Noltes, "Zinc Chemicals", Zinc Development Association, London, 1973.
5. A. C. Tolcin, "2006 Minerals Yearbook: Zinc", United States Geological Survey, Washington, D.C., 2008.
6. R. S. Lehto, "The Encyclopedia of the Chemical Elements", Reinhold Book Corporation, New York, 1968.
7. A. C. Tolcin *Mineral Commodity Summaries: Zinc*; United States Geological Survey: Washington, D.C., 2009.
8. A. C. Tolcin *Mineral Commodity Summaries: Zinc*; United States Geological Survey: Washington, D.C., 2008.
9. D. Panagapko, "Canadian Minerals Yearbook 2007: Zinc", Natural Resources Canada,

Ottawa, 2008.
10. G. Rossini and A. M. Bernardes, *Journal of Hazardous Materials*, 2006, **131**, 210-16.
11. E. Sayilgan, T. Kukrer, G. Civelekoglu, F. Ferella, A. Akcil, F. Veglio and M. Kitis, *Hydrometallurgy*, In press.
12. P. A. Tasker, P. G. Plieger and L. C. West, "Comprehensive Coordination Chemistry II", Elsevier Ltd, Oxford, 2004.
13. C. Young, A. Alfantazi, C. Anderson, A. James, D. Dreisinger and B. Harris, Proceeding of Hydrometallurgy, 2003, 501-700.
14. A. Deep and J. M. R. de Carvalho, *Solvent Extraction and Ion Exchange*, 2008, **26**, 375-404.
15. M. K. Jha, V. Kumar and R. J. Singh, *Solvent Extraction and Ion Exchange*, 2002, **20**, 389-405.
16. K. C. Nathsarma and N. Devi, *Hydrometallurgy*, 2006, **84**, 149-54.
17. A. Mellah and D. Benachour, *Chemical Engineering and Processing*, 2006, **45**, 684-90.
18. A. Ocio and M. P. Elizalde, *Solvent Extraction and Ion Exchange*, 2003, **21**, 259-71.
19. M. R. C. Ismael and J. M. R. Carvalho, *Minerals Engineering*, 2003, **16**, 31-39.
20. F. Principe and G. P. Demopoulos, *Hydrometallurgy*, 2004, **74**, 93-102.
21. F. Principe and G. P. Demopoulos, *Hydrometallurgy*, 2005, **79**, 97-109.
22. J. Gnoinski, K. C. Sole, D. R. Swart, R. F. Maluleke, G. Diaz and F. Sanchez, international Solvent Extraction Conference 2008, Tucson, US, 2008, 201-8.
23. E. D. Nogueira, L. A. Suarez-Infazon and P. Cosmen, Zinc 83, 13th Annual CanadaHydrometallurgical Meeting, Canada, 1983.
24. G. Diaz, J. M. Regife, C. Frias and F. Parrilla, *Publications of the Australasian Institute of Mining and Metallurgy*, 1993, **7/93**, 341-6.
25. M. Kunzmann and Z. Kolarik, *Solvent Extraction and Ion Exchange*, 1992, **10**, 35-49.
26. F. J. Alguacil, A. Cobo and C. Caravaca, *Hydrometallurgy*, 1992, **31**, 163-74.
27. G. Kyuchoukov and S. Zhivkova, *Solvent Extraction and Ion Exchange*, 2000, **18**, 293-305.
28. A. Grzeszczyk and M. Regel-Rosocka, *Hydrometallurgy*, 2007, **86**, 72-79.
29. S. G. Galbraith, Q. Wang, L. Li, A. J. Blake, C. Wilson, S. R. Collinson, L. F. Lindoy, P. G. Plieger, M. Schroder and P. A. Tasker, *Chemistry - A European Journal*, 2007, **13**, 6091-107.
30. K. Smith, PhD Thesis, University of Edinburgh, 2008.
31. M. Tramontini and L. Angiolini, *Tetrahedron*, 1990, **46**, 1791-837.
32. M. Tramontini, *Synthesis*, 1973, 703-75.
33. R. A. Fairhurst, H. Heaney, G. Papageorgiou and R. F. Wilkins, *Tetrahedron Letters*, 1988, **29**, 5801-4.
34. H. Adams, N. A. Bailey, D. E. Fenton and G. Papageorgiou, *Dalton Transactions*, 1995, 1883-6.
35. J. Clayden, N. Greeves, S. Warren and W. Peter, "Organic Chemistry", Oxford University Press, Oxford, 2001.
36. T. Jerphagnon, G. P. M. van Link, J. G. de Vries and G. van Koten, *Organic Letters*, 2005, **7**, 5241-44.
37. K. D. Collins and M. W. Washabaugh, *Quarterly Reviews of Biophysics*, 1985, **18**, 323-422.
38. M. Wenzel, K. Gloe, K. Gloe, G. Bernhard, J. K. Clegg, X.-K. Ji and L. F. Lindoy, *New Journal of Chemistry*, 2008, **32**, 132-37.

39. K. Kavallieratos, R. A. Sachleben, G. J. Van Berkel and B. A. Moyer, *Chemical Communications (Cambridge)*, 2000, 187-88.
40. K. Wichmann, B. Antonioli, T. Soehnel, M. Wenzel, K. Gloe, K. Gloe, J. R. Price, L. F. Lindoy, A. J. Blake and M. Schroeder, *Coordination Chemistry Reviews*, 2006, **250**, 2987-3003.
41. K. Gloe, H. Stephan and M. Grotjahn, *Chemical Engineering & Technology*, 2003, **26**, 1107-17.
42. R. F. Kruh and C. L. Standley, *Inorganic Chemistry (Washington, DC, United States)*, 1962, **1**, 941-3.
43. D. F. C. Morris, E. L. Short and D. N. Waters, *Journal of Inorganic and Nuclear Chemistry*, 1963, **25**, 975-83.
44. D. L. Wertz and J. R. Bell, *Journal of Inorganic and Nuclear Chemistry*, 1973, **35**, 861-8.
45. Y. Yongyai, S. Kokpol and B. M. Rode, *Journal of the Chemical Society, Faraday Transactions*, 1992, **88**, 1537-40.
46. P. Butterworth, I. H. Hillier, N. A. Burton, D. J. Vaughan, M. F. Guest and J. A. Tossell, *Journal of Physical Chemistry*, 1992, **96**, 6494-500.
47. O. G. Parchment, M. A. Vincent and I. H. Hillier, *Journal of Physical Chemistry*, 1996, **100**, 9689-93.
48. D. J. Harris, J. P. Brodholt, J. H. Harding and D. M. Sherman, *Molecular Physics*, 2001, **99**, 825-33.
49. J. A. Tossell, *Journal of Physical Chemistry*, 1991, **95**, 366-71.
50. Y. Zhang, S. Mukherjee and E. Oldfield, *Journal of the American Chemical Society*, 2005, **127**, 2370-71.
51. G. E. Maciel, L. Simeral and J. J. H. Ackerman, *Journal of Physical Chemistry*, 1977, **81**, 263-7.

CHAPTER 4

ANION BINDING AND SELECTIVITY OF POLYTOPIC SALICYLALDIMINE LIGANDS

Content

4.1 Introduction

The work presented in this chapter continues the development and investigation of the polytopic ligands in chapter 3 for the hydrometallurgical recovery of zinc chloride. As shown in Figure 4.1, the salicylaldimine ligands bearing pendant amine groups can form ditopic and tritopic assemblies with a variety of anions. This chapter focuses on the anion binding and anion selectivity of these extractants and their metal complexes.

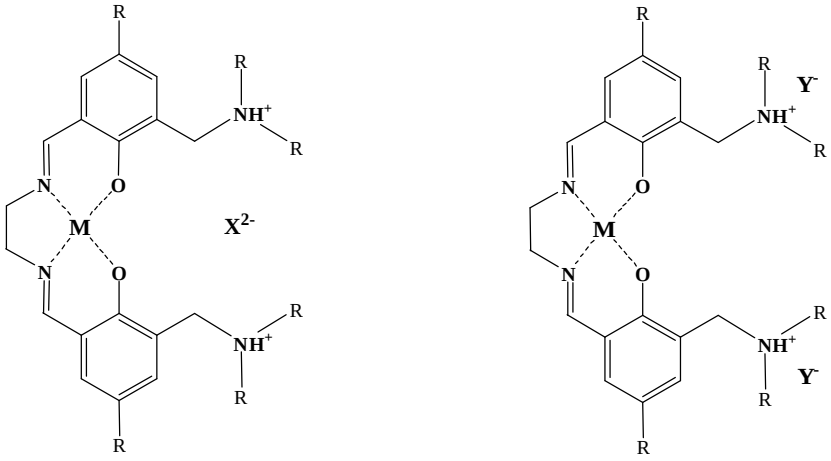

Figure 4.1 A ditopic assembly to recover divalent metal salts $M^{II}X$ and a tritopic arrangement for M^{II} salts of monoanions

4.1.1 Feature of Anions in Comparison to Cations

Anions are of great significance in biology, medicine, environment and industry.[1] More than 70% of natural enzymes and cofactors selectively bind anionic substrates among which phosphate and carboxylate anions are dominant and carbonate, sulfate, nitrate and chloride are also essential.[1] One of the many examples of anion analysis and control in medicine is the so-called "unmeasured" anions that are sulfate and a

number of serum proteins contributing to metabolic acidosis in a variety of disease states with the "measured" anions being chloride, bicarbonate and phosphate.[2] A whole series of environmental problems are directly connected with anionic species,[1] e.g. the eutrophication of water bodies caused by the entry of nitrate and phosphate from agricultural activities, the pollution of heavy metals such as chromate from the leathering industry and so on.[1] In addition there are still many anion-containing processes and waste solutions in industry to be decontaminated or recovered,[1] some of which are hydrometallurgical processes related to those in this thesis.

Despite the importance of anions in these areas, the studies of selective binding and extraction of anions were restricted for many years compared to the well-established and diverse development of metal cation extraction. Anion coordination chemistry came into being when the first synthetic anion-including complex was reported by Park and Simmons in 1968.[3] The organic cavity of a macrobicyclic amine was occupied by a guest halide as shown in Figure 4.2.[3]

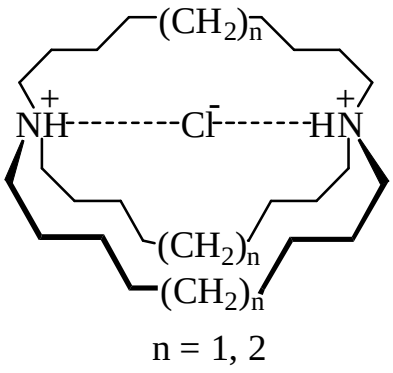

Figure 4.2 The first example of a synthetic anion-including complex[3]

Such ion pair formation of corresponding anionic species with hydrophobic ammonium cations of secondary and tertiary amines or quaternary ammonium compounds became the basis of the early work on anion complexation.[1] One of the

industrial applications in hydrometallurgy based on ion pairing is the reagent Aliquat 336 (tricaprylmethylammonium chloride)[4] mentioned in chapter 3. In recent years, the complexation of anions has undergone impressive development with the advance of supramolecular chemistry to create various new approaches,[5-8] which will be addressed in section 4.1.3.

The reasons for the restricted development of anion extraction are rooted in the different features of anions in comparison with cations.[1] For metal cations, the receptor defined as a Lewis base donates a pair (or pairs) of electrons to the metal to form covalent bonds; while in anion coordination the lone pair of electrons is donated in the reverse fashion, from the anion to the ligand.[9] Binding affinities between anions and the hosts are mostly attributed to hydrogen bonding and/or electrostatic interactions. Hydrogen bonding is more influential in promoting selective binding through topological complementarity,[9] which is much more challenging to design and achieve.

The simple physical property such as the size of ion is another difference. Anions are usually larger than cations,[1] which is clearly shown by the comparison of isoelectronic ions in Table 4.1.[10] Consequently anions have much lower charge to radius ratios, and are more difficult to bind electrostastically.[11]

Cation	r / Å	Anion	r / Å
Na^+	0.95	F^-	1.36
K^+	1.33	Cl^-	1.81
Rb^+	1.48	Br^-	1.95
Cs^+	1.69	I^-	2.16

Table 4.1 Radius of some isoelectronic cations and anions[10]

The sizes of anions also require that the complexing agents must be larger to ensure encapsulation.[1] Also the approach for the differentiation of cations on the basis of the ion sizes is not so effective because of the smaller differences in the relative sizes of anions.[1]

Anionic species also have a variety of different geometric arrangements as illustrated in Table 4.2 with some examples of interest in extractive metallurgy.[1, 12] The design of receptors is therefore specific for the anion's particular geometry and far more complicated than for the inherently spherical cations.[1, 12]

Anion Structure	Geometry	Examples
	Spherical	F^-, Cl^-, Br^-, I^-
	Linear	N_3^-, SCN^-, OH^-
	Trigonal Planar	CO_3^{2-}, NO_3^-
	Square Planar	$PdCl_4^{2-}$, $AuCl_4^-$
	Tetrahedral	PO_4^{3-}, SO_4^{2-}, $CoCl_4^-$
	Octahedral	$PdCl_6^{2-}$, $PtCl_6^{2-}$

Table 4.2 Typical anion geometries and the examples of each relevant to hydrometallurgy.[1, 12]

Another difficulty associated with the extraction of anions is that they are subject to

acid base equilibria in aqueous solutions. The presence of a specific ionic species is therefore connected to defined pH conditions, e.g. PO_4^{3-}, HPO_4^{2-} or $H_2PO_4^-$, and receptors must be designed to work in a specific pH range.[1]

One of the biggest challenges for the selective extraction of anions into non-polar water-immiscible liquids comes from their hydrophilic properties which result from the ion sizes, electronic peculiarities and hydrogen bonding natures.[1, 9] These are discussed in the following section.

4.1.2 Hofmeister Bias

Hydrophilicity tends to govern the selective anion extraction simply because the hydrate shells of anions have to be largely removed in an aqueous-organic phase transfer.[1, 9] This phenomenon is much related to the so-called Hofmeister series. In 1886 Franz Hofmeister conducted experiments to rank the ability of various ions to precipitate a mixture of hen egg white proteins,[13] and concluded the ordering from strongly hydrated anions on the left to weakly hydrated anions on the right:[13]

$$Citrate^{3-} > SO_4^{2-} = tartrate^{2-} > HPO_4^{2-} > CrO_4^- > OAc^- > HCO_3^- > Cl^- > NO_3^- > ClO_4^-$$

Much research has been done following this remarkable discovery,[14, 15] and extends not only the number of ion species studied but also the general utility of the series to *ca.* 40 observed phenomena,[14, 15] including the graduated effects on the structuring or denaturation of biological macromolecules,[16] influences on interfacial hydration,[17] effects on pH measurements[18] and so on. This ranking has huge implications in the field of anion extraction and can generally predict why anions such as ClO_4^- are extracted from aqueous solutions into non-polar solvents with more ease than anions such as SO_4^{2-}. The reason is that sulfate is much more hydrated than perchlorate, and

therefore has a greater hydrophilicity which favours its retention in an aqueous environment.

The relative positions of anionic species in the Hofmeister series can change or even reverse with the variation of applied phenomena and corresponding conditions such as protein, counter cation, pH and temperature.[14, 15] In order to avoid the confusion, Moyer *et al*[19] proposed that the term Hofmeister bias be used to describe the effects of anion solvation on extraction. In the liquid/liquid extraction of anions, the following series is usually observed, with the most readily extracted anions on the left and poorly extracted anions on the right:[1, 20]

$$ClO_4^- > I^- > NO_3^- > Br^- > Cl^- >> SO_4^{2-} > CO_3^{2-} > PO_4^{3-}$$

For the above anions, the values of the absolute enthalpies of hydration are given in Table 4.3.[21] The ranking is also proved by experimental work such as IR studies.[22]

Anion	ClO_4^-	I^-	NO_3^-	Br^-	Cl^-	SO_4^{2-}	CO_3^{2-}	PO_4^{3-}
$\Delta_{hyd}H^o$ (kJ/mol)	-205	-287	-316	-328	-359	-1099	-1486	-2921

Table 4.3 Standard absolute molar enthalpies of hydration of selected anions[21]

The rationale of the Hofmeister bias is still under debate, e.g. whether the surface charge density or the polarizability is the important determinant effect,[23, 24] and how much the natural hydrogen-bonded network of water is changed due to the interaction between the ions and water molecules.[25, 26] However, this does not affect the eventual ranking and its application in the anion extraction. In general, anions become more hydrated when the charges increase. For anions of the same charges, the larger anions show lower hydrophilicity because they are less charge-condensed

or polarized. This results in the more facile extraction of more charge-diffuse and larger anions which are less hydrated.[27]

The Hofmeister bias indicates the natural selectivity of anion extraction. However, selectivity against the bias is often required. Truly selective anion receptors must involve some elements of strategic design to overcome the dehydration in the aqueous-organic phase transfer of the target species, which has been achieved in recent years with the development of supramolecular chemistry.

4.1.3 Anion Receptor Development

Dimensionality, hydrogen-bond donors, preorganization effects and charge complementarity have been exploited to develop anion receptors and attenuated the Hofmeister bias to achieve desirable anion binding and selectivity.[9] Extensive research is reported and has been comprehensively reviewed[1, 5-9] with only a few examples discussed in this section.

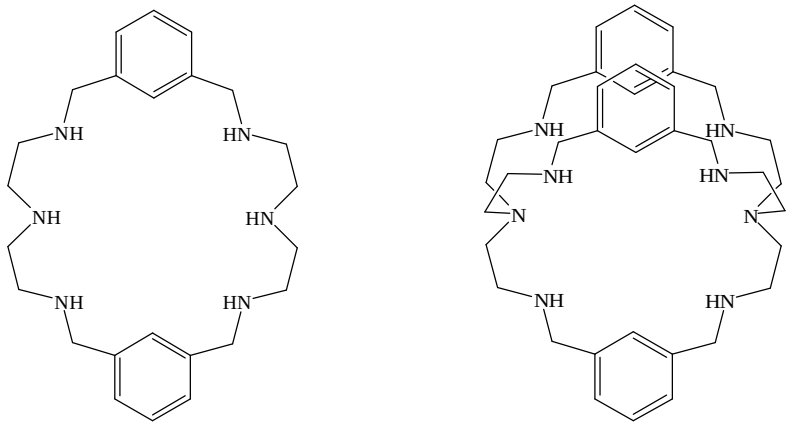

Figure 4.3 Examples of macrocyclic and macrobicyclic amines studied for anion binding[28]

Since the discovery of the first synthetic anion-including complex (see Figure 4.2), a large number of macrocyclic or macrobicyclic amines and amides has been studied for anion binding.[7, 9] A couple of them in Figure 4.3 are investigated by Bowman-James *et al*,[28] comparing monocyclic versus bicyclic binding of anions in polyammonium systems.[9]

The monocycles are usually prone to flatten or to remain flat because of solvation effects;[28] while the macrobicyclic ligands usually form organic cages for hosting anions,[28] and the size of the cavity can be adjusted by the length of linking alkyl chain. Consequently dimensionality can be utilized to achieve size selectivity of anions. Schmidtchen and co-workers put this to the test by investigating the macrotricyclic quaternary ammonium compounds in Figure 4.4.[29] The cavity diameters were estimated as spheres of 4.6 Å and 7.6 Å respectively for the two compounds with n = 6 or 8 in Figure 4.4.[29] The smaller tetrahedral host shows much stronger binding of bromide than iodide and chloride in water, because the size of bromide ion fits the cavity best.[29] The larger host selectively binds iodide among all the halides as a result of the large cavity size.[29]

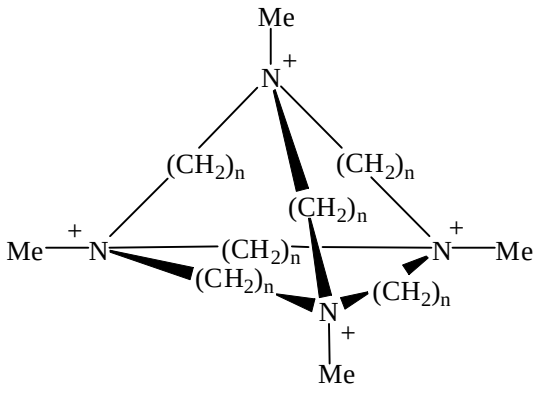

n = 6, 8

Figure 4.4 The macrotricyclic quaternary ammonium compounds studied for size selectivity of anions[29]

Hydrogen bonding can provide favourable interactions with the bound anions and becomes a major structure-defining aspect in anion coordination chemistry.[9] Increasing the hydrogen-bond donor functionality of macrocyclic receptors such as the octamethyl-octaundecylcyclo[8]pyrolle designed by Moyer *et al*[30] in Figure 4.5, can favour the extraction of larger, more complex anions. This is the first reagent to selectively extract sulfate in the presence of high nitrate concentrations.

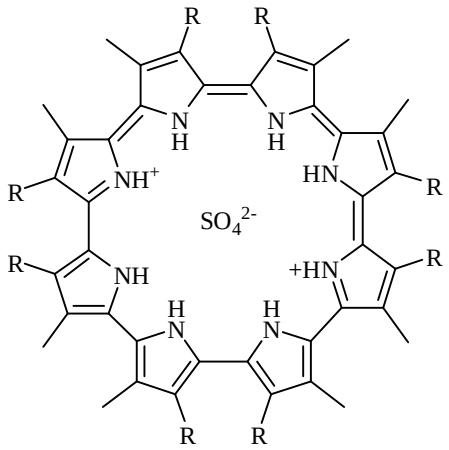

$R = C_{11}H_{23}$ or C_2H_5

Figure 4.5 Octamethyl-octaundecylcyclo[8]pyrolle for the extraction of sulfate.[30]

Topology can be considered in the placement of hydrogen-bond acceptors in the ligands to achieve preorganized arrangement and selective recognition of anions,[9] e.g. trigonal receptors could be ideal for anions of tetrahedral symmetries such as phosphates.[31] The tripodal ligand studied by Bowman-James *et al*[32] in Figure 4.6 provides a trigonal array of hydrogen-bond acceptor groups and binds $H_2PO_4^-$ and HSO_4^- more strongly than halides.

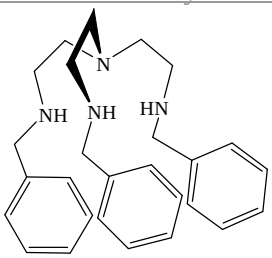

Figure 4.6 A tripodal amine studied for anion bindings[32]

All these features for designing a truly selective anion receptor are often combined,[9] e.g. polyammonium ligands are normally polyprotonated for charge complementary, with significant binding commencing after several protons are added to the macrocycle.[33] A highly organised, singly charged, steroid-based receptor with urea H-bond donors developed by Davis *et al*[34] in Figure 4.7 has shown to extract bromide and iodide more strongly than hexafluorophosphate and perchlorate. The complexity of the structure illustrates the difficulties in synthesizing receptors with appropriate geometries and H-bond donors to achieve selective anion transport against the Hofmeister bias.

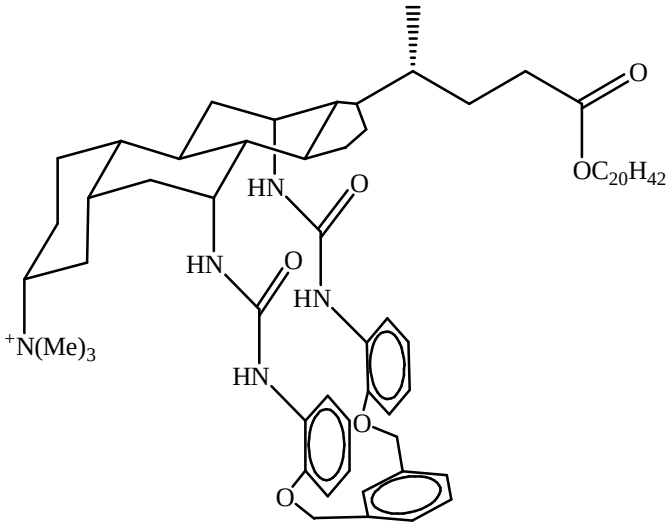

Figure 4.7 Steroid based anion receptor of Davis *et al*.[34]

4.1.4 Anion Analysis and Anion Selectivity Determination

Along with the advance of anion coordination chemistry, many methods have been developed to analyze anions and determine anion selectivity. Most literature techniques involve single phase measurements of anion concentration and the stability of anion complexation. NMR is probably most widely used to measure anion binding constants in either aqueous or non-aqueous solvents.[35, 36] The experimentally measurable NMR parameters such as chemical shifts, coupling constants, integration of peaks and so on can give information not only on the strength of binding but also solution structure. The NMR sensitive nuclei showing the greatest perturbation in chemical shift are usually most heavily involved in the binding of the anion, and therefore the location of binding in solution can be confirmed in most cases.[35] Changes of the NMR parameters can be used to determine complex stability constants. Slow or fast exchanges of the NMR sensitive nuclei give different information.[36] In the case of slow exchange the amount of free and complexed species present in equilibrium can be determined and allows an estimate of the stability constants. Under fast exchange, weight averaged signals of chemical shifts are obtained and used to calculate equilibrium constants.[36] However, NMR techniques can show low sensitivity due to the relatively high concentrations of both the anion and the receptor required to attain signals with appropriate intensities for use.[37] The technique also suffers from its intolerance to paramagnetic nuclei, including some common metal centres such as Cu(II) ion.[10]

Another well-defined method for measuring stability constants in aqueous solutions is based on potentiometry, more often pH-metry,[38, 39] which analyzes the consumption or liberation of protons as the receptor binds the anion by monitoring the pH of the solution. The basicity constants of the ligand and the anion(s) involved in the experiment are required and previously determined. Subsequently pH titrations

are carried out using a solution of the receptor, anion and protons to determine the pH changes. Stability constants can then be extracted from the data using computer programs.[40] This technique is limited to only aqueous solutions and heavily depends on the understanding of all equilibria in the solution which can be very complicated.

The optical and electrochemical properties of the anion and/or the receptor can be affected by anion coordination, and allow the possible use of UV-Vis, IR and other spectroscopies. The changes of the peaks can unveil structural information. The intensities of the spectra are often related with the concentrations of different species, and hence can be used to calculate equilibrium constants for anion-binding.[37, 41] The advantage of these methods is less restriction. They can be applied regardless of solvent, concentration or pH. However, they are often less accurate than other methods. In recent years, there have been some novel approaches in this area with the development of anion sensing, e.g. the inclusion of ruthenium chromophores[42] or fluorophores[43] in receptors to facilitate anion detection by UV-Vis spectroscopy or fluorimetric analysis.

Anion selective electrodes are popular options for measuring anion concentrations mainly in aqueous solutions. Particularly halide selective electrodes are successfully utilized. They conveniently provide the activities of free halide ions in water or polar solvents such as acetonitrile. However, interfering anions and complexing agents are potential problems. For chloride selective electrode, since it detects only free chloride ions, the presence of certain transition metal cations results in the formation of chlorometallate anions and affects the measured chloride concentration through Equation 4.1. This will be discussed further in section 4.2.

$$M^{x+} + yCl^- \rightleftharpoons MCl_y^{(x-y)-} \qquad \textbf{Equation 4.1}$$

ICP-OES analysis has been successfully used to measure metal ion concentration in extraction experiments as shown in chapter 2 and 3. Generally the technique requires at least one atomic or ionic emission line in the 160 to 900 nm region to detect the element accurately.[44] Unfortunately the emission spectra of most non-metallic elements lie in the wrong region or have intensities too low for reliable detection.[44] Consequently elements such as halogens are not applicable for ICP-OES analysis. Sulfur is a rare exception and the content of sulfate can be measured by ICP-OES in both aqueous and organic phases.[44]

Ion exchange chromatography is one of the applications of coordination chemistry, and its development has been exploited in anion analysis.[44-48] This technique is applied in aqueous or water-miscible solvents and commonly used for the determination of simple anions such as chloride and sulfate.[44] The disadvantage is that ion exchange chromatography can be fragile, target specific and expensive.[44] Concentrations of the analytes need to be carefully controlled to avoid overloading the column.[44] The optimum performance of the column depends heavily on the type of samples and the methods for sample preparation.[44] Consequently columns must be periodically replaced due to wear and tear or the changing analytical requirements.[44]

4.1.5 Aim of This Work

As shown above, anion coordination chemistry is a fascinating and rapid developing area which attracts many attentions from academia and industry. The Tasker group has contributed by investigating anion binding and selectivity in solvent extraction for hydrometallurgical uses.[49-51] Much of the research focused on sulfate and chloride selective extraction along with base metal recovery,[49, 50] which is also covered by the work presented in this chapter. However, there are many unique features due to the counter cation Zn^{2+}. As discussed in chapter 3, chlorozincates can be formed and

extracted as anions, which results in the complication of anion analysis and selectivity. This chapter aims to provide novel approaches for anion determination, particularly chloride analysis, and unveil the anion selectivity involving simple anions and chlorometallates in solvent extraction by the polytopic ligands.

4.2 Chloride Analysis

The determination of chloride contents loaded into the organic phase is key but challenging in this work. As mentioned above, the zinc and sulfur contents can be simultaneously measured by ICP-OES analysis of the organic phase,[44] and provide reliable information on the extraction of metal values and sulfate anion. Chloride analysis by ICP-OES was attempted in both aqueous phase and organic phase (butan-1-ol as solvent). Unfortunately the lines in chloride emission spectra are too weak to be properly calibrated. Alternative methods are required to carry out chloride analysis.

4.2.1 Chloride Selective Electrode

Among the other techniques discussed in section 4.1.4, the chloride selective electrode was firstly chosen due to the accuracy and availability of the facilities. The Orion 96-17 ionplus electrode employed works in aqueous solutions. Consequently direct chloride analysis in the organic phase was not possible. There were two options to solve the problem, one of which was to use the aqueous phase of solvent extraction to carry out the analysis. The difference of the chloride concentrations before and after the extraction in the aqueous feed would be the chloride content loaded by the ligand. However, the conditions of the extraction experiments determined this method would not be very accurate, e.g. from 1 M $ZnCl_2$ solution only *ca.* 0.02 M $ZnCl_2$ could be extracted. The difference in chloride concentrations

would be in the error range of the electrode. Also the recommended working range of chloride selective electrode is 10^{-3}-10^{-2} M, and therefore the high tenor chloride feed would not be suitable for direct measurement. The necessary dilution could result in further errors. Another option for chloride analysis by the electrode is to transfer the chloride content in the organic phase back into equivalent volume of an aqueous solution. Since nitrate is not an interfering anion for chloride selective electrode, nitric acid was used to strip all the zinc chlorides. The concentrations of the new aqueous solutions are well within the working range of the electrode.

Another big problem associated with chloride selective electrode is the formation of zinc chloride complexing species as shown in Equation 4.2. The electrode only measures free chloride activity, and the presence of zinc will result in a major error.

$$Zn^{2+} + nCl^- \rightleftharpoons ZnCl_n^{2-n} \qquad \textbf{Equation 4.2}$$

The equilibria for zinc chloride complex formation are highly dependent on the concentrations of both ions. The back extractions discussed above give mildly concentrated zinc chloride solutions. Tests for the electrode using $ZnCl_2$ standards were carried out in hope of minimal interference. Unfortunately the measured chloride concentrations were 10-20% lower than expected. Reported work[52] indicates that $ZnCl^+$ forms under such conditions and interferes with the electrode measurement, which is consistent with the observed results. Masking agents for zinc such as ethylenediaminetetraacetic acid (EDTA)[53, 54] were attempted to cancel the interference. These agents form complexes with Zn^{2+} to free all the chloride ions,[53, 54] and initially showed promising progresses. However, specific pH ranges were needed for EDTA and others to thoroughly complex the zinc cation,[53, 54] and therefore pH-buffering agents were brought into the system. This caused the complication of the species and the ion strength in the analyte. No satisfactory test results were

obtained, and chloride selective electrode had to be abandoned for chloride analysis at the presence of zinc.

4.2.2 Silver ICP-OES Analysis

The failure of the chloride selective electrode excludes the possibility of direct chloride analysis. A novel approach indirectly measuring the chloride contents by ICP-OES was invented in this work.

The method involves precipitating all chloride in the analyte by adding an excess of $AgNO_3$ standard solution, determining the concentration of the remaining Ag^+ in solution by ICP-OES, and then calculating the chloride concentration by the difference of silver(I) concentrations. This design includes several successful features. Silver is ICP-OES active and measure instead of chloride to take advantage of the accurate and facile ICP-OES technique. The method is applicable to the analysis of the total chloride content even in the presence of zinc, provided the chlorometallate is substitution-labile and the formation of AgCl solid by Equation 4.3 is thermodynamically favourable, which is the case for zinc[53-55] and proven by tests using concentrated $ZnCl_2$ reference solutions.

$$MCl_x^{y-} + zAg^+ \rightleftharpoons xAgCl_{(s)} + M^{x-y} + (z-x)Ag^+ \qquad \textbf{Equation 4.3}$$

Silver chloride precipitation is a well-studied reaction.[53] Only one species forms and the solubility of silver chloride is negligible in water at room temperature. The possible interferences are lead, copper(I), palladium(II), mercury(I) and thallium(I) cations as well as cyanides and thiosulfates,[53] which do not exist in the target system. In order to generate the aqueous analyte, the nitric acid stripping discussed in section 4.2.1 was applied. The resulting solution with dilute nitric acid provided an excellent

medium for the precipitation of silver chloride.[53] The presence of dilute nitric acid further reduces the solubility of silver chloride, prevents the precipitation of other silver salts, and also produces a more readily filterable precipitate.[53] To control the error range, the quantity of Ag^+ added to the analyte is about twice the expected molar Cl^- content, so that approximately half of the Ag^+ is precipitated. Silver chloride is light sensitive, and decomposition occurs into silver and chlorine when directly exposed to sunlight.[53] Consequently light was excluded as much as possible during the formation of silver chloride. The method was tested with satisfactory results, and used for the chloride analysis throughout this chapter.

4.3 Dependence of Zinc Transport Efficiency on the Nature of Counter Anions

As discussed in chapter 3, zinc uptakes by the polytopic ligands **L12** and **L13** are much greater from chloride solutions than sulfate solutions under comparable conditions, which indicates that zinc transport efficiency is very dependent on the nature of counter anions. Further work extended the research to zinc nitrate which is another common zinc salt and the anion NO_3^- ranks high in the Hofmeister bias for its hydrophobicity.[1, 20] Solvent extractions by **L12** and **L13** were carried out from 1 M $ZnCl_2$, $ZnSO_4$ or $Zn(NO_3)_2$ aqueous solution. The results in Figure 4.8 show that it is difficult to extract the metal from aqueous solutions to non-polar solvents when the counter anions are heavily hydrated, i.e. SO_4^{2-}, and the transport efficiency significantly increases with the decreasing hydrophilicity of the anions such as Cl^- and NO_3^-. The Hofmeister bias[1, 20] can be generally applied to predict the ease of the solvent extraction by the polytopic ligands. The abnormally high loadings of zinc chlorides are likely due to the extraction of chlorozincates as discussed in chapter 3. If $[ZnCl_4]^{2-}$ or $[ZnCl_3]^-$ is included in the Hofmeister bias, it should rank on the hydrophobic side, which will be further addressed in the section 4.4.

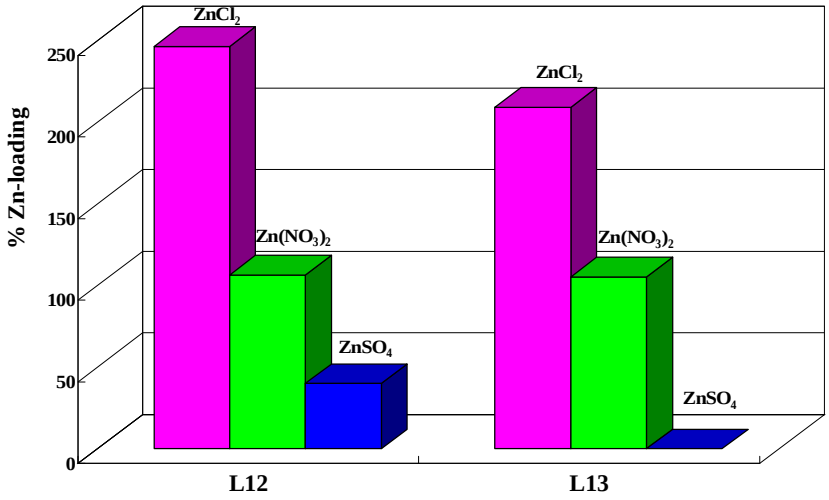

Figure 4.8 Zinc loadings by **L12** (0.01 M) or **L13** (0.01 M) from 1 M $ZnCl_2$, $ZnSO_4$ or $Zn(NO_3)_2$ aqueous solution. The 100% loading is based on 1:1 Zn:L.

To confirm the role of counter anions in the zinc extraction, another experiment was carried out by adding 2 M NaCl or $NaNO_3$ to the aqueous feed solution after the extraction by **L12** from 1 M $ZnSO_4$ solution. When the new equilibrium was reached, the zinc and sulfate contents in the organic phase were measured to compare with those before the addition of other anions. The results in Figure 4.9 show that the zinc concentrations increased in the organic phase with the complete disappearance of the sulfate content. It indicates that zinc transport efficiency increases when the poorly extracted anions are replaced. The dependence of metal value extraction on the nature of counter anions is much related with the anion selectivity in the following section.

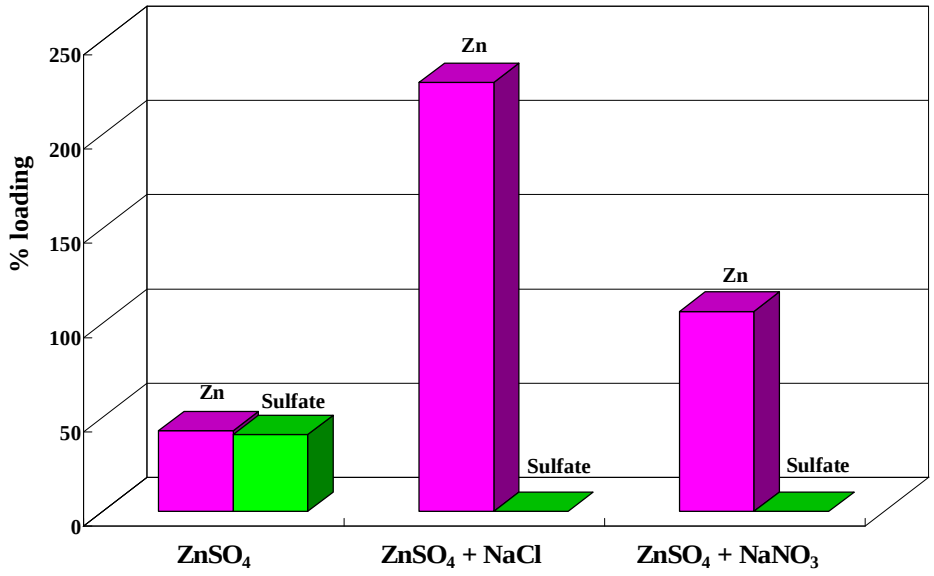

Figure 4.9 Zinc and sulfate loadings by **L12** (0.01 M) from 1 M $ZnSO_4$ aqueous solutions before and after the addition of 2 M NaCl or $NaNO_3$. The 100% loading is based on 1:1 Zn:L or SO_4^{2-}:L.

4.4 Chloride over Sulfate Selectivity

The selectivities of chloride and sulfate in solvent extraction have been of great interest because both are present in media used for hydrometallurgical processes in the industry. In this work the anion selectivity involves not only simple Cl^- or SO_4^{2-} ions but also chlorozincates such as $[ZnCl_4]^{2-}$ and $[ZnCl_3]^-$ which could form under high tenor $ZnCl_2$ feed and be extracted by the polytopic ligands.

Solvent extraction experiments were carried out by contacting chloroform solutions of 0.01 M **L12** with equal volumes of 1 M $ZnCl_2$, 0.03 M $ZnCl_2$ or 1 M $ZnSO_4$ solutions under stirring overnight. The zinc, chloride and sulfate contents loaded in the organic phase were measured. As shown in Figure 4.10, the transport efficiency of sulfate is much lower than that of chloride. The stoichiometry of zinc to sulfate is

1:1 and that of zinc to chloride are generally 1:2. But as the proposed mechanism in chapter 3 suggests, mainly Cl^- ions are extracted by **L12** from 0.03 M $ZnCl_2$ aqueous feed when achieving 100% Zn loading, and chlorozincates such as $[ZnCl_4]^{2-}$ are favourably extracted instead of Cl^- to achieve more than 200% Zn loading from 1 M $ZnCl_2$ aqueous solution. Combined these results, it can be concluded that the anion selectivity follows the order $[ZnCl_4]^{2-} > Cl^- > SO_4^{2-}$. This suggests that $[ZnCl_4]^{2-}$ should be ranked in Hofmeister bias as a poorly hydrated species, which is consistent with theoretical calculation and Raman spectroscopy studies.[56-58]

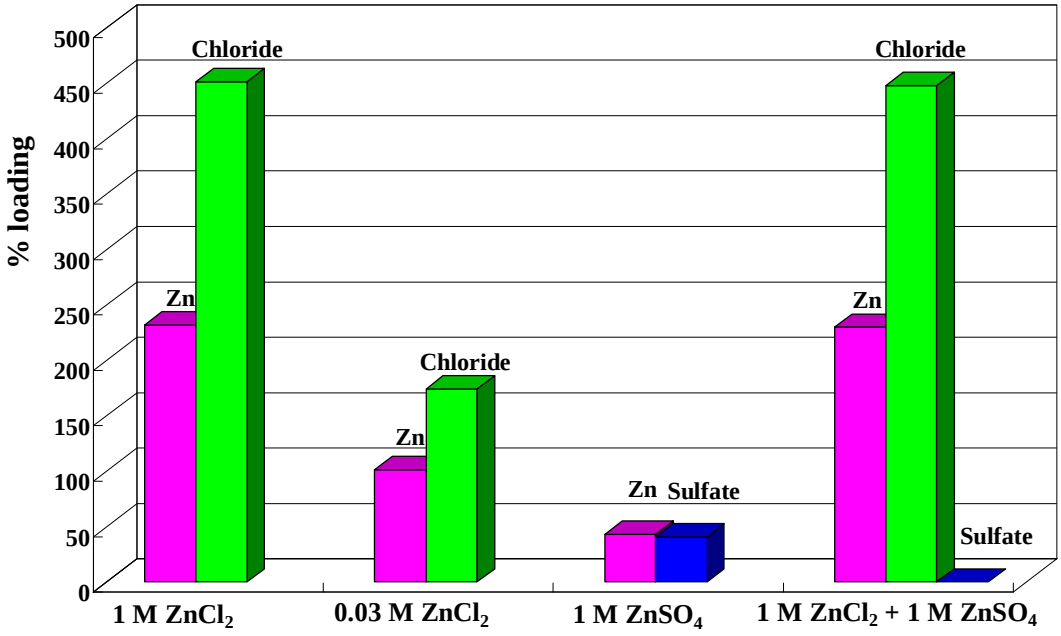

Figure 4.10 The zinc, chloride and sulfate loadings by chloroform solutions of 0.01 M **L12** from equal volumes of 1 M $ZnCl_2$, 0.03 M $ZnCl_2$, 1 M $ZnSO_4$ or a mixture of 1 M $ZnCl_2$ and 1 M $ZnSO_4$ aqueous solutions. The 100% loading is based on 1:1 Zn:L, Cl:L or SO_4^{2-}:L.

To confirm the above selectivity, another extraction experiment by **L12** was performed using a mixture of 1 M $ZnCl_2$ and 1 M $ZnSO_4$ aqueous solution. Since all

the target anions exist in the feed, the loaded species in the organic phase directly demonstrate the anion selectivity. The results in Figure 4.10 show that 230% zinc and 448% chloride were extracted without any sulfate content, which strongly supports the proposed selectivity.

4.5 Chloride Extraction

The chloride over sulfate selectivity by the polytopic ligand **L12** is established above. To investigate the extraction mechanism and evaluate the potential for commercial application, the chloride contents extracted by **L12** under various conditions were determined. The zinc chloride dependent extractions in section 3.5 provided a series of organic solutions containing different complexes formed by **L12**, zinc and chloride from $ZnCl_2$ feed solutions of various concentrations. The chloride analysis was carried out for these organic analytes as discussed in section 4.2.2. The chloride loadings were shown in Figure 4.11 along with the zinc loadings.

Multiple loadings of chloride were achieved by the polytopic ligands **L12**, which is desirable for designing excellent material balances in hydrometallurgical processes. Generally the stoichiometry of chloride to zinc extracted into the organic phase is very close to 2:1, which confirms the uptake as $ZnCl_2$ and is consistent with the proposed mechanism in chapter 3. There are a few reasons for the observed stoichiometry being slightly lower than 2:1. It could be that the cation binding is slightly more favoured than the anion binding, and small portions of the polytopic ligands function only as cation exchange reagents. It could also result from the incomplete acid stripping of chlorides. However, this possibility is rather slim. To generate the aqueous analyte, the organic solution was contacted with concentrated nitric acid under stirring overnight. After the stripping, the organic phase was analyzed for zinc contents by ICP-OES, and all zinc was confirmed to be transferred

into the aqueous phase. It is reasonable to assume that all chlorides are stripped along with the zinc contents. Also there are a large excess of nitrate ions which are more hydrophobic than Cl^- ions.[1, 20] Consequently it will be difficult to extract chloride back into the organic phase. Other possible error sources are from the analysis method, e.g. superficial decomposition of silver chloride under light, very fine AgCl precipitate getting through the syringe filter, *etc*. Despite these potential problems, the method has provided reliable chloride analysis and information on the extraction mechanism.

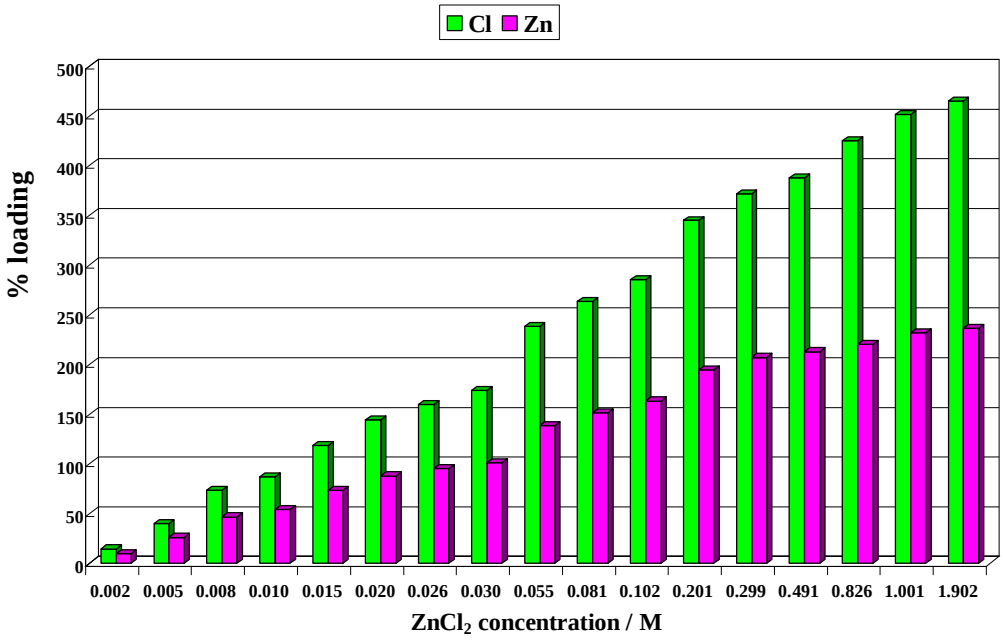

Figure 4.11 Chloride and zinc loadings by **L12** (0.01 M) from equivalent volumes of $ZnCl_2$ solutions of various concentrations. The 100% loading is based on 1:1 Zn:L or Cl:L.

4.6 Anion Extraction of Copper-Only Complex

The complex of the polytopic ligand **L12** containing only copper(II) cation, [Cu(**L12**-2H)] (see Figure 4.12), was investigated for anion extraction from zinc chloride and zinc sulfate solutions. This copper-only complex is chosen because

copper forms the most stable complexes with "salen" type ligands among the first row transition metals due to the almost perfect fit of Cu^{2+} in the square planar $N_2O_2^{2-}$ site.[10, 55, 59] The copper centre should not be stripped or replaced by zinc during the anion extraction. Since the cation binding site is occupied, the extraction process will be simplified and reflect solely the anion binding and selectivity. Also the coordination of the copper(II) cation templates the configuration of the ligand for the formation of the anion-binding site, and therefore could enhance the anion extraction. Another advantage of using the thermodynamically stable copper-only complex is that any detected zinc content in the organic phase should be present as chlorozincate anions.

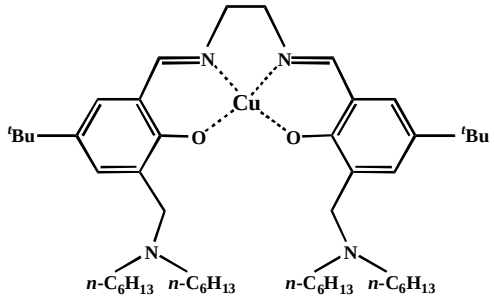

Figure 4.12 Structure of the copper-only complex [Cu(**L12**-2H)]

4.6.1 Synthesis and Characterization of the Copper-Only Complex

The copper-only complex [Cu(**L12**-2H)] was prepared from the polytopic ligand **L12** and copper acetate as shown in Figure 4.13. A solution of **L12** and equivalent $Cu(OAc)_2 \cdot H_2O$ in ethanol was stirred overnight. After removing the solvent, the crude complex was then dissolved in chloroform and washed with a pH 9 ammonia solution to remove excess copper acetate and to ensure the pendant amine groups were free of protons.

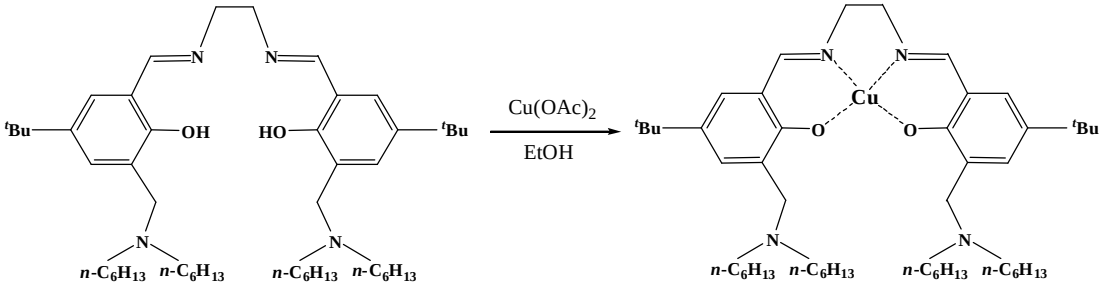

Figure 4.13 Synthesis of [Cu(**L12**-2H)]

Colour change occurred immediately in the reaction solution, indicating the complex formation. The pure complex [Cu(**L12**-2H)] was fully characterized by elemental analysis and mass spectrometry. ESI MS showed the molecular ion $[Cu(\mathbf{L12}\text{-}2H)]H^+$, confirming the success of the synthesis.

4.6.2 Anion Binding and Selectivity of the Copper-Only Complex

Solvent extraction experiments were carried out by contacting chloroform solutions of 0.01 M [Cu(**L12**-2H)] with equal volumes of 0.50 M $ZnSO_4$, 0.03 M $ZnCl_2$ or 0.50 M $ZnCl_2$ solutions under stirring overnight. The copper, zinc and sulfate contents loaded in the organic phase were measured simultaneously by ICP-OES as shown in Figure 4.14.

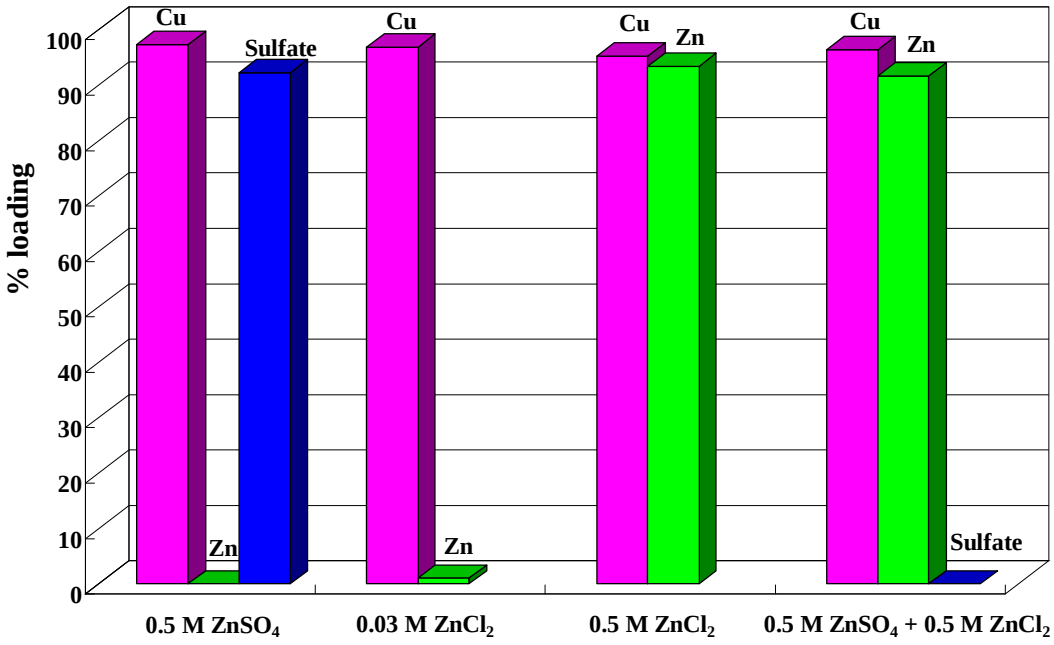

Figure 4.14 The copper, zinc and sulfate contents loaded by chloroform solutions of 0.01 M [Cu(**L12**-2H)] from equal volumes of 0.50 M $ZnSO_4$, 0.03 M $ZnCl_2$, 0.50 M $ZnCl_2$ or a mixture of 0.50 M $ZnCl_2$ and 0.50 M $ZnSO_4$ aqueous solutions. The 100% loading is based on 1:1 Cu:L, Zn:L or SO_4^{2-}:L.

The copper loadings (see Figure 4.14) are all very close to 100%, which indicates the cation binding sites were still occupied by Cu^{2+} in all cases. The sulfate loading by the complex from zinc sulfate media (92% in Figure 4.14) is remarkably high compared to that by the free ligand (41% in section 4.4). The 0.5 M $ZnSO_4$ solution is slightly acidic (*ca.* pH 5) due to the hydrolysis of the zinc salt. The protonation of the pendant amine groups in the copper-only complex and the extraction of the sulfate anion occur as shown in Equation 4.4.

$$[Cu(\mathbf{L12}\text{-}2H)]_{(org)} + 2H^+ + SO_4^{2-} \rightleftharpoons [Cu\mathbf{L12}SO_4]_{(org)} \qquad \textbf{Equation 4.4}$$

The high loading efficiency of sulfate by the complex suggests that the templating by Cu^{2+} enhances the anion binding, and the anion transport efficiency depends on the

nature of the counter cation. The origin of the synergic Cu^{2+} and SO_4^{2-} loading likely arises from the planarity of the CuN_2O_2 unit which aligns the pendant alkylamine groups to "chelate" the sulfate ion. Such an arrangement was confirmed by the X-ray structure of $CuSO_4$ complex of 3-(N-morpholinomethyl)-substituted salen ligand reported by the Tasker group.[60]

Negligible zinc was extracted by the copper-only complex from 0.50 M $ZnSO_4$ and 0.03 M $ZnCl_2$ solutions, which confirms that Zn^{2+} does not replace Cu^{2+} in the square planar $N_2O_2^{2-}$ site. Also under these conditions, very little chlorozincate anion was formed in the aqueous feed and consequently none was extracted by the complex. In contrast, *ca.* 100% zinc loading from the 0.5 M $ZnCl_2$ solution with copper remaining in the complex suggests that chlorozincates such as $[ZnCl_4]^{2-}$ are readily transferred to the organic phase. These anion binding results by the copper-only complex are very consistent with the extraction mechanism of the free ligand **L12**, and strongly support the possible extraction of chlorozincate as an anion species.

The anion selectivity by the complex [Cu(**L12**-2H)] involving SO_4^{2-}, Cl^- and $[ZnCl_4]^{2-}$ was also briefly investigated by extraction experiment using a mixture of 0.5 M $ZnCl_2$ and 0.5 M $ZnSO_4$ aqueous feed solution. The results (on the right in Figure 4.14) show that 92% zinc was extracted in the possible form of $[ZnCl_4]^{2-}$ without any sulfate loading. Considering the Hofmeister bias,[1, 20] it could be concluded that the anion selectivity by the copper-only complex follows the order $[ZnCl_4]^{2-} > Cl^- > SO_4^{2-}$, which is exactly the same for the free ligand **L12**. Consequently this confirms the anion selectivity obtained in section 4.4.

4.7 Experimental

4.7.1 Chemicals and Instrumentation

Unless otherwise specified a reagent or solvent was used as obtained from Aldrich, Fisher or Acros. Standards for inductively coupled plasma optical emission spectroscopy (ICP- OES) were purchased from Alfa Asar.

Mass spectrometry was performed on a Micromass ZMD instrument with a z-spray ESI source. CHN analytical data were obtained by the University of St Andrews Microanalytical Service. ICP-OES analysis was performed on a Perkin Elmer Optima 5300DV spectrometer. Initial chloride analysis by selective electrode was carried out on an Orion 96-17 ionplus electrode.

4.7.2 Complex Synthesis

[Cu(L12-2H)] A solution of **L12** (3.88 g, 0.005 mol) in ethanol (100 ml) was added to a solution of $Cu(CH_3COO)_2 \cdot H_2O$ (1.00 g, 0.005 mol) in ethanol (100 ml). The mixture was stirred overnight and the solvent was removed *in vacuo*. The resulting black solid was dissolved in chloroform (100 ml) and washed with a pH 9 ammonia solution (2 × 100 ml). The organic fraction was dried with $MgSO_4$, filtered and concentrated *in vacuo* to yield [Cu(**L12**-2H)] as a black solid (4.12 g, 98%). (Anal. Calc. for $C_{50}H_{84}Cu\,N_4O_2$: C, 71.77; H, 10.12; N, 6.70. Found: C, 71.52; H, 10.38; N, 6.57%). ESIMS *m/z* 837 (MH^+).

4.7.3 Chloride Determination by Silver ICP-OES Analysis

The analyte was prepared by nitric acid stripping of the loaded organic fraction

separated from solvent extraction experiment. A 0.4 M nitric acid solution was contacted with an equivalent volume of the organic solution in a tightly sealed, screw top glass jar. The two-phase system was stirred at 500 r.p.m at room temperature for 18 h. The aqueous fraction forms the analyte, and the organic fraction was analyzed for metal values by ICP-OES to make sure the acid stripping is complete.

A stock solution of silver nitrate was prepared by accurately weighing out $AgNO_3$, dissolving in water and making up to volume in a volumetric flask. A 2.50 ml aliquot was taken from the analyte and added into a sample vial with a rubber lined cap. $AgNO_3$ solution (2.50 ml) was added and the mixture was stirred vigorously for 4 h. The vial was covered with aluminium foil to avoid superficial decomposition of silver chloride under light. The suspension was transferred into an ICP tube and centrifuged for 10 min to separate the solid. The supernatant liquid was then sucked into a 5 ml syringe and ejected through a single-use syringe filter (0.2 μm). A 1.00 ml aliquot was diluted with water and made up to a known volume to ensure that the silver concentration was appropriate for ICP-OES analysis. The silver content was determined by ICP-OES and the total chloride content of the analyte was calculated by the number of mol of Ag^+ added to the analyte deducting the number of mol of Ag^+ remaining in supernatant after removal of AgCl.

4.8 Conclusions

The work in this chapter continued the development and investigation of polytopic salicylaldimine ligands in chapter 3, and aimed to study the anion binding and selectivity involving simple anions and chlorometallates in solvent extraction by these ligands and their complexes. Also it was necessary to develop novel and reliable chloride analysis method at the presence of complexing metal cations. All these objectives have been achieved.

The polytopic ligand **L12** has shown multiple loadings of chloride, which is desirable for achieving excellent material balances in hydrometallurgical processes. The *ca.* 400% chloride loadings along with *ca.* 200% zinc loadings under high tenor zinc chloride feed solutions suggest that chlorozincates such as $[ZnCl_4]^{2-}$ are likely extracted as anion species with Zn^{2+} cation by **L12**. Combined with the chloride loadings in zinc chloride dependent extractions, these results further prove the extraction mechanism in chapter 3 that a tritopic assembly [Zn**L12**Cl_2] forms from $ZnCl_2$ feed of low concentration by binding the Zn^{2+} cation within the $N_2O_2^{2-}$ site and two Cl^- anions with the protonated pendant amine groups and then a ditopic assembly [Zn**L12**($ZnCl_4$)] forms by extracting the $[ZnCl_4]^{2-}$ anion when the $ZnCl_2$ loading is increased with high tenor $ZnCl_2$ feed. The anion binding of the copper-only complex [Cu(**L12**-2H)] also supports this mechanism by indicating that *ca.* 100% zinc loading from 0.5 M $ZnCl_2$ solution, but negligible zinc content from 0.03 M $ZnCl_2$ solution was achieved. Since the cation binding site is still occupied by Cu^{2+}, zinc should be extracted only in the form of anion species, i.e. $[ZnCl_4]^{2-}$, which is consistent with the proposed mechanism.

The polytopic ligand **L12** and its complex [Cu(**L12**-2H)] show the same anion selectivity following the order $[ZnCl_4]^{2-} > Cl^- > SO_4^{2-}$. This suggests that $[ZnCl_4]^{2-}$ anion should rank highly on the hydrophobic side in the Hofmeister bias,[1, 20] which is consistent with theoretical calculations and Raman spectroscopy studies on chlorozincate species.[56-58] Consequently the Hofmeister bias can be expanded and used to predict the anion selectivity by the polytopic ligand. The solvent extractions from $ZnCl_2$, $ZnSO_4$, $Zn(NO_3)_2$ or mixed feed solutions indicate that the dependence of zinc transport efficiency on the nature of counter anions is closely related with the anion selectivity and can also be explained by the Hofmeister bias.

Because the chloride selective electrode failed to determine the chloride content

interfered by zinc as a complexing agent, a novel chloride analysis method was developed using silver ICP-OES technique. The method involves precipitating all chloride in the analyte by adding an excess of $AgNO_3$ standard solution, determining the concentration of the remaining Ag^+ in solution by ICP-OES, and then calculating the chloride concentration by the difference of silver(I) concentrations. The successful design results from relating the determination of one element with another by the stoichiometry of a well-studied reaction. This universal principle can be applied to the analysis of many other species that are difficult to analyze.

In summary, the anion binding and selectivity by the polytopic ligand **L12** has provided information on the extraction mechanism and further indicated great potential for application of these extractants in the industry.

4.9 References

1. K. Gloe, H. Stephan and M. Grotjahn, *Chemical Engineering & Technology*, 2003, **26**, 1107-17.
2. H. E. Corey, *Journal of Laboratory and Clinical Medicine*, 2006, **147**, 121-25.
3. C. H. Park and H. E. Simmons, *Journal of the American Chemical Society*, 1968, **90**, 2431-2.
4. M. K. Jha, V. Kumar and R. J. Singh, *Solvent Extraction and Ion Exchange*, 2002, **20**, 389-405.
5. C. Caltagirone and P. A. Gale, *Chemical Society Reviews*, 2009, **38**, 520-63.
6. P. A. Gale, S. E. Garcia-Garrido and J. Garric, *Chemical Society Reviews*, 2008, **37**, 151-90.
7. P. A. Gale, *Coordination Chemistry Reviews*, 2003, **240**, 191-221.
8. P. A. Gale and R. Quesada, *Coordination Chemistry Reviews*, 2006, **250**, 3219-44.
9. K. Bowman-James, *Accounts of Chemical Research*, 2005, **38**, 671-78.
10. D. F. Shriver, P. W. Atkins, T. L. Overton, J. P. Rourke, M. T. Weller and F. A. Armstrong, "Inorganic Chemistry", Oxford University Press, Oxford, 2006.
11. R. D. Shannon, *Acta Crystallographica, Section A: Crystal Physics, Diffraction, Theoretical and General Crystallography*, 1976, **A32**, 751-67.
12. P. D. Beer and P. A. Gale, *Angewandte Chemie, International Edition*, 2001, **40**, 486-516.
13. F. Hofmeister, *Arch. Exp. Pathol. Pharmakol.*, 1888, 247-60.
14. K. D. Collins and M. W. Washabaugh, *Quarterly Reviews of Biophysics*, 1985, **18**, 323-422.
15. W. Kunz, P. Lo Nostro and B. W. Ninham, *Current Opinion in Colloid & Interface Science*, 2004, **9**, 1-18.

16. Y. Zhang and P. S. Cremer, *Current Opinion in Chemical Biology*, 2006, **10**, 658-63.
17. S. Romsted Laurence, *Langmuir : the ACS journal of surfaces and colloids*, 2007, **23**, 414-24.
18. M. Bostroem, V. S. J. Craig, R. Albion, D. R. M. Williams and B. W. Ninham, *Journal of Physical Chemistry B*, 2003, **107**, 2875-78.
19. K. Kavallieratos and B. A. Moyer, *Chemical Communications (Cambridge, United Kingdom)*, 2001, 1620-21.
20. B. A. Moyer and P. V. Bonnesen, "Physical factors in anion separations", Wiley-VCH, New York, 1997.
21. J. Barrett, "Inorganic Chemistry in Aqueous Solution." Royal Society of Chemistry, Cambridge, 2003.
22. P. A. Bergstroem, J. Lindgren and O. Kristiansson, *Journal of Physical Chemistry*, 1991, **95**, 8575-80.
23. N. V. Nucci and J. M. Vanderkooi, *Journal of Molecular Liquids*, 2008, **143**, 160-70.
24. P. Lo Nostro, B. W. Ninham, S. Milani, A. Lo Nostro, G. Pesavento and P. Baglioni, *Biophysical Chemistry*, 2006, **124**, 208-13.
25. R. Leberman and A. K. Soper, *Nature*, 1995, **378**, 364-6.
26. A. W. Omta, M. F. Kropman, S. Woutersen and H. J. Bakker, *Science*, 2003, **301**, 347-49.
27. B. A. Moyer, P. V. Bonnesen, L. H. Delmau, T. J. Haverlock, K. Kavallieratos and T. G. Levitskaia, International Solvent Extraction Conference, Cape Town, South Africa, Mar. 17-21, 2002, 2002, 299-306.
28. T. Clifford, A. Danby, J. M. Llinares, S. Mason, N. W. Alcock, D. Powell, J. A. Aguilar, E. Garcia-Espana and K. Bowman-James, *Inorganic Chemistry*, 2001, **40**, 4710-20.
29. F. P. Schmidtchen and M. Berger, *Chemical Reviews (Washington, D. C.)*, 1997, **97**, 1609-46.
30. L. R. Eller, M. Stepien, C. J. Fowler, J. T. Lee, J. L. Sessler and B. A. Moyer, *Journal of the American Chemical Society*, 2007, **129**, 11020-21.
31. P. D. Beer, P. A. Gale and D. K. Smith, "Supramolecular Chemistry", Oxford University Press, Oxford, 1999.
32. M. A. Hossain, J. A. Liljegren, D. Powell and K. Bowman-James, *Inorganic Chemistry*, 2004, **43**, 3751-55.
33. A. Bencini, A. Bianchi, E. Garcia-Espana, E. C. Scott, L. Morales, B. Wang, T. Deffo, F. Takusagawa, M. P. Mertes and et al., *Bioorganic Chemistry*, 1992, **20**, 8-29.
34. A. L. Sisson, J. P. Clare and A. P. Davis, *Chemical Communications (Cambridge, United Kingdom)*, 2005, 5263-65.
35. K. A. Connors, "Binding Constants: The Measurements of Molecular Complex Stability", 1987.
36. T. Ramstad, C. E. Hadden, G. E. Martin, S. M. Speaker, D. L. Teagarden and T. J. Thamann, *International Journal of Pharmaceutics*, 2005, **296**, 55-63.
37. H. Xie, S. Yi and S. Wu, *Journal of the Chemical Society, Perkin Transactions 2: Physical Organic Chemistry*, 1999, 2751-54.
38. A. Bianchi, M. Micheloni and P. Paoletti, *Coordination Chemistry Reviews*, 1991, **110**, 17-113.
39. R. M. Izatt, K. Pawlak, J. S. Bradshaw and R. L. Bruening, *Chemical Reviews (Washington,*

DC, United States), 1991, **91**, 1721-85.

40. P. Gans, A. Sabatini and A. Vacca, *Journal of the Chemical Society, Dalton Transactions: Inorganic Chemistry (1972-1999)*, 1985, 1195-200.
41. H. Xie, S. Yi, X. Yang and S. Wu, *New Journal of Chemistry*, 1999, **23**, 1105-10.
42. P. D. Beer and E. J. Hayes, *Coordination Chemistry Reviews*, 2003, **240**, 167-89.
43. T. Gunnlaugsson, M. Glynn, G. M. Tocci, P. E. Kruger and F. M. Pfeffer, *Coordination Chemistry Reviews*, 2006, **250**, 3094-117.
44. F. A. Settle, "Handbook of Instrumental Techniques for Analytical Chemistry", Prentice Hall, New Jersey, 1997.
45. M. Amin, L. W. Lim and T. Takeuchi, *Journal of Chromatography, A*, 2008, **1182**, 169-75.
46. A. Markowska and P. Stepnowski, *Analytical Sciences*, 2008, **24**, 1359-61.
47. H.-B. Meng, T.-R. Wang, B.-Y. Guo, Y. Hashi, C.-X. Guo and J.-M. Lin, *Talanta*, 2008, **76**, 241-45.
48. N. Hirayama, W. Umehara, H. Makizawa and T. Honjo, *Analytica Chimica Acta*, 2000, **409**, 17-26.
49. S. G. Galbraith, Q. Wang, L. Li, A. J. Blake, C. Wilson, S. R. Collinson, L. F. Lindoy, P. G. Plieger, M. Schroeder and P. A. Tasker, *Chemistry--A European Journal*, 2007, **13**, 6091-107, S91/1-S91/5.
50. R. S. Forgan, J. E. Davidson, S. G. Galbraith, D. K. Henderson, S. Parsons, P. A. Tasker and F. J. White, *Chemical Communications (Cambridge, United Kingdom)*, 2008, 4049-51.
51. R. J. Warr, A. N. Westra, K. J. Bell, J. Chartres, R. Ellis, C. Tong, T. G. Simmance, A. Gadzhieva, A. J. Blake, P. A. Tasker and M. Schroder, *Chemistry--A European Journal*, 2009, **15**, 4836-50, S36/1-S36/10.
52. J. W. Bixler and T. M. Larson, *Journal of Inorganic and Nuclear Chemistry*, 1974, **36**, 224-6.
53. A. I. Vogel, J. Bassett, R. C. Denney, J. Mendham and G. H. Jeffery, "Vogel's Textbook of Quantitative Inorganic Analysis Including Elementary Instrumental Analysis", Longman, London, 1979.
54. M. Farnsworth, C. H. Kline and J. G. Noltes, "Zinc Chemicals", Zinc Development Association, London, 1973.
55. N. N. Greenwood and A. Earnshaw, "Chemistry of the Elements", Butterworth-Heinemann Ltd, Oxford, 1984.
56. O. G. Parchment, M. A. Vincent and I. H. Hillier, *Journal of Physical Chemistry*, 1996, **100**, 9689-93.
57. D. F. C. Morris, E. L. Short and D. N. Waters, *Journal of Inorganic and Nuclear Chemistry*, 1963, **25**, 975-83.
58. P. Butterworth, I. H. Hillier, N. A. Burton, D. J. Vaughan, M. F. Guest and J. A. Tossell, *Journal of Physical Chemistry*, 1992, **96**, 6494-500.
59. E. Suresh, M. M. Bhadbhade and D. Srinivas, *Polyhedron*, 1996, **15**, 4133-44.
60. R. A. Coxall, L. F. Lindoy, H. A. Miller, A. Parkin, S. Parsons, P. A. Tasker and D. J. White, *Dalton Transactions*, 2003, 55-64.

CHAPTER 5

CONCLUSIONS

5.1 Conclusions

The aims of this thesis were to develop new types of reagents for use in the hydrometallurgical recovery of base metals, and to understand ligand design features which are needed to control the strength, transport efficiency and selectivity of new solvent extractants. Both these objectives have been achieved.

3-Substituted and N-substituted salicylaldehyde hydrazones, **L1**-**L10,** were investigated as cation exchange extractants for the hydrometallurgical recovery of copper, and polytopic salicylaldimine ligands bearing pendant tertiary amine groups, **L12** and **L13**, were developed for the solvent extraction of zinc chloride salts. All the solvent extraction data were measured after the equilibria were reached, and thermodynamic products were obtained in all cases.

L1-**L10** extract Cu^{2+} to form complexes of a 1:2 M:L ratio (see Figure 5.1) in a similar manner to commercially successful salicylaldoxime extractants which account for 20-30%[1, 2] of the world's copper production.

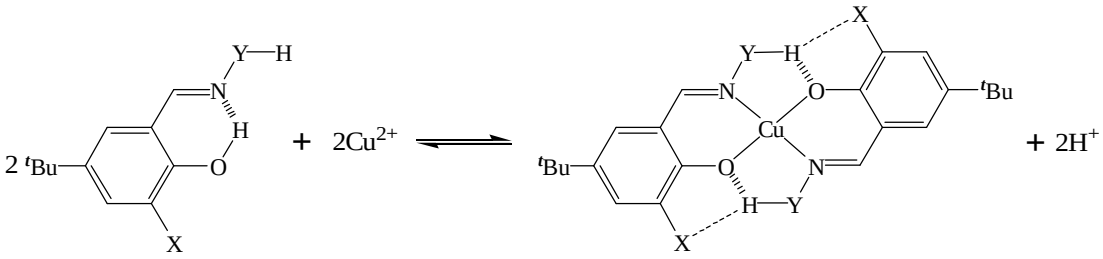

Figure 5.1 Copper extraction mechanisms of the hydrazones and oximes

The hydrazones are weaker extractants than the oximes, and the strength varies in the order: oximes > methylhydrazones > phenylhydrazones. This order likely arises from a combination of variations in the phenol acidities and the strength of the hydrogen

bonding motifs as shown in Figure 5.1. It was observed that 3-substituent such as NO_2 or Br can make the methylhydrazones (**L3** and **L4**) comparably strong extractants to the unsubstituted oximes. This emphasizes the importance of the substitution effects, and shows the potential of salicylaldehyde hydrazones for industrial application.

The polytopic ligands, **L12** and **L13**, show remarkably high zinc loadings from chloride media (246% and 209% respectively) and achieve high $ZnCl_2$ over $ZnSO_4$ selectivity in solvent extraction experiments. This could allow these extractants to be exploited in circuits which take advantage of chloride leaching techniques[3] and effectively recover zinc in chloride media from sulfide or oxide ores and from secondary sources. Most of the currently available reagents for zinc recovery requires one or two moles of ligands to extact one mole of zinc,[3, 4] while **L12** and **L13** have been shown to take up two zinc ions per ligand. Also they recover both metal values and counter anions as metal salt reagents, which is desirable for achieving good material balance in industrial circuits. The extraction mechanism of zinc chloride shown in Figure 5.2 is proposed on the base of the elemental analysis and ESI MS spectra of the complexes formed, the comparison of **L12** with the monotopic ligand **L11** as well as the dual host system **L11** and **L14**, the zinc chloride dependent extraction and stripping results and the ^{1}H NMR solution studies which indicate two different complexes are successively formed by increasing the concentration of $ZnCl_2$ aqueous feeds. As shown in Figure 5.2, a tritopic assembly [Zn**L12**Cl_2] forms from $ZnCl_2$ solutions of low concentrations by binding the Zn^{2+} cation with the $N_2O_2^{2-}$ site and two Cl^- anions with the protonated pendant amine groups and then a ditopic assembly [Zn**L12**($ZnCl_4$)] forms on extracting the $[ZnCl_4]^{2-}$ anion when the $ZnCl_2$ loading is increased with high tenor $ZnCl_2$ feeds. The possible formation of the tritopic assembly [Zn**L12**$(ZnCl_3)_2$] is able to account for the observed Zn-loading of more than 200%.

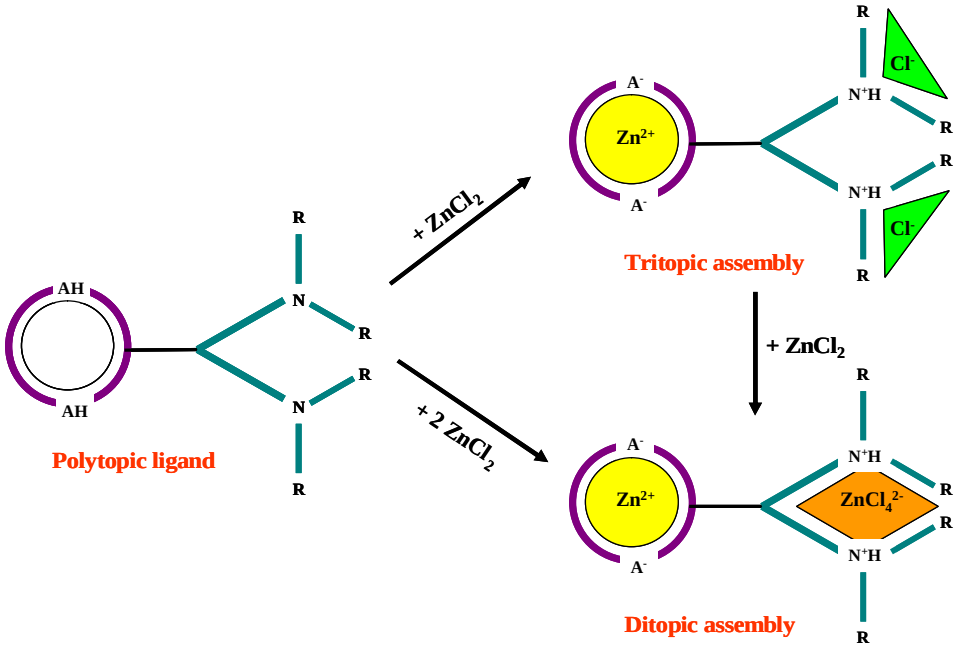

Figure 5.2 Proposed tritopic and ditopic assemblies involved in the extraction mechanism of $ZnCl_2$ by the polytopic ligand **L12**

An understanding of the ligand design features has been achieved as part of the development of the above extractants. The strength of the hydrazone extractants is readily tuned by substituent effects, e.g. electronic, steric and particularly "buttressing" of ligand-ligand hydrogen bonding (see Figure 5.1). The distribution coefficient for copper extraction is increased by more than three orders of magnitudes along the series of 3-substituents: Me < OMe ≤ H < Br < NO_2. Electron-withdrawing groups which also act as hydrogen bond acceptors (NO_2 or Br) are particularly effective in enhancing the strength of the methylhydrazones. The buttressing effect is well illuminated by the 3-methoxy substituted **L5**. Despite the electron-donating effect of the methoxy group, **L5** is a stronger extractant than its methyl analogue **L2**, and has a similar $pH_{0.5}$ value to the unsubstituted ligand **L1**. The transport efficiency of zinc chloride by the polytopic ligands is significantly increased by combining both the cation and anion binding sites in the same extractant. The deprotonation of the phenolic group and the protonation of the amine group can

occur as a simultaneous intramolecular proton exchange instead of an intermolecular or interfacial reaction, and both zinc cation and chlorozincate anion species are readily extracted. The inclusion of the pendant amine groups on the phenol moiety also makes the "salen" component stronger at cation binding, which is indicated by the results that **L12** achieved much higher Zn loadings than the combination of **L11** and trihexylamine at low $ZnCl_2$ concentrations. The anion selectivity of **L12** and its copper-only complex [Cu(**L12**-2H)] follows the order $[ZnCl_4]^{2-} > Cl^- > SO_4^{2-}$. This is rationalized by the Hofmeister bias[5, 6] which can be expanded and include $[ZnCl_4]^{2-}$ anion on the hydrophobic side.

In order to investigate the extractants presented in this thesis, new synthetic strategy, systematic NMR studies, modified ICP-OES techniques and novel chloride analysis methods were developed. The synthetic route employed for **L1**-**L10** minimizes the number of starting materials and steps required, and it is viable for industrial manufacture. A variety of 1D and 2D NMR spectroscopy was used to establish the assembly of the hydrazone ligands in solution and to study the substitution effect on the phenol acidity, hydrogen bonding and intermolecular association. ^1H NMR in two-phase system ($CDCl_3$ and D_2O) is employed to unveil the extraction mechanism of zinc chloride by the polytopic ligands **L12** and **L13**. For the salicylaldehyde hydrazones, a new approach to ICP-OES analysis of the loaded organic phase using nitrobenzene as the diluent is established to solve the issues of some of the copper complexes with low solubilities. Due to the interference of zinc as a complexing agent, the chloride selective electrode could not be used to determine the chloride loaded by the polytopic ligands. An alternative chloride analysis method was developed by adding an excess of $AgNO_3$ standard solution to the analyte to precipitate all chloride, determining the concentration of the remaining Ag^+ in solution by ICP-OES, and then calculating the chloride concentration by the difference of silver(I) concentrations. All the above methods have contributed to the

successful development of the novel extractants for the recovery of base metals, and they can also be applied in relevant systems.

5.2 References

1. P. J. Mackey, *CIM Magazine*, 2007, **2**, 35-42.
2. G. A. Kordosky, International Solvent Extraction Conference, Cape Town, South Africa, 2002, 853-62.
3. A. Deep and J. M. R. de Carvalho, *Solvent Extraction and Ion Exchange*, 2008, **26**, 375-404.
4. M. K. Jha, V. Kumar and R. J. Singh, *Solvent Extraction and Ion Exchange*, 2002, **20**, 389-405.
5. K. Gloe, H. Stephan and M. Grotjahn, *Chemical Engineering & Technology*, 2003, **26**, 1107-17.
6. B. A. Moyer and P. V. Bonnesen, "Physical factors in anion separations", Wiley-VCH, New York, 1997.

CHAPTER 6

APPENDIX

The following files are located in the appendix CD.

6.1 Publications

Polytopic Salicylaldimine ligands for the Recovery of Zinc Chloride, T. Lin, V. Gasperov, K. J. Smith, C. C. Tong and P. A. Tasker, *International Solvent Extraction Conference Proceedings*, Tucson, Arizona, USA, 2008, 1451-6.

6.2 Contents of Chapter 2

6.2.1 Crystal structure data and cif files for **L6** and **L9**

6.2.2 Solvent extraction results by **L1**-**L5**

6.2.3 Material balance of copper in two-phase extraction by **L1**-**L5**

6.2.4 ^{1}H NMR spectra for phenol acidity of the hydrazones and oximes

6.2.5 NOESY and 1D NOE difference spectra of **L1**-**L5**

6.2.6 ^{1}H NMR spectra for 3-substituent effect on phenol acidity

6.2.7 ^{1}H NMR spectra of concentration and temperature dependence

6.3 Contents of Chapter 3

6.3.1 Initial extraction results

6.3.2 Solvent extraction results of **L12** compared with dual host systems

6.3.3 Zinc chloride dependent extraction

6.3.4 Stripping results

6.3.5 ^{1}H NMR spectra for the speciation studies

6.4 Contents of Chapter 4